UNIVERSITAT DE BARCELONA

TRESK in nociceptive neurons: functional insights and modulation of peripheral sensitivity

Anna Pujol Coma

UNIVERSITAT DE BARCELONA

TRESK in nociceptive neurons: functional insights and modulation of peripheral sensitivity

Doctoral thesis dissertation presented by

Anna Pujol Coma

to apply for the degree of doctor at the University of Barcelona

Directed by

Prof. Xavier Gasull Casanova
Prof. Núria Comes Beltran
(University of Barcelona, IDIBAPS)

Doctoral Program in Biomedicine
School of Medicine and Health Sciences. University of Barcelona.
February 2024

Index

Abbreviations and acronyms

AITC	Allyl IsoThioCyanate
AP	Action Potential
APH	AfterPotential Hyperpolarisation
ASIC	Acid-Sensing Ion Channel
Calca	calcitonin related peptide
CFA	Complete Freud's Adjuvant, compound containing heat-killed *Mycobacterium tuberculosis* used to induce an inflammatory reaction that results in persistent inflammatory pain
CGRP	Calcitonin Gene-Related Peptide
CIPS	Calcineurin-Inhibitor-induced Pain Syndrome
C_m	Membrane capacitance
CNS	Central Nervous System
Ct	Cycle threshold for quantitative real-time PCR
DALY	Disability Adjusted Life-Years
DNA	DeoxyriboNucleic Acid
DRG	Dorsal Root Ganglia
GAPDH	GlycerAldehyde 3-Phosphate DeHydrogenase, used as endogenous control in quantitative Real-Time PCR of DRG tissues to normalise levels of gene expression
HT	High Threshold temperatures (between 26.5 and 19 ºC)
HTMR	High Threshold MechanoReceptors
IASP	International Association for the Study of Pain
IB_4	Isolectin B4,

IP	IntraPeritoneal administration
ISH	*In Situ* Hybridisation
KCl	Potassium Chloride
Kcnk	Potassium (K^+) Channel of subfamily K, family of genes codifying for K_{2P} channels
KO	Knock-Out
K_{2P}	Two-Pore domain K^+ channel
LT	Low Threshold temperatures (higher than 26.5 ºC)
LTMR	Low Threshold MechanoReceptors
MARK	Microtubule Affinity-Regulating Kinase
MIA	Mono-IodoAcetate
Mrgpr	Mas-Related G-Protein coupled Receptor
mRNA	messenger RiboNucleic Acid
Na_V	Sodium voltage-gated channels
P	Pore domain of ion channels
PBS	Phospate Buffered Saline solution used to dilute β-alanine and Tacrolimus and as a control solution in behavioural experiments
PCR	Polymerase Chain Reaction
PKA	Protein Kinase A
PKC	Protein Kinase C
PNS	Peripheral Nervous System
R_{in}	Input resistance
Rlp19	Receptor Like Protein 19, used as endogenous control in quantitative Real-Time PCR of nervous tissues to normalise levels of gene expression

RMP	Resting Membrane Potential
RNA	RiboNucleic Acid
SC	Spinal Cord
SEM	Standard Error of the Mean
TG	Trigeminal Ganglia
ThT	Threshold temperature
TM	TransMembrane domain of ion channels
TRAAK	Twirk-Related Arachidonic Acid-stimulated K^+ channel
TREK1	Twirk-RElated K^+ channel 1
TREK2	Twirk-RElated K^+ channel 1
TRESK	Twirk-RElated Spinal cord K^+ channel
TRP	Transient Receptor Potential
TRPA	Transient Receptor Potential Ankyrin
TRPM	Transient Receptor Potential Melastatin
TRPV	Transient Receptor Potential Vanilloid
Tubb3	Tubulin Beta 3 class III, used as neuronal marker in *in situ* hybridisation as it is more than 10 times more expressed in neurons than in other types of cells in sensory ganglia (Zeisel et al. 2018)
vHT	very High Threshold temperatures (lower than 19 ºC)
WT	Wild-type

Abstract

Sensing stimuli from our internal and external environments is critical to react appropriately and to guarantee our survival. Primary sensory neurons from dorsal root ganglia (DRG) and trigeminal ganglia are the first connection between our tissues and the central nervous system. Different populations of primary sensory neurons are involved in the detection of specific stimuli, and the tuning of their excitability is crucial to modulate our sensitivity. TRESK background potassium channel plays a critical role in modulating the action potential firing and excitability of primary sensory neurons. It is selectively expressed in populations of neurons involved in the perception of touch (low-threshold mechanoreceptors) and pain (nociceptors) and its depletion results in enhanced pain sensitivity.

Here, using RNA in situ hybridisation, calcium imaging and electrophysiological assays in DRG labelled neurons from wild type (WT) and TRESK knock-out (KO) mice, we explore the role of the channel in a population of nociceptors expressing the MrgprD receptor. We validate that TRESK is expressed in 70 % of MrgprD+ neurons and that it modulates their excitability, reducing the number of neurons activated by the MrgprD specific agonist β-alanine in male and female mice and by cold in female mice.

Using calcium imaging, we also study the role of TRESK in the modulation of the responsiveness of DRG neurons to cold temperatures and specific agonists. In concordance with previous studies showing that TRESK modulates the excitability of DRG neurons, we reveal that knocking out the channel enhances the number of neurons being activated by the noxious molecule capsaicin or cold temperatures, an effect present in females but not in sensory neurons from male mice. In contrast, deleting TRESK enhances the activation of neurons by menthol and the chemical irritant AITC but only from male mice.

Considering the effects of TRESK in the modulation of DRG neurons' responsiveness to cold and chemical compounds activating nociceptors and cold-sensitive neurons, we evaluated the cold, heat and mechanical sensitivity of WT and TRESK KO mice in physiological and pathological conditions. Knocking out TRESK does not change mice's cold and plantar mechanical sensitivity but increases their heat sensitivity in physiological but not under inflammatory conditions. Surprisingly, WT mice are more sensitive to joint mechanical friction than TRESK KO animals in both physiological and osteoarthritic conditions. Finally, treatment

with the calcineurin-inhibitor Tacrolimus increases wild-type mice's plantar sensitivity to heat and mechanical, but not to cold stimuli. The increased heat sensitivity after TRESK indirect inhibition by Tacrolimus in WT male mice resembles the heat allodynia observed in TRESK KO animals.

In summary, the presented data indicates that TRESK modulates the excitability of MrgprD+ nociceptors and prevents the responsiveness to chemical compounds and cold temperatures of DRG neurons in a sex-dependent manner. Genetically depleting the channel results in increased plantar heat sensitivity and decreased joint mechanical sensitivity, but, surprisingly, does not affect cold and plantar mechanical sensitivity of mice.

Resum

El canal de potassi TRESK participa en la modulació de l'excitabilitat de les neurones sensorials primàries. S'expressa en poblacions de neurones implicades en la percepció del dolor (nociceptors) i del tacte, i la seva eliminació provoca un augment de la sensibilitat al dolor.

En aquest estudi multidisciplinar, demostrem que TRESK s'expressa en nociceptors que presenten el receptor MrgprD i en modula l'excitabilitat, reduint l'activació d'aquestes neurones per un agonista selectiu de MrgprD, o pel fred en ratolins femella.

També mostrem que l'expressió del canal redueix el nombre de neurones que s'activen en resposta al proalgèsic capsaïcina, i a temperatures fredes, cosa que només s'observa en ratolins femella, però no de ratolins mascle. En canvi, TRESK també redueix el nombre de neurones de ratolins mascle, però no de ratolins femella, que s'activen en resposta a mentol o al compost irritant AITC.

D'altra banda, en condicions fisiològiques, eliminar TRESK no canvia les respostes dels ratolins a estímuls mecànics i de fred, però augmenta la seva sensibilitat a la calor. Tot i això, l'expressió de TRESK no protegeix als ratolins de la hipersensibilitat mecànica o a l'escalfor en un model inflamatori. Sorprenentment, tant en condicions fisiològiques com en un model d'osteoartritis, els ratolins que expressen TRESK són més sensibles a la fricció en les articulacions que els que no l'expressen. El tractament amb l'inhibidor de calcineurina Tacrolimus augmenta la sensibilitat plantar dels ratolins a la calor i als estímuls mecànics, però no al fred. La sensibilitat a la calor induïda pel tractament en els ratolins mascle que expressen TRESK és similar a la que presenten els ratolins sense el canal en condicions basals.

En resum, els nostres resultats indiquen que TRESK modula l'excitabilitat dels nociceptors MrgprD+ i redueix la resposta de les neurones sensorials primàries a estímuls químics i de fred. L'eliminació o inactivació indirecta del canal provoca una major sensibilitat a la calor, però no afecta la sensibilitat mecànica plantar i al fred dels ratolins. D'altra banda, els ratolins que no expressen el canal presenten una sensibilitat mecànica reduïda a les articulacions.

Introduction

1. Somatic sensation, perception and adaptation

Conscious or unconsciously, we are constantly receiving inputs from our body and the environment surrounding us. Our capacity to perceive and process this information allows us to adapt to the internal and external conditions. From Descartes, who believed that animals are mechanical devices that transform sensory stimuli into motor responses, several scientists and philosophers have studied and contributed to our current ideas and knowledge about sensory perception. Since kids, we learn about five senses that give us information about the external world: “vision, hearing, olfaction, taste and touch”. However, there are more stimuli that we can sense from inside and outside our body.

Somatic sensations group those sensations arising from skin, muscles, tendons, joints, and viscera, including temperature perceiving, touch, itch and pain sensing and proprioception. More than a century ago, Charles Sherrington, a physiologist that studied the nervous systems though which we adapt to the environment, already described three major functions for the somatosensory system: the exteroception, the interoception and the proprioception, which allow us to react to external inputs, to our own organism functioning and to our own body position and movement, respectively.

In most of the cases, the information we perceive from sensory inputs do not reach consciousness but produces responses. It is the case of blood pressure regulation or the maintenance of our body posture, for example. In some other cases, we can perceive the information from our internal and external organs. Sensory perception is a complex system that includes both sensory inputs, translated into sensory information by receptor cells, and cognitive and emotional components, integrated by higher areas of the central nervous system (Kandel et al. 2021; Levine 2007).

For example, we can distinguish nociception from pain, as the first one refers to the resultant effect of the activity of the receptor cells and does not consider the psychological and social factors involved in pain perception, which is both a sensory and emotional experience (International Association for the Study of Pain Terminology Working Group 2020).

1.1. Cold perception

The ability to detect changes in temperature is fundamental for the survival of warm-blooded animals. Detection of cold temperature is essential to activate conscious and unconscious mechanisms to maintain body temperature. Moreover, extreme temperatures can provoke serious damage to our tissues, and pain sensing in response to these temperatures is also crucial to avoid tissue harm (Tattersall et al. 2012).

1.2. Pain perception

According to the last revision of the International Association for the Study of Pain (IASP), pain is “an unpleasant sensory and emotional experience associated with, or resembling that associated with, actual or potential tissue damage”. This way, pain is a necessary mechanism that alerts us from potential harmful stimuli to allow us to protect from it. In fact, people that have decreased or absent pain sensitivity show high risk to self-mutilate (by uncontrolled scratching or fingers chewing, for example), have burning lesions, frequent contractures, fractures, and even decreased life-expectancy (Axelrod and Hilz 2003).

As reviewed in Woolf 2010, pain can be classified into nociceptive pain, which appears in response to an intense stimulus, inflammatory pain, which appears in response to the activation of the immune system, and pathological pain, which is maintained without a real or potential noxious stimuli or inflammation.

Apart from the continuous or intermittent pain, both inflammatory and pathological pain can curse with allodynia and hyperalgesia. While hyperalgesia is an increased pain sensation from a stimulus that normally provokes pain, allodynia is pain sensation provoked by a stimulus that does not normally provoke pain (**Figure 1**) (International Association for the Study of Pain Terminology Working Group 2020).

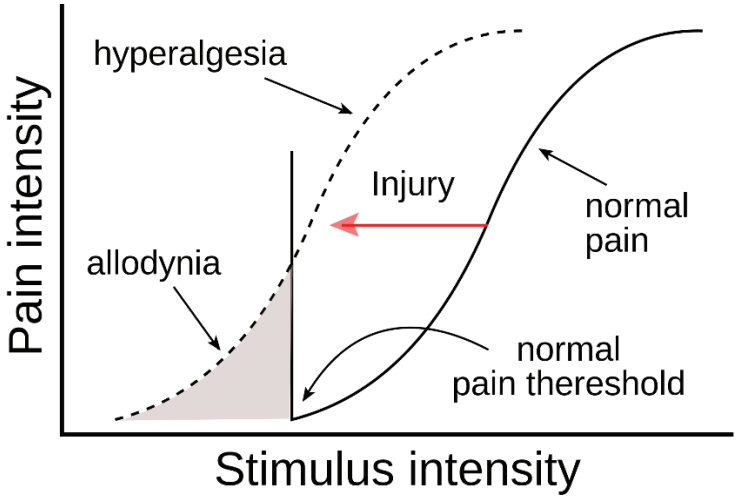

Figure 1. Characteristics of pain sensitisation. *Comparison of the pain intensity perceived in relation to the intensity of the stimuli received. While allodynia consists in the perception as painful of a stimuli of a lower intensity than the one considered the threshold for noxious stimuli (gray area), hyperalgesia is the perception of a noxious stimuli as more painful than in physiological conditions. Image by Jmarchn, CC BY-SA 3.0. Obtained from https://commons.wikimedia.org/w/index.php?curid=134350549.*

When pain persists beyond normal tissue healing time, it is considered chronic (International Association for the Study of Pain Terminology Working Group 2020). Chronic pain is one of the major health problems worldwide. In fact, the Global Burden of Diseases, Injuries, and Risk Factors Study of 2019, which collects data on incidence, prevalence, and mortality of hundreds of diseases and injures worldwide, identified low back pain as the 9th leading cause of years lived with disability (DALY) in people from all ages, and headache disorders as the top 5 of causes of DALY in people from 10 to 49 years old worldwide. When dividing the causes by gender, low back pain raises to the 6th position and headache disorders enter in the 10th position of the ranking in women (Abbafati et al. 2020).

More than it can be imagined by people that do not suffer it, living with daily pain interferes with functional abilities and with social and psychological well-being. In fact, chronic pain has been considered both a symptom and a primary disease, as it can be cause for other diseases such as mental disorders or depression. Although in this thesis we focus on one biological mechanism involved in sensory perception, is it important to consider that biological, psychological, socio-demographic and lifestyle elements are both determinants and outcomes of chronic pain (Breivik et al. 2006; Mills, Nicolson, and Smith 2019; Raja et al. 2020).

2. Somatosensory system

As mentioned, the transmission of sensory information is a complex process that integrates, not only the sensory stimuli, *per se*, but also cognitive and emotional components. While in the peripheral nervous system (PNS) the sensory information is detected, many components of the central nervous system (CNS) participate in the processing and integration of this information and the elaboration of the responses to it (**Figure 2**).

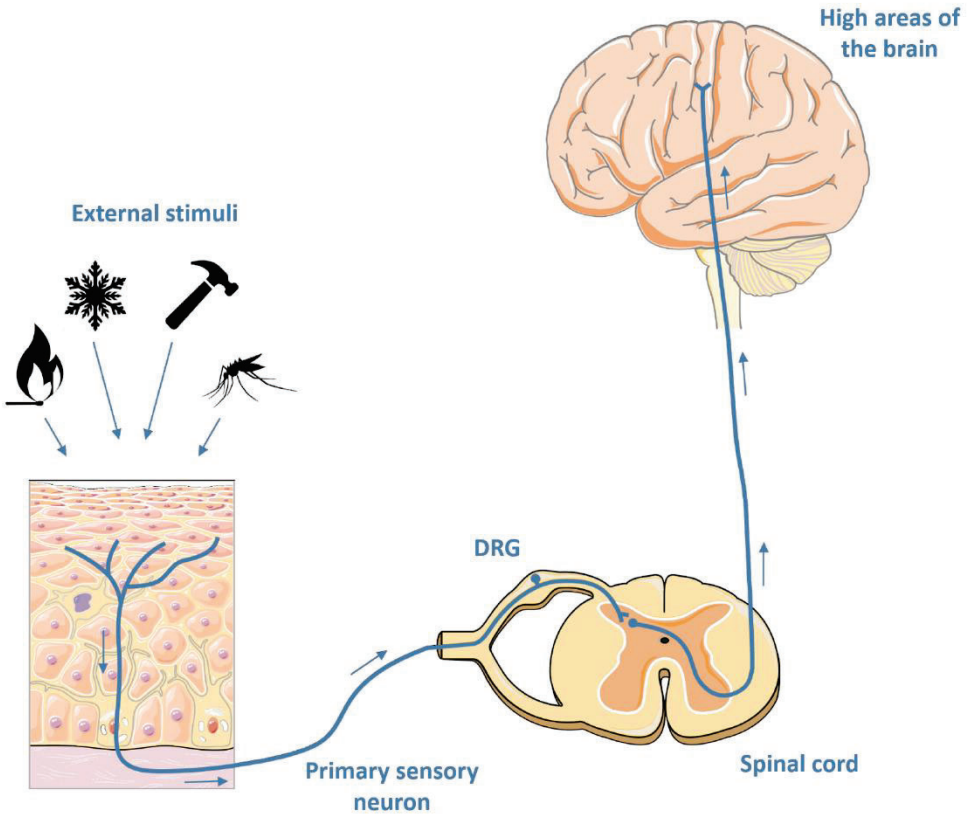

Figure 2. Main elements of the somatosensory system *including the primary sensory neurons that transduce the stimuli (in this scheme from the skin), has its soma in the dorsal root ganglia (DRG) and makes synapsis with second order neurons in the spinal cord. Most of the information from primary sensory neurons terminates in high areas of the brain, including the somatosensory cortex, where information is processed (more detailed in* ***Figure 5****). Image extracted from* (Andres-Bilbe 2020).

2.1. Primary sensory neurons

Primary or peripheral sensory neurons are the main neural connexion from the internal and external organs to the central nervous system. They are pseudounipolar neurons with one branch connecting to the internal or external organs and the other making synapses to the CNS. The primary sensory neurons that innervate the head and face have their somas in the trigeminal ganglia (TG) and project to the upper regions of the spinal cord or to the trigeminal nuclei located in the brainstem, while the primary sensory neurons that innervate the rest of

the body have their somas in the dorsal root ganglia and project to different levels of the spinal cord.

Thermal, mechanical and chemical stimuli activate specific receptors located in the peripheral terminals of primary sensory neurons, which depolarise the cell membrane in this area. If the depolarization reaches a threshold, the information is transduced into an action potential (AP) and transmitted to the central terminal of the axon. The transduction and transmission of the sensory information can be modulated at several levels by endogenous and exogenous factors (see Chapter Primary sensory neurons' sensitivity). The intensity and duration of the sensory stimuli is translated into the frequency and duration of the AP trains.

Primary sensory neurons are a heterogeneous family of neurons. Differential expression of receptors, ion channels and proteins involved in the transmission of information through the axons confer primary sensory neurons selective sensitivity to specific stimuli at specific intensities.

Primary sensory neurons have been classically classified according to the area of the body that they innervate, their soma size, their conduction velocity, and their physiological function. Lately, new techniques including single-cell sequencing, genetic tools to label specific populations of cells, and calcium imaging of cultured or skin-nerve preparations of primary sensory neurons have allowed a better understanding to the heterogeneity of these neurons and their functions in our body (Kandel et al. 2021; Xie et al. 2023).

Sensory transducers

An intuitive strategy to classify primary sensory neurons and understand their functions is analysing the receptors that they have and that might confer them capacity to respond to mechanical, thermal and chemical stimuli. Nevertheless, it is important to consider that other cells in the environment of primary sensory neurons, including cells of specialised sensory organs in the skin, glial cells or immune cells, can also respond to different types of stimuli and transmit the information to sensory neurons.

The most known stimuli transducers in the primary sensory neurons is the family of transient receptor potential channels (TRPs). TRPs are ligand-gated nonselective cation channels activated by a variety of biophysical and chemical stimuli and expressed in many neuronal and non-neuronal cells in the body. To date, 28 types of TRP channels have been identified

and classified into 6 families. The main TRPs expressed in primary sensory neurons and participating in their somatic sensitivity are TRPA1, TRPM8, TRPV4, TRPV3, TRPM3, TRPV1 and TRPV2 (**Figure 3**) which are expressed in specific populations. TRPs are considered polymodal integrators, because they show different domains that can respond to a variety of stimuli, including temperature, pH, osmolarity or immune or noxious compounds (Kandel et al. 2021; Mickle, Shepherd, and Mohapatra 2016; Tsagareli and Nozadze 2020).

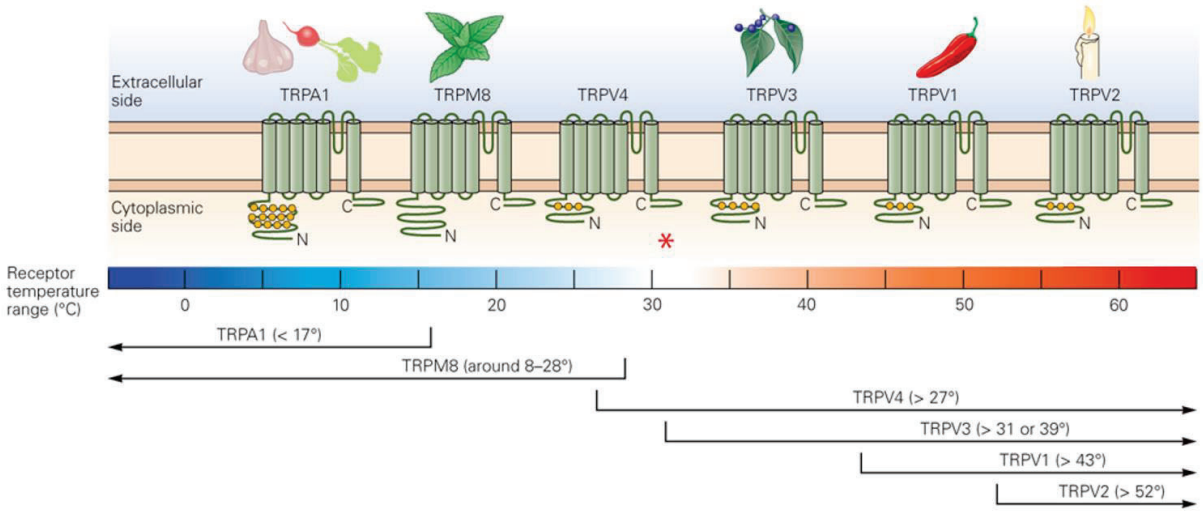

Figure 3. Thermosensitive TRP channels expressed in primary sensory neurons*. Scheme of the temperature of activation and the chemical agonists of each channel. The asterisk (*) indicates the resting skin temperature (around 32 ºC). TRPM3, which is active at temperatures from 30 to 45 ºC does not appear in the figure. Image extracted from* (Kandel et al. 2021).

Out of the TRPs expressed in primary sensory neurons, TRPM8 and TRPA1 are the only cold-sensitive. TRPM8 is activated by cooling and by temperatures below 25 ºC, by menthol and mints, and by voltage, and inactivated by warming. Neurons expressing this channel are involved in cold but not in heat sensing. Lack of TRPM8^{+} neurons results in a dramatic decrease of noxious cold sensing (Pogorzala, Mishra, and Hoon 2013). The TRPA1 channel is also activated by cooling and cold temperatures below 17 ºC, by chemical irritants such as AITC or the active principle of wasabi, by high concentrations of menthol and by mechanical stimuli, and inactivated by warming (Karashima et al. 2007). In some studies, TRPA1$^{-/-}$ animals show unaltered cold sensitivity. However, animals lacking the channel show increased aversive behaviours than wild-type (WT) animals when were stimulated with cold temperatures for long periods. Considering this, the high threshold temperature for TRPA1 activation and that injection of AITC in mice produce heat and cold hyperalgesia, it is proposed that TRPA1 might be mediating the cold sensitivity especially in pain situations. There are also

some disagreements regarding the role of TRPA1 in mechanical sensitivity as behavioural and electrophysiological studies show opposite results. It has been proposed that TRPA1 might be modulating the mechanical sensitivity of the neurons expressing the channels but that they are not the main mechanical transducers.

TRPV1 and TRPV2 are the main responsible for noxious heat sensing and their activation produce burning pain sensations. TRPV1 and TRPV2 are activated at 42 ºC and 52 ºC, respectively. TRPV1 is also activated in response to mechanical stimuli, extracellular acidic medium and noxious substances and toxins, including capsaicin, while TRPV2 is also activated by mechanical stimuli. While TRPV1 is essential for the detection of noxious heat and warm sensations (Ran and Chen 2019; Ran, Hoon, and Chen 2016), TRPV2 KO animals do not show impaired thermal, mechanical or chemical sensitivities. The loss of TRPV1-expressing neurons results in a high loss of the acute heat pain sensitivity even after inflammation, and do not affect mechanical and cold sensitivity, although it facilitates the development of mechanical hypersensitivity in inflammation conditions (Cavanaugh et al. 2009; Pogorzala, Mishra, and Hoon 2013).

Finally, TRPV3, TRPV4 and TRPM3 are the only TRP channels expressed in primary sensory neurons that are active at resting skin temperatures. They are activated at temperatures above 31 ºC, 27 ºC and 30 – 45 ºC, respectively. Thus, the neurons expressing these channels are the main responsible of innocuous warm sensing. Nevertheless, neurons expressing TRPV3 and TRPM3 are also involved in pain sensing. TRPV4 is also sensitive to mechanical and osmotic stimuli, while TRPM3 is also sensitive to mechanical stimuli.

The theoretical activation of just one TRP channel or just one population of TRP-expressing primary sensory neurons can not explain the sensations resulting from the stimulation by different stimuli. As an example, when $TRPA1^+$ and $TRPM8^+$ neurons are activated, the resultant sensation is the corresponding to noxious cold while, when the $TRPA1^+$ but not $TRPM8^+$ neurons are activated, the sensation is the corresponding to itch. In a similar way, when $TRPV1^+$, $TRPV2^+$ and $TRPV3^+$ neurons are activated, heat pain is perceived, while when $TRPV1^+$ but not $TRPV2^+$ and $TRPV3^+$ neurons are activated, itch is perceived. In a similar way, warm sensation has also been proposed to be a result of the absence of aversive temperature stimuli (Pogorzala, Mishra, and Hoon 2013).

Apart from the TRP family of channels, other receptors are activated by biophysical stimuli. In the recent years, the channels responsible for mechanotransduction in sensory neurons have been identified. It is the case of the nonselective cationic channels Piezo2, TACAN and TTN3 (TMEM150c), which are activated by mechanical stimuli and expressed in mechanosensitive primary sensory neurons, among other mechanosensitive cells, and participate in innocuous touch and proprioception, mechanical nociception, and proprioception, respectively (Beaulieu-Laroche et al. 2020; Hong et al. 2016; Ranade et al. 2014; Woo et al. 2015).

Finally, acid-sensing ion channels (ASICS) 1, 2 and 3 are nonselective cation channels activated by extracellular acid medium and participate in acidic pain sensing.

Populations of primary sensory neurons

As seen, expression of specific receptors confer sensitivity to different mechanical, thermal and chemical stimuli to specific populations of primary sensory neurons. However, primary sensory neurons are not expressing a single receptor and many other proteins or conditions can modulate their activity (see Chapter Primary sensory neurons' sensitivity). Thus, most of the primary sensory neurons are polymodal. As mentioned previously, primary sensory neurons can also be classified according to their size, their degree of myelinisation, their velocity of conduction, their patterns of expression and their function.

Classically, mammal primary sensory neurons innervating the skin have been classified into four classes. From largest and fastest conducting, to smaller and slower conducting, somatic sensory fibres are be classified into: Aα, Aβ and Aδ fibres, which are myelinated, and C fibres, which are unmyelinated (**Figure 4**). Fibers innervating the muscles and viscera have similar group distribution.

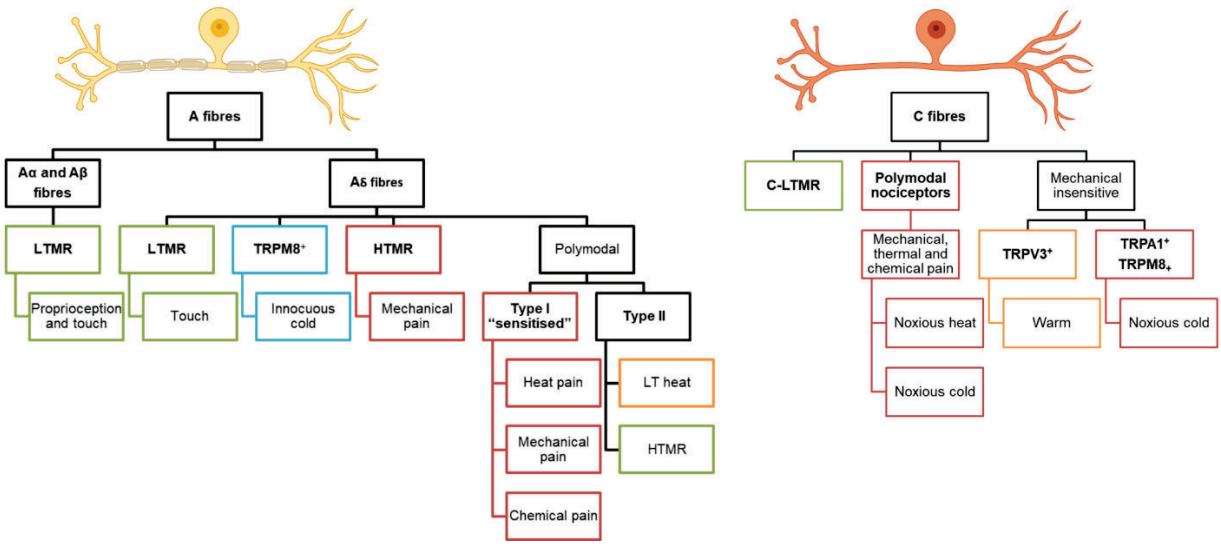

Figure 4. Classical classification of primary sensory neurons *according to their degree of myelinisation, their soma size, their conduction velocity (from left to right: gradation from the most myelinated, largest-sized and with faster conduction velocity, to the non- myelinated, smallest-sized and with slowest conduction velocity), and their function. Acronyms: LTMR – low threshold mechanoreceptors, HTMR – high threshold mechanoreceptors, and LT – low threshold.*

Aα and Aβ fibres are low threshold mechanoreceptors (LTMR) expressing the Piezzo 2 mechano-transducer that innervate specialised organs in the skin, including Paccinian corpuscles and hair follicles, and participate in the sensation of vibration, texture, light pressure and pleasant touch (Kandel et al. 2021; Ranade et al. 2014; Woo et al. 2015).

Aδ fibres are classified into five subpopulations according to their functions. The polymodal Aδ fibres of type I, also called "sensitising" Aδ fibres, are polymodal nociceptors that express the TRPV2 mechano- and thermo-transducer and participate in chemical, thermal and mechanical pain. This population of neurons can be activated by temperatures over 50 ºC or by sustained heat at lower thresholds. The polymodal Aδ fibres of type II, by their side, are TRPV1$^+$ TRPV2$^+$ Aδ fibres activated by low threshold heat (over 43 ºC) and high threshold mechanical stimuli. Polymodal Aδ fibres are inactivated by cold temperatures below 0 ºC. Non-polymodal Aδ fibres are Aδ low threshold mechanoreceptors (LTMR), that express Piezo 2 and are involved in touch; Aδ high threshold mechanoreceptors (HTMR), involved in mechanical pain, and TRPM8$^+$ Aδ fibres, involved in detecting innocuous skin cooling below 25 ºC.

Finally, C fibres are also classified into five different populations including one LTMR, two polymodal nociceptors and two thermal receptors. Both populations of polymodal

nociceptors express the chemical, mechanical and thermo-transducers TRPV1 and TRPA1, and participate in the sensing noxious mechanical stimuli, chemical irritants, and itch. While one of the polymodal populations participate in the sensitivity of noxious cold stimuli, the other one is sensitive to noxious heat (over 45 ºC) and inactivated by cooling. A subset of these polymodal C fibres sensitive to heat is classified as “silent” nociceptors, as they only respond to mechanical stimuli after being activated by inflammation compounds, such as histamine. The two mechanical insensitive populations of C fibres can be distinguished by their patterns of expression of TRP channels: while the population expressing TRPV3 is responsible for the sensing of warm temperatures over 35 ºC, the population expressing TRPA1 and TRPM8 participates in sensing noxious cold temperatures below 5 ºC.

Aδ and C fibres are involved in different types of nociception. While Aδ fibres are mostly related to immediate and localised pain, which is also called first pain, C fibres are the main responsible for poorly localised differed second pain (Basbaum et al. 2009; Kandel et al. 2021).

Lately, single-cell sequencing studies have allowed the classification of primary sensory neurons according to their patterns of expression. Several studies analysing the neurons of the DRG and TG from mice, rats, humans and non-human primates have pooled primary sensory neurons into different subpopulations. Some populations were identified in most of the studies while others were found only in specific publications, which is probably due to differences in the cell processing, region studied, technique used or number of neurons analysed, most of them found groups with multiple similarities (Chiu et al. 2014; Jung et al. 2023; Nguyen, Le Pichon, and Ryba 2019; Tavares-Ferreira, Shiers, et al. 2022; Usoskin et al. 2015; Xie et al. 2023; Zeisel et al. 2018; Zheng et al. 2019). In a recent study, (Jung et al. 2023) integrated data from different species to facilitate the comparison of populations between species (**Table 1**). They classified LTMR into four groups (proprioceptor & Aβ SA-LTMR, Aβ RA-LTMR, Aδ-LTMR and C-LTMR), created a new separated group for Aδ and C fibres expressing the cold sensor TRPM8 (Cold Trmp8), and classified the nociceptors into non-peptidergic (NP1-3) and peptidergic (PEP1-3). In mice, those nociceptors that release the neuropeptides substance P, somatostatin and/or calcitonin related peptide (Calca) to communicate with cells nearby are named non-peptidergic nociceptors and are populations of C and Aδ fibres, while the C-fibres responding to noxious stimuli that do not release these neuropeptides are called non-peptidergic nociceptors. In mice, most of the non-peptidergic nociceptors express Mas-

related G-protein coupled receptors (Mrgpr) and purinergic receptors such as $P2X_3$ and have membrane components that bind to the isolectin B4 (IB_4) (Jung et al. 2023).

mice

	LTMR				nociceptors						Cold
	Aβ SA-	Aβ RA-	Aδ	C	NP1	NP2	NP3	PEP1	PEP2	PEP2	Trpm8
Trpv1	4.94	11.76	4.21	7.21	34.78	34.02	81.32	89.71	19.9	18.05	35.42
Trpa1	2.47	2.94	2.11	30.21	60.87	43.99	28.57	36.27	10.68	7.52	1.04
Trpm8	0	0.98	0	1.04	0	0	0	11.76	3.88	24.06	81.25
Mrgprd	6.17	7.84	8.42	4.69	85.71	41.68	15.38	4.9	5.83	1.5	1.04
Mrgpra3	1.23	2.94	2.11	2.08	8.07	45.7	6.59	2.45	3.4	3.76	1.07
Kcnk18	0	2.94	43.16	2.08	36.02	41.58	5.49	4.41	7.28	5.26	0

human

	LTMR				nociceptors						Cold
	Aβ SA-	Aβ RA-	Aδ	C	NP1	NP2	NP3	PEP1	PEP2	PEP2	Trpm8
Trpv1	2.37	26.99	17.02	70.59	87.9	79.7	79.22	65.1	36.46	43	51.52
Trpa1	0	6.75	3.19	35.29	38.71	9.02	48.05	45.3	3.39	20	36.36
Trpm8	2.37	3.68	0	0	0	0	3.9	18.46	6.77	18	42.42
Mrgprd	0	0	0	0	0	0	0	0	0	0	0
Mrgpra3	0	0	0	0	0	0	0	0	0	0	0
Kcnk18	0	4.29	0	0	20.97	19.55	2.6	0	2.86	0	0

Table 1. Percentage of neurons from mice and human DRGs expressing specific TRPs, Mrgprs and Kcnk18 transcripts on each population of neurons. *Classification of neurons according to* (Jung et al. 2023). *Data of specific genes obtained from XSpecies DRG Atlas (http://research-pub.gene.com/XSpeciesDRGAtlas/#, consulted on 7th February 2024). Dark blue and yellow colours indicate the lower and higher percentages of neurons of each population expressing the specific genes, respectively. The populations of neurons expressing Kcnk18 in DRGs from mice (Aδ-LTMR, NP1 and NP2) are highlighted in orange. Acronyms: LTMR – low threshold mechanoreceptors, NP – non-peptidergic nociceptors, and PEP – peptidergic nociceptors. Although this table show no expression of Mrgprd in human, other studies proved that is expressed in some populations of human DRGs* (Wooten et al. 2014).

In mice, the Twirk-related Spinal cord K^+ channel (TRESK), which is involved in the sensitivity to diverse mechanical, thermal and chemical stimuli (see Chapter 4. TRESK), is expressed in high percentages of neurons of Aδ-LTMR, NP1 and NP2 subpopulations. In humans TRESK is also expressed in neurons of NP1 and NP2 populations, but not in the Aδ-LTMR population. Interestingly, high proportions of the populations non-peptidergic nociceptors NP1 and NP2 also express the member D of the Mrgpr family in mice (MrgprD, **Table 1**) (Jung et al. 2023).

MrgprD-expressing primary sensory neurons

Since their identification, it was already found that Mrgprs co-express with nociceotor markers and that some of them were selectively expressed in some populations (Klein et al. 2021). It is the case of MrgprD, that was first described in (Dong et al. 2001) and (Shinohara et al. 2004) and is clearly expressed at very high levels in subsets of non-peptidergic small nociceptors (Dong et al. 2001; Jung et al. 2023; Rau et al. 2009; Shinohara et al. 2004; Usoskin et al. 2015; Zheng et al. 2019; Zylka, Rice, and Anderson 2005). MrgprD$^+$ neurons innervate the epidermis of both glabourous and hairy skin but are not part of specific cutaneous structures (Zylka, Rice, and Anderson 2005). In DRG of mice, MrgprD shows a high co-expression with TRPA1 (C. Wang et al. 2019).

Although Jung et al. 2023 showed no expression of MrgprD in human DRGs (**Table 1**), Wooten et al. 2014 found that, in human DRGs, *MRGPRD* is co-expressed with the *MRGPRX1*, the human homologous of the mice *MrgpA3* gene, which is expressed in a high proportion of NP2 nociceptors from mice.

β-alanine is a specific agonist of MrgprD. Although it has been shown that a subset of MrgprD$^+$ neurons with differential electrophysiological characteristics are not responsive to β-alanine, it is also true that MrgprD KO neurons are not responsive to the agonist. The activation of MrgprD by β-alanine mediates the activation of different kinases, including PKA and it has been proposed that the increase of TRPA1 activity due to its phosphorylation is mediating the intracellular calcium increases induced by β-alanine (C. Wang et al. 2019).

The differential gene expression in MrgprD$^+$ neurons characterise their electrophysiological properties. MrgprD$^+$ neurons fire at low frequency and show no delay or adaptation in response to depolarising stimuli (Zheng et al. 2019). Neurons lacking the receptor show decreased excitability, while the activation of the receptor using β-alanine results in an increase in the neuronal excitability (Rau et al. 2009).

Although MrgprD is not sensitive to mechanical stimuli (Zheng et al. 2019), MrgprD$^+$ neurons are sensitive to mechanical, cold and heat stimuli. In line with the effects on the excitability, lacking MrgprD results in a decrease in the neuronal firing rate in response to mechanical stimuli and in an increase in the cold and heat thresholds for neuronal activation in this population of nociceptors (Rau et al. 2009).

Ablation of the MrgprD$^+$ line has revealed its determinant role in noxious mechanical sensing. In another direction, the ablation of the line does not affect mice sensitivity to heat and cold stimuli (Cavanaugh et al. 2009). Nevertheless, when this line is ablated together with TRPM8$^+$ or TRPV1$^+$ fibres, the role of MrgprD$^+$ neurons as components of cold and noxious heat sensitivity, respectively, emerges (Pogorzala, Mishra, and Hoon 2013). In relation to the MrgprD receptor, it has been proposed that it participates in mechanical pain and cold allodynia in neuropathic pain conditions (C. Wang et al. 2019). Moreover, it has been shown that β-alanine produces itch sensations in both mice and humans (Klein et al. 2021; Wooten et al. 2014).

2.2. Central nervous transmission of sensory information

Transmission of sensory information: spinal cord pathways

As said, primary sensory neurons project their central terminals to the spinal cord (SC). Most of primary sensory neurons are excitatory glutamatergic neurons and make synapsis with second order projection neurons in the dorsal horn of the spinal cord. Some populations of primary sensory neurons also release peptides in the synapses: peptidergic nociceptors, for example, can release substance P and the calcitonin gene related peptide – CGRP, but other neuropeptides can also be released by non-peptidergic nociceptors.

The dorsal horn of the spinal cord is organised anatomically and electrophysiologically into six cellular and laminaes (from I to VI). Each laminae contains specific populations of second order neurons that receive input from specific populations of primary sensory neurons. In a simplified scheme, most C and Aδ fibres carrying thermal and nociceptive information innervate laminaes I and II, Aβ- -LTMR innervate laminaes III to V, and lamina V receive convergent stimuli from Aβ, Aδ and C fibres. Some primary sensory neurons innervating viscera project to laminaes of the ventral horn of the SC. Second order neurons are classified according to the laminae that they innervate and often maintain selectivity for stimuli in a similar manner as primary sensory neurons (see Chapter 2.3 for an example on temperature coding). Second order neurons are also called projection neurons as their axons organise into tracts to transmit sensory information to higher order areas in the CNS (Basbaum et al. 2009; Häring et al. 2018; Kandel et al. 2021; Ma 2010; Ran and Chen 2019).

The SC is an important centre for sensory modulation. The majority of the neurons of the dorsal horn are interneurons, which are a very diverse population of neurons that can be excitatory or inhibitory. Moreover, SC glial cells and neurons from higher areas of the CNS that project their axons to the SC, also modulate the activity of second order neurons.

Some sensory input can activate the reflex arc, which initiates a response before higher centres process the information thanks to direct synapses of sensory neurons with effector neurons or interneurons that connect with other effector neurons in the SC. In most of the cases, this process has protective or regulatory functions (for example, closing your eyes when something is touching them) (Kandel et al. 2021).

Somatosensation in the brain: higher ascending pathways

Second order neurons project into higher areas of the CNS grouped in ascending pathways. Simplifying, the main ascending pathways are the spinothalamic tract, which projects to the thalamus and typically transmit descriptive information about the location or the type of stimuli, and the spinoreticulothalamic tract, which projects to different areas of the brainstem and typically transmit painful information. Most of the information arriving to the thalamus is then transmitted to the somatosensory cortex, which is mainly associated to sensory discrimination. On the other way, most of the information arriving to the brainstem is transmitted to different areas more related to the emotional processing to the sensory information, including the amygdala, the cingulate gyrus and the insular cortex (**Figure 5**).

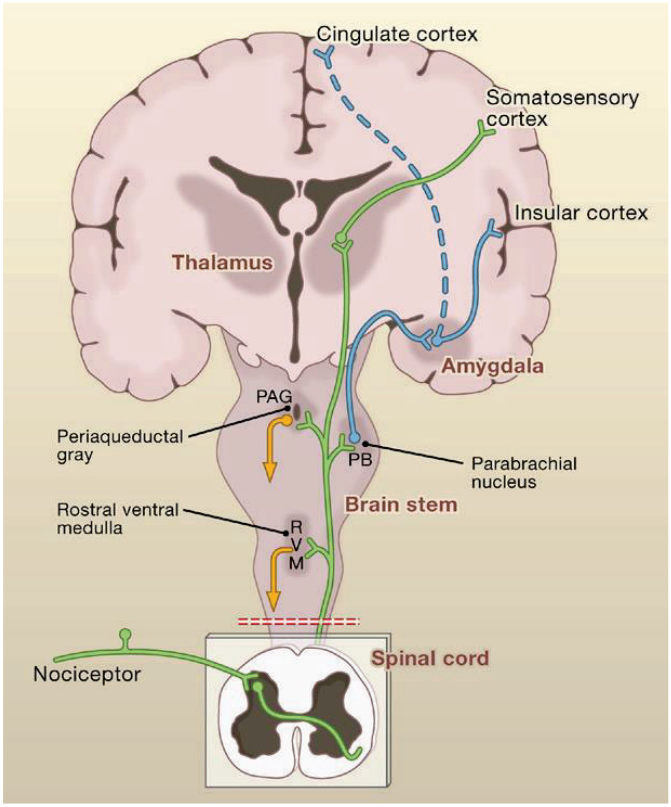

Figure 5. High brain areas involved in the processing of pain. *Primary sensory neurons make synapses in the dorsal root of the spinal cord with second order neurons. Second order neurons group mainly into the spinothalamic and spinoreticulothalamic tracts. Information from these tracts terminate mainly in the somatosensory cortex and in emotional areas of the brain, respectively, in order to correctly perceive and respond to the pain stimuli. Obtained from* (Basbaum et al. 2009).

As mentioned, sensory perception is a complex system and requires the coordination of multiple areas. When a noxious stimuli is processed, for example, several brain areas involved in both the sensory and emotional components of pain are activated in a coordinated manner. The activation of the circuits of the somatosensory system can result, then, in both autonomic physiological responses and voluntary behaviours (Basbaum et al. 2009; Kandel et al. 2021; Lindsay et al. 2021; Xiao and Xu 2020).

2.3. Temperature coding

For years, the strategy of the somatosensory system to code distinct sensory modalities in a way that allows their differentiation in the brain processing has been under debate. Two main theories were disputed. The defenders of the specificity theory provided evidence suggesting that each sensory modality is processed in a maintained labelled line from primary sensory neurons to the brain circuits. On the other side, the defenders of the pattern theory had proofs consistent with specific sensations being generated in the brain by the combination of

inputs initiated by different sensory neurons. This debate was also present in the study of temperature discrimination. Considering the data presented in the introduction until here, it may be deduced that both theories are true and combinable, and this is the reality. In fact, the more accepted theory now is that labelled lines exists but is the crosstalk among these lines the phenomenon necessary for sensory discrimination (Ma 2010; F. Wang et al. 2018).

We perceive as noxious temperatures below 15 ºC. For years, different studies have shown that primates are more capable to distinguish temperatures in the innocuous cold range than in the noxious cold range. Those discoveries suggested that different circuits might be activated by different temperatures, which required different adaptative responses, supporting the labelled line theory (Chen, Rainville, and Bushnell 1996; Rainville, Chen, and Bushnell 1999; Yarmolinsky et al. 2016). In fact, as shown in Chapter 2.1, different populations of primary sensory neurons respond to different ranges of temperature. Other experiments, however, found that signals from different neuronal populations activated by similar ranges of temperature interact to create the perception of different temperatures (accurately reviewed in Ma 2010; Xiao and Xu 2020).

Oppositely to the described perception of heat temperatures, recent studies proposed that both DRG primary sensory neurons and second order neurons responded to cold in a graded manner. This means that cold-sensitive neurons are more sensitive to decreases in temperature than to absolute temperatures, although they are not activated over a threshold temperature. This way, in *in-vivo* calcium experiments, most of cold-sensitive primary and second order neurons peaked at the beginning of a cold stimulation with a peak of an amplitude independent of the temperature, and rapidly adapted to the change of temperature. It is also proposed that, using a different mechanism, sensory neurons are activated at discrete temperatures in the noxious range. In fact, Yarmolinsky et al. 2016 found that, apart from the non-noxious cold-adapting primary sensory neurons, small subsets of TG neurons responded to noxious cold temperatures in a sustained manner or showing a combination of both responses (Ran and Chen 2019; Wang et al. 2018; Yarmolinsky et al. 2016).

2.4. Sex, gender and sensory perception

In clinics, many types of chronic pain, including osteoarthritis, cancer pain, low back pain, neuropathic pain, migraine or fibromyalgia, are more prevalent in woman than in man. Moreover, some types of chronic pain, including back pain, osteoarthritic pain and abdominal pain are perceived as more intense by woman, and cancer pain and musculoskeletal pain trigger depression as a secondary effect in more woman than man. In physiological conditions, woman also present lower thresholds to heat and cold stimuli than man. Moreover, the responsiveness to treatments against chronic pain also variate depending on the sex and gender of the treated people (Abbafati et al. 2020; Fillingim et al. 2009; Jiménez-Trujillo et al. 2019; Litwic et al. 2013; Mogil 2020; Plotnikoff et al. 2015; Racine et al. 2012).

These differences should be studied considering the sex variable, which refers to the biological based differences, and the psychosocial influences, including the gender roles. Briefly, some gender conditions that might influence the increased prevalence of pathological pain conditions in woman include the greater willingness of woman to seek for medical help and to report pain compared to man, among others (Fillingim et al. 2009; Mogil 2020).

The lack of studies in females and in the sex dimorphism in different areas of biology, and especially in neurosciences, is not a novelty. Some factors including misogyny, false beliefs in the greater variability among female animals compared to males, and reduced likelihood of reporting negative results on studies finding no differences between male and female animals, result in a male-biased literature (Fillingim et al. 2009; Mogil 2020).

As reviewed by Mogil 2020, studies in animals have revealed sexual differences in the genetic, neural and neuroimmune mediation of pain and in the processes of pain chronification. A recent study of Tavares-Ferreira et al. 2022 identified 66 proteins differentially expressed in the DRGs of male and female mice, including genes involved in cell communication and signalling and a prostaglandin synthase involved in nociception.

3. Primary sensory neurons' sensitivity

As mentioned, primary sensory neurons respond to exogenous stimuli. Specific receptors and ion channels are involved in the depolarisation of neurons' membrane in response to stimuli and, if this depolarisation reaches a threshold, APs are generated and the sensory information

is propagated through the cell. Apart from the sensory transducers (see Chapter 2.1), many other components participate in the capacity of primary sensory neurons to activate second order neurons in the SC. Those components include voltage-gated sodium and potassium channels, which underlie AP generation. Interestingly, different populations of primary sensory neurons express different combinations of voltage-gated channels, which results in different conducting properties (Zheng et al. 2019), and alterations in different subtypes of voltage-gated channels result in alterations of specific sensitivities. For example, inhibitors of the voltage-gated potassium channel Kv1 reduce the sensitivity to cold but do not modulate the sensitivity to mechanical stimuli.

Apart from sensory transducers and voltage-gated channels, other channels participate in the modulation of primary sensory neurons capacity to respond to sensory stimuli by generating APs. It is the case of the family of two-pore domain background potassium channels (K_{2P}), that participate in setting the resting membrane potential (RMP) or countersting depolarising currents.

3.1. Two-pore domain background potassium (K_{2P}) channels

K_{2P} channels are a family of 15 potassium-selective channels encoded by *Kcnk* genes grouped into 6 families according to their sequence, function, and pharmacological similarities. These channels are highly selective for potassium ions and are the main responsible of the potassium outflow currents in the range between RMP and the threshold voltage to fire APs. For this reason, K_{2P} channels have been traditionally named background or *leak* potassium channels.

K_{2P} channels subunits are conformed by four transmembrane domains, two pore domains, and intracellular T- and C-terminal domains. These subunits assemble as dimers forming a pseudotetrameric pore. Recent studies have shown that, contrary to previous theories, K_{2P} channels are sensitive to voltage and chemical gradients through a non-canonical mechanism mediated by the selectivity filter (Schewe et al. 2016). Nevertheless, the members of the K_{2P} family allow potassium currents in a broad range of membrane potentials and are involved in setting or stabilising the RMP, but especially in modulating the excitability, counteracting subthreshold and AP depolarizations, and participating in potassium transport of the cells.

Several members of the K_{2P} family are expressed in sensory ganglia. The properties, patterns of expression and involvement in pain sensing of each of the members of the family are carefully reviewed in (Busserolles, Gasull, and Noël 2018; Enyedi and Czirják 2010).

4. TRESK

TRESK (TWIRK-Related Spinal cord K^+ channel) was the last member of the K_{2P} family of background potassium channels to be identified. It was first isolated from human spinal cord by Sano et al., 2003 and later isolated from mouse testis by Kang et al., 2004. It shows low homology with the other members of the K_{2P} family and, thus, it conforms a subfamily by itself (Sano et al. 2003).

TRESK gene is named *KCNK18* and presents 3 exons and 2 introns. In humans, it is found in the chromosome 10 and its transcription results in a sequence of sequence of 385 amino acids (Sano et al. 2003), while in mice is found in the chromosome 19 and results in a sequence of 394 amino acids, and in rats it is found in the chromosome 1 and results in a sequence of 405 amino acids. Human and mouse orthologs present a 67 % of sequence identity (Czirják, Tóth, and Enyedi 2004; Kang, Mariash, and Kim 2004).

4.1. TRESK structure

Like the other K_{2P} channels, each TRESK channel subunit has four transmembrane domains (T_1-T_4), two pore forming domains (P_1 and P_2), intracellular N- and C-terminals, and an extended extracellular loop between the first transmembrane domain (TM_1) and the first pore domain (P_1). As a particularity out of the other members of the family, TRESK have 2 extracellular N-glycosylation sites, short C- and T-terminal regions, and an extended intracellular loop between the TM_2 and the TM_3 domains (**Figure 6**) (Kang, Mariash, and Kim 2004; Sano et al. 2003). The long intracellular loop sequence is highly conserved among different species and is critical for the regulation of TRESK activity (see below).

TRESK subunits ensemble as homodimers of two identical monomers or as heterodimers with TREK1 or TREK2 subunits. In this chapter we are introducing the electrophysiological properties of TRESK homodimers. The characteristics of heterodimers including the TRESK monomers are a mix of the properties of each subunit (Lengyel et al. 2020; Royal et al. 2019).

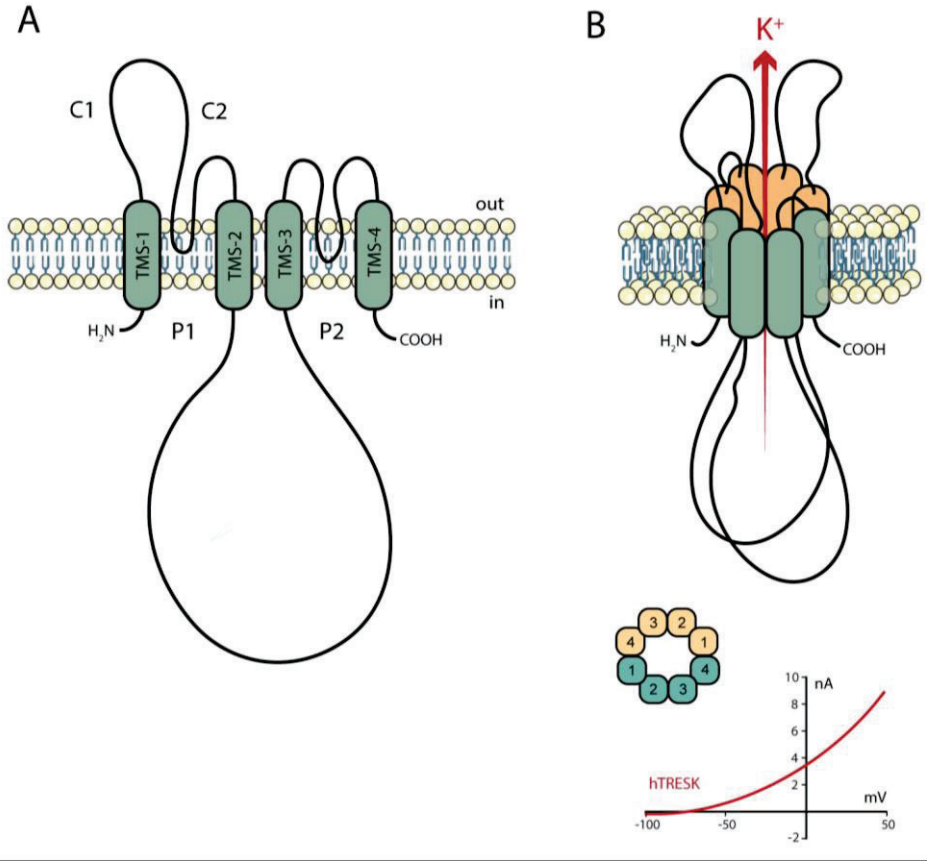

Figure 6. TRESK structure. *TRESK channels are homodimers* ***(b)*** *of two TRESK subunits* ***(a)****, which present four transmembrane domains (TMS), two pore domains (Ps), two extracellular domains (Cs) and a long intracellular loop. Like in other* K_{2P}*s, TRESK potassium currents are outwardly rectifying* ***(b)****. Figure obtained from* (Aida n.d.).

4.2. Electrophysiological properties of TRESK

Electrophysiological and modulating properties of the channel are interestingly reviewed in (Enyedi, Braun, and Czirják 2012; Enyedi and Czirják 2015).

Human, mouse and rat TRESK show similar single-channel behaviours and sensitivity to channel blockers. Like almost all the other K_{2P} channels, TRESK is an outward rectifying channel highly selective for potassium ions. Its single-channel current is low (Kang and Kim 2006; Kang, Mariash, and Kim 2004) and it shows a characteristic opening kinetics, resulting in well-defined, quare wave-like openings in the outward direction and bursts of very short openings in the inward direction (Czirják, Tóth, and Enyedi 2004).

TRESK rapidly activates when stimulated by depolarising stimuli and loose its voltage dependency when activated by specific modulators (Sano et al. 2003; Schewe et al. 2016). Due to these characteristics and the high differences between the intra and extracellular

concentrations of potassium, TRESK is one of the main responsible of the potassium outflux in the cells.

4.3. TRESK expression

Neural tissues

When TRESK was first identified in humans, its RNA expression was localised in the spinal cord and brain (Liu et al. 2004; Sano et al. 2003). Sánchez-Miguel et al., 2013 also found TRESK expression in motor neurons from human spinal cord.

TRESK was also cloned from the cerebellum and testis of mice and its transcript was found in their brain, cerebellum, brainstem and spinal cord (Czirják, Tóth, and Enyedi 2004; Dobler et al. 2007; Kim et al. 2020). W. Huang et al., 2021 found that TRESK transcript expression is especially enriched in the dentate gyrus, CA1 and CA3 of the hippocampus of mice. Immunostainings also show that TRESK is expressed in the dorsal and ventral neurons of the spinal cord of mice (Kim et al. 2020). In a study pointing to other nervous systems, Cadaveira-Mosquera et al., 2012 also found high expression of TRESK transcripts in the neurons but not in the ganglionic satellite cells of the afferent and efferent autonomic ganglia of mice, which was translated into functional effects of TRESK in these neurons.

Yoo et al., 2010 found that TRESK is highly expressed in the dentate gyrus of the hippocampus, the amygdala, the thalamus and in different brain cortex areas including the somatosensory, the motor and the cingulate cortex of rats. They also found moderate expression in the cerebellum and weak expression in other areas of the CNS of rats. Importantly, different studies found TRESK expression in the neurons of the dorsal and ventral horns of the spinal cord of rats. Using immunostainings, it was found that TRESK expression is enhanced in the dorsal horn region of the spinal cord, especially in the superficial lamina I and II and with medium density in the ventral horn (Hwang et al. 2015; Kim et al. 2020; Zhou et al. 2017).

Although, as seen, TRESK was found in the spinal cord and brain of humans, mice and rats, which are also involved in pain and cold perception, its expression is enriched in the sensory ganglia compared to these other areas of the CNS. Guo et al., 2019 found TRESK expression only in the neurons but not in non-neuronal cells of sensory ganglia.

Sensory ganglia and primary sensory neurons

Out of K_{2P}, TRESK is the more expressed and functional abundant channel in the DRG neurons of mice, followed by TREK1, TREK2 and TRAAK channels (Dobler et al. 2007; Kang and Kim 2006; Marsh et al. 2012).

Different studies differ in the selective expression of TRESK among the different neuronal populations of trigeminal and dorsal root ganglia.

On one hand, Dobler et al., 2007 and Guo et al., 2019 found TRESK transcript expression in most of the DRG and TG neurons of all sizes of mice. Moreover, Guo et al., 2019 and Lengyel et al., 2019 also found TRESK currents in important percentages of TG and DRG neurons.

On the other hand, Weir et al., 2019 identified the channel transcript only in selective neuronal populations of TG of mice. They showed that around 50 % of TG neurons of all sizes present the TRESK transcript and that most of them bind to the lectin IB_4, which is characteristic of the non-peptidergic populations of nociceptors. The authors identified expression of the *Kcnk18* transcript in neurons expressing characteristic proteins of the NF1 and NF2 populations of low-threshold mechanoreceptors, and of the NP2, PEP1 and PEP2 populations of nociceptors, which is in line with single-cell sequencing studies identifying *Kcnk18* expression in these populations (**Table 1**) (Jung et al. 2023; Usoskin et al. 2015). Low proportions of neurons with the characteristic markers of the NF3, NF4 and NF5 populations of low-threshold mechanoreceptors and proprioceptors also expressed the *Kcnk18* transcript (Weir et al. 2019).

In DRGs from rats, TRESK transcript was identified mainly in small- and medium-sized neurons (Kang and Kim 2006). Using immunohistochemistry, it was found mainly in small-sized neurons (Yoo et al. 2010). In humans, TRESK is mainly expressed in NP1 and NP2 populations of non-peptidergic nociceptors (**Table 1**) (Jung et al. 2023).

Other tissues and cells

Different studies have found TRESK expression in tissues and cells of the immune system. In mice and rats, TRESK is expressed in the thymus, the spleen and the small intestine (Dobler et al. 2007; Kang, Mariash, and Kim 2004; Kim et al. 2020). Moreover, Sánchez-Miguel et al., 2013 found TRESK expression in mice lymphoblastic T-cells in the lymphocytes in the lymph

nodes but not in the peripheral blood. After spinal cord contusion, TRESK was also found in inflammatory cells of rats (Kim et al. 2020).

In humans, the K_{2P} channel is also expressed in the thymus and in the lymphocytes in the lymph nodes but not in the peripheral blood (Ruck et al. 2022; Sánchez-Miguel et al. 2013). Moreover, TRESK has recently been involved in in the in the differentiation of regulatory T cells in humans (Ruck et al. 2022).

Apart from the immune system, TRESK is expressed in the testis, heart and muscle of murine animals. Moreover, mice present TRESK expression in the ovary, kidney, liver and lung, and rats in the uterus and the placenta (Dobler et al. 2007; Kang, Mariash, and Kim 2004; Kim et al. 2020).

Although its wide expression, knock out experiments have demonstrated that TRESK is not necessary for survival and that its overexpression does not result in dramatic effects in murine animals' behaviour. Moreover, TRESK is not involved in the motor function or in anxiety behaviours in mice (Castellanos et al. 2018, 2020; Chae et al. 2010; Guo et al. 2019; Kim et al. 2020; Pettingill et al. 2019; Ruck et al. 2022; Weir et al. 2019).

4.4. Modulation of TRESK activity

Modulation of TRESK activity by physicochemical stimuli

Detecting physicochemical stimuli gives the cells the capacity to react to their environment. The capacity of a channel that regulates neuronal excitability to respond to environmental stimuli is specially interesting in the complex modulation of the neuronal responses to these stimuli.

Some K_{2P} channels are directly modulated by mechanical stimuli, as it is the case of TRAAK or TREK1 (Brohawn, Su, and MacKinnon 2014), or by thermal stimuli, as it is the case of TREK1, TREK2 and TRAAK channels (Kang, Choe, and Kim 2005). TRESK, by its side, is not sensitive to direct mechanical stimulation, but mechanical deformation of the cell membrane activate its currents in a process probably mediated by conformational changes of the channel (Callejo, Giblin, and Gasull 2013). In a similar way, although TRESK is not thermosensitive (Sano et al. 2003), the thermal dependency of the other K_{2P} channels more expressed in DRG of rats,

makes TRESK the main responsible for background potassium current at room temperature (24 ºC) (Kang, Choe, and Kim 2005; Kang and Kim 2006).

TRESK is also sensitive to inflammation markers, which may participate in the sensitization in inflammatory pain in the peripheral nervous system. TRESK is inhibited by intracellular and extracellular arachidonic acid and by other cytoplasmatic unsaturated fatty acids (Callejo, Giblin, and Gasull 2013; Kang, Mariash, and Kim 2004; Sano et al. 2003), which also modulate the activity of other K_{2P} channels. Moreover, TRESK activity is also modulated by intracellular and extracellular pH. The channel is inhibited at acid pH and activated at basic pH. This process is probably not relevant in physiological conditions in humans, as the modulation is not important in the physiological range of pH, but the murine orthologs of TRESK are inhibited by extracellular acidic pH in the physiological range (Callejo, Giblin, and Gasull 2013; Kang, Mariash, and Kim 2004; Keshavaprasad et al. 2005; Sano et al. 2003).

Modulation of TRESK activity by phosphorylation and protein interactions

In most of K_{2P} channels, the regulation depends on the intracellular C-terminal. However, in TRESK, the principal modulation is in the highly conserved long intracellular loop.

Nevertheless, although the TRESK C-terminal is short (only 29 amino acids), it is critical for the membrane trafficking of the channel (Callejo, Giblin, and Gasull 2013) and participates in the activation of TRESK currents after calcineurin-mediated dephosphorylation of the channel (see below) (Debreczeni et al. 2023). Like in other K_{2P}, N-glycosilation of asparagine amino acids of the extracellular loop is also necessary for the trafficking of the channel to the plasma membrane and its dimerization (Egenberger et al. 2010).

As said, TRESK intracellular loop is one of the main domains responsible for the regulation of TRESK activity. The serine amino acids 264, 274, 276 and 279 (positions of the mouse orthologue) of TRESK intracellular loop are probably phosphorylated constitutively. Phosphorylation of these serine aminoacids inhibit the activity of the channel (Czirják and Enyedi 2010).

Czirják et al., 2004 described that TRESK is activated by intracellular calcium in a fast process dependent on calcineurin **Figure 7**. Among all K_{2P} channels, TRESK is the only channel regulated by intracellular calcium levels. Calcineurin is a calcium and calmodulin-dependent phosphatase that is activated in response to high intracellular calcium levels. When active,

calcineurin dephosphorylates the residues serine 276 and serine 264 of the intracellular loop (positions of the mouse TRESK ortholog), which results in a high and fast increase of the potassium flow through the channel.

In the TRESK mouse orthologue, calcineurin needs to bind to the PQIVID domain of the intracellular loop to dephosphorylate the channel. The homologous calcineurin biding sites in the human orthologue are the PQIIID and LQLP domains. Nevertheless, the lack of interaction with these domains do not completely abolish the calcineurin-mediated activation of TRESK in humans (Czirják and Enyedi 2014).

After dephosphorylation, the return to a phosphorylated state is a slow process mediated by protein kinase A (PKA) and microtubule affinity-regulating kinases (MARK) 1, 2 and 3. PKA phosphorylates the serine residue 264 of the mouse orthologue (serine 252 in the human orthologue) while MARKs phosphorylate the serine aminoacids 264, 274, 276 and 279 of the TRESK mouse orthologue (252, 262, 264 and 267 of the human orthologue) (Braun et al. 2011; Czirják and Enyedi 2010).

Rephosphorylation processes are finely regulated by the adapter protein 14-3-3 and the novel-type isoforms of the Protein Kinase C (PKC). PKCs inhibit the kinases responsible for the phosphorylation of the serine 264 in the TRESK mouse orthologue, thus slowing down the return of the channel to an inactivated state and allowing the dephosphorylation of the serine residue by other phosphatases in a process independent on calcineurin (Pergel et al. 2019). In a similar way, 14-3-3 adapter protein prevents TRESK return to the resting state by inhibiting the kinases responsible for their returning to resting state (probably by inhibiting MARK kinases). Moreover, 14-3-3 can bind to the RSNSCPE motif of the TRESK long intracellular loop when the second serine of the sequence is phosphorylated (serine in the 264 position in the mouse orthologue and in the 252 position in the human orthologue) and maintain the activation effect of calcineurin-dependent dephosphorilation. However, 14-3-3 binding to the RSNSCPE site also increases and maintains the inhibitory effect of phosphorylation in time (Czirják and Enyedi 2010).

Yang et al., 2018 found that calcineurin inactivation results, not only in an increase of TRESK phosphorylation, but also in a decrease in its RNA expression in DRG neurons from rats. In

fact, calcineurin administration in a rat model with decreased TRESK expression results in a rescue of the channel expression (Yang et al. 2018).

The channel resulting of the dimerization of TRESK and TREK2 subunits is also activated through calcineurin (Lengyel et al. 2020).

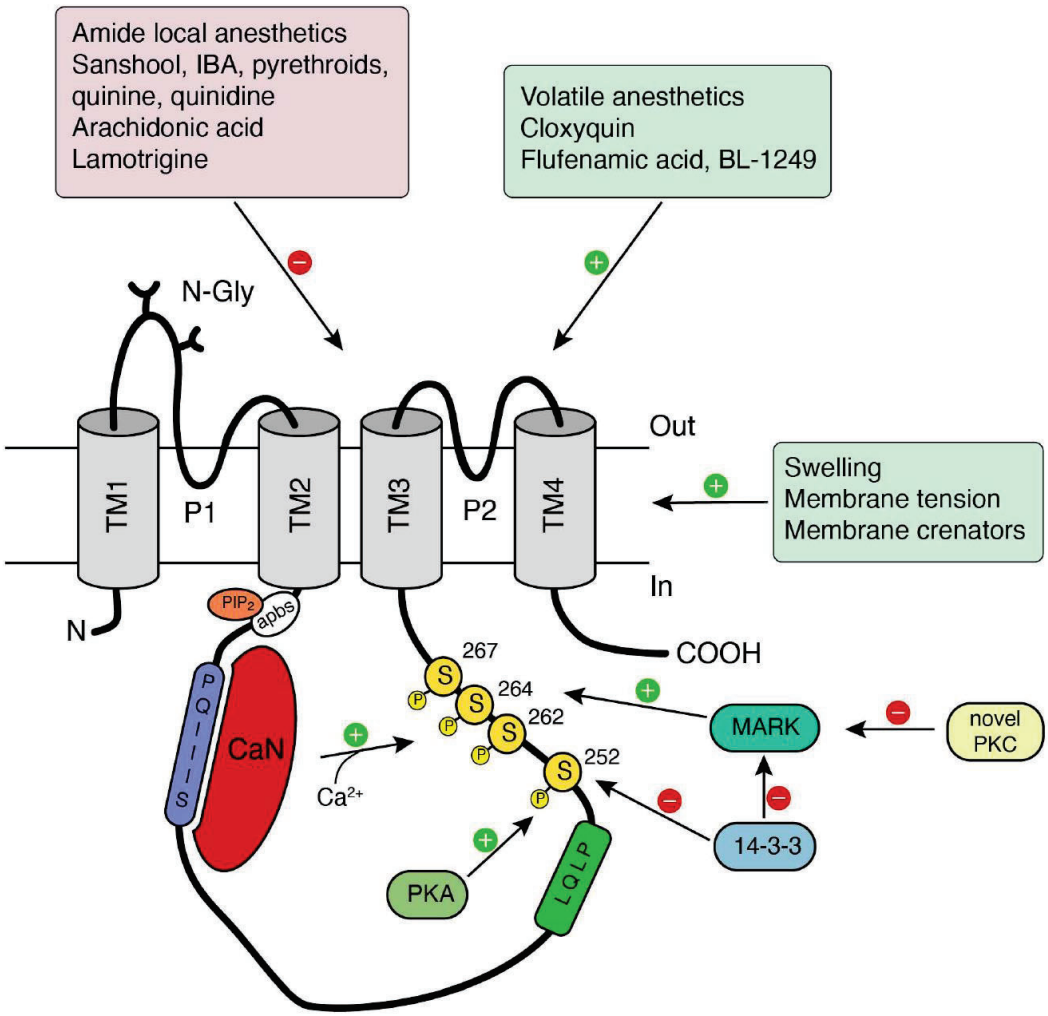

Figure 7. Modulation of TRESK activity by endogenous factors and pharmacologic molecules. *Extracellular and membrane components involved in the activation of TRESK are in green, while the ones involved in the blocking of TRESK are in red. Phosphorylated TRESK is not active. While PKA and MARK contribute to its phosphorylation, calcineurin dephosphorylates the channel. Other proteins such as 14-3-3 or a novel PKC participate in the regulation of this process. Figure obtained from* (Andres-Bilbe et al. 2020).

Pharmacological modulation of TRESK activity

Pharmacological modulation of background potassium channels' activity is compactly reviewed in (Kamuene, Xu, and Plant 2021).

Most of the compounds modulating TRESK activity are not specific for the channel and, thus, its application to distinguish TRESK currents in complex systems or with the intention to target the channel as a possible strategy for treatment are still difficult.

Just a few time after TRESK discovery, Keshavaprasad et al., 2005 and Liu et al., 2004 described its activation by volatile anaesthetics, being this channel the more sensitive member of the K_{2P} family to these compounds. It took more time to identify more specific compounds for TRESK activation. On one side, the antimicrobial drug cloxyquin is a potent slow reversible activator of murine and human TRESK orthologues. It does not modulate the activity of any of the other K_{2P} channels except for the low activation of TASK2. Cloxyquin stabilises an activated state of TRESK receptor in a mechanism independent of the calcium-calcineurin and PKA pathways, and it can further increase human but not mice TRESK activation in its phosphorylated state. (Lengyel et al. 2017; Pettingill et al. 2019; Schreiber et al. 2023; Wright et al. 2013). On the other hand, a recent study identified nitroxoline, a compound with a similar molecular structure to cloxyquin used as an antibiotic to treat urinary tract infections without reported adverse effects, as an activator of human TRESK currents. The molecular mechanisms behind TRESK activation by nitroxoline are still unknown (Ruck et al. 2022).

Like other K_{2P} channels, open TRESK is blocked by extracellular barium cations and inhibited by the zinc cation. However, it is possible to distinguish TRESK from other zinc-sensitive K_{2P} channel because it is insensitive to ruthenium red, which inhibits the other K_{2P} channels. Mouse TRESK is also irreversible inhibited by the cation mercury, which, on the other side, activates other K_{2P} channels. Human TRESK ortholog, however, is not sensitive to zinc and mercury cations (Czirják and Enyedi 2006; Keshavaprasad et al. 2005; Sano et al. 2003).

TRESK is not inhibited by the classical voltage-gated potassium channel blockers 4-aminopyridine, apamin, glybenclamide and TEA. However, it is inhibited by the unspecific potassium channel blockers profanolone, glybidine, quinine, quinidine and triethanolamine, and by the sodium channel blockers lidocaine and bupivacaine. Among sodium channel blockers, TRESK is the only K_{2P} channel inhibited by lamotrigine (Guo and Cao 2014; Kang, Mariash, and Kim 2004; Sano et al. 2003; Tulleuda et al. 2011).

TRESK is also inhibited by the non-selective K_{2P} inhibitors hydroxy-α-sanshool and the isobutylalkenyl amid and by pyrethroids and local anaesthetics, which also have effects in

other K_{2P} channels (Bautista et al. 2008; Castellanos et al. 2018; Kang and Kim 2006; Keshavaprasad et al. 2005; Liu et al. 2004; Sano et al. 2003; Tulleuda et al. 2011).

Finally, the chemically modified derivative of cloxyquin A2764, which specially inhibits calcineurin-activated TRESK, is one of the most selective TRESK inhibitors, although it also inhibits other K_{2P} channels in a lesser extent (Lengyel et al. 2019).

4.5. Physiological and pathological roles of TRESK

Although TRESK is expressed in different tissues (see Chapter 4.2) and recent studies have involved the channel in different functions in the body, here we are going to focus on the role of TRESK in primary sensory neurons in physiological and pathological conditions. TRESK effects on the modulation of the excitability of primary sensory neurons and its pain-related consequences have been nicely reviewed in (Andres-Bilbe et al. 2020).

TRESK in neuronal excitability

TRESK is a significant component of the background potassium currents in DRG neurons, and, as mentioned previously, the more significant at room temperature (Dobler et al. 2007; Kang and Kim 2006).

Here, we review some studies that modulate TRESK expression or activity in primary sensory neurons to study the effects of the channel in neuronal excitability. Although some of the studies differ when evaluating the effects of TRESK in certain parameters involved in neuronal excitability, all of them conclude that this K_{2P} channel is preventing primary sensory neurons from hyperexcitability.

Input resistance (R_{in}) is an electrophysiological indicative of the cellular membrane capacity to retain charges. If many channels are active in a cell, it has lower capacity to retain charges and, thus, its R_{in} is low. Low R_{in} is related to a low capacity of cells to maintain differences in the membrane voltage and, thus, it has been related with decreased neuronal excitability. TRESK depletion results in an increase in the R_{in} of small- and medium-sized DRG neurons and of TG small- but not medium-sized neurons (Castellanos et al. 2020; Guo et al. 2019). The effects of TRESK depletion in the R_{in} of TG neurons is increased in the subpopulation of $TRPM8^{+}$ neurons (Guo et al. 2019). In a similar line, decreased TRESK expression in DRG neurons of rats results in increased R_{in}, while overexpression of the channel in TG and

pyramidal neurons of the hippocampus results in decreased R_{in} (Guo and Cao 2014; W. Huang et al. 2021; Tulleuda et al. 2011).

Another indicator of the excitability of a neuron is its resting membrane potential (RMP). As mentioned in chapter 3.3, some members of the K_{2P} channels are involved in the modulation of this membrane parameter. However, the loss of TRESK expression or function in DRG and TG neurons from mice and in human nociceptors has low effects in their RMP (Castellanos et al. 2020; Pettingill et al. 2019). Restitution of TRESK expression in a neuropathic model of rats, however, results in a recovery of neurons' RMP (Yang et al. 2018).

TRESK channel has a major impact in the range between RMP and AP threshold. In fact, depletion or reduction of TRESK currents results in a decrease in the minimal currents necessary to inject to primary sensory neurons of DRG and TG for them to fire an action potential (rheobase) (Castellanos et al. 2020; Dobler et al. 2007; Guo et al. 2019; Pettingill et al. 2019; Yang et al. 2018). Guo et al., 2019 only found this effect in small- but not in medium-sized neurons from TG. In a similar way, increase of TRESK levels result in increased rheobases in TG neurons and hippocampal pyramidal neurons (Guo and Cao 2014; W. Huang et al. 2021; Pettingill et al. 2019). In a different study, however, Tulleuda et al., 2011 found that the voltage threshold for AP firing of DRG neurons is not reduced after a decrease in TRESK expression.

Not surprisingly given the described effects of TRESK in the neuronal electrophysiological properties, several studies described that TRESK function prevent from disproportionate neuronal firing in response to depolarising stimuli. Decrease or depletion of TRESK expression or function results in an increase in the number of APs fired by DRG neurons from rats and mice and nociceptor-like neurons from humans in response to depolarising currents (Castellanos et al. 2020; Pettingill et al. 2019). Moreover, TRESK overexpression results in a decrease in the number of APs fired by DRG and TG neurons in response to depolarising stimuli (Guo and Cao 2014; Tulleuda et al. 2011; Yang et al. 2018). Studying deeper the effects of TRESK in different populations of primary sensory neurons, Guo et al., 2019 found that peptidergic small neurons from TG, and especially $TRPM8^+$ neurons, fire more APs in response to depolarising currents when they lack the K_{2P} channel, an effect that is not found in non-peptidergic small-neurons or medium-sized neurons. Only one of the reviewed studies describes spontaneous AP firing in neurons lacking TRESK (Guo et al. 2019).

As a potassium channel activated at depolarised potential, TRESK also participates in the modulation of the characteristics of the APs fired by sensory neurons, although different studies show variable effects of the channel. On one side, Guo & Cao, 2014 and Guo et al., 2019 described no effects of TRESK depletion or overexpression in the duration and hyperpolarising afterpotential (HAP) of APs fired by TG neurons. On the other side, Dobler et al., 2007 observed that DRG neurons lacking TRESK fired APs with decreased duration, while Castellanos et al., 2020 found that small- and medium-sized DRG neurons without the channel fired APs with increased duration. As TRESK is a member of the *leak* potassium channels family, a decrease in the HAP of APs fired by neurons lacking this current is expected. However, these results were only described in small- and medium-sized DRG neurons (Castellanos et al. 2020), while another study examining the whole population of DRG neurons found that the lack of the channel in neurons result in fired APs with larger HAP (Dobler et al. 2007). These differences might be due to the different composition of ion channels within the different populations of neurons studied on each case (DRG *vs.* TG neurons, and all DRG *vs.* only small- and medium-sized DRG neurons). TRESK does not participate in setting the amplitude of APs fired by DRG and TG neurons (Castellanos et al. 2020; Dobler et al. 2007; Guo et al. 2019; Guo and Cao 2014).

Summing everything up, we can conclude that TRESK is protecting from neuronal hyperexcitability DRG and TG primary sensory neurons and pyramidal hippocampal neurons, and that it participates in shaping the APs fired by primary sensory neurons. However, it is also observed that different studies show opposite results in different cases, which might be related to differential expression of the channel or of other channels involved in the same functions in different populations of neurons (see chapters 3.3 and 4.3) (Usoskin et al. 2015).

In fact, intracellular calcium experiments reveal that TRESK modulates differently the responsiveness to different agonists of characteristic receptors of each population of neurons from different tissues. For example, Castellanos et al., 2020 described that TRESK increases the number of DRG $TRPA1^+$ neurons responding to its specific agonist, while it does not modulate the responsiveness of this population of neurons in TG. The same authors described that TRESK is not modulating the responsiveness of $TRPM8^+$ and $TRPV1^+$ DRG and TG neurons to their specific agonists, thus proposing a different role of TRESK in different populations of primary sensory neurons as it was already hypothesised by (Guo et al. 2019), that found

differences in the role of TRESK between small- and medium-sized neurons and in the cold-sensitive population of TRPM8^{+} neurons.

Pointing to this way, a recent study in the laboratory, which is still under review for publication, show that the MrgprA3-expressing population of TG neurons, mainly overlapping with the population of non-peptidergic nociceptors NP2 (Usoskin et al. 2015), show increased excitability identified by shorter time to reach the AP peak and increased firing in response to depolarising stimuli, but not by changes in the RMP, R_{in} or rheobase when lacking TRESK. TRESK does not participate in the characteristics of the APs fired by this population of neurons. (Llimós-Aubach et al. n.d.).

In a similar way, there are differences in the expression of channels involved in neuronal excitability between males and females, and, thus, the role of TRESK in neurons from animals of the different sexes might also vary. However, no studies comparing possible sex differences in the role of TRESK in the neuronal excitability have been published to date.

TRESK in pain models and diseases

Since its isolation from human genome in 2003 (Sano et al. 2003), alterations in TRESK expression and function in primary sensory neurons have been related to sensory misfunction and nociceptive phenotypes.

Different models of neuropathic pain, including axotomizing injury, spinal nerve ligation and spared nerve injury, curse with a decrease of TRESK expression in sensory ganglia of male rats (Hwang et al. 2015; Tulleuda et al. 2011; Zhou et al. 2013, 2017). In a similar way, Tulleuda et al., 2011 found that dissociating neurons from DRG tissue also result in a decrease in TRESK expression, although experiments using cultures of DRG neurons show that that decrease is not sufficient to completely ablate TRESK currents (Castellanos et al. 2020; Dobler et al. 2007; Guo et al. 2019; Kang and Kim 2006). In a similar fashion, decrease of *Kcnk18* and calcineurin transcript levels with reduced TRESK-like currents in DRG is associated with pain in a rat model of bone metastasis (Yang et al. 2018) and induced-inflammatory pain curses with decreased expression of TRESK, TASK 1, 2 and 3 and THIK2 in DRGs (Marsh et al. 2012). Added to the effects of these models in the TRESK expression in sensory ganglia, inflammatory mediators such as the arachidonic acid or the decreased pH can also reduce TRESK activity (Callejo, Giblin, and Gasull 2013). In this line, Weir et al., 2019 showed that TRESK increased the effects

of the inflammatory sensitisation on the excitability and responsiveness of TG neurons from mice. Moreover, spinal nerve ligation also curses with a reduction of TRESK expression in neurons from the spinal cord (Zhou et al. 2017).

The decrease of TRESK expression and function in sensory ganglia and the spinal cord are related with the pain phenotypes in these models. However, other models of neuropathic pain curse with increases in TRESK expression, probably as a compensating mechanism for the hyperexcitability or malfunction of primary sensory neurons. For example, in a model of spinal cord contusion, rats showed increased TRESK expression in DRGs, in the neurons of the dorsal and ventral horn of the spinal cord and in inflammatory cells (Kim et al. 2020). Contrary to the previous presented study of Zhou et al., 2017, Hwang et al., 2015 found that spinal nerve ligation in male rats increase TRESK expression in the neurons of the dorsal horn of the spinal cord. As expected, in other models, TRESK expression did not vary in the course of inflammation pain (Marsh et al. 2012).

Apart from animal models, TRESK misfunction has been associated with a high spectrum of pain-associated diseases.

Different loss-of-function mutations affecting the human *KCNK18* gene have been linked to migraine with aura, although other mutations resulting in inactivation of the channel are also found in humans without migraine pathology. The F139WfsX24 mutation in the *KCNK18* human gene is associated with migraine with aura with an autosomal dominant heritage. The expression of the mutated subunit results in a premature truncation of the TRESK subunit. This frameshift mutation is especially interesting because, apart from the decrease of channel function related to an increase in the nociceptor's excitability, one of the resulting aminoacids sequences is capable to retain TRESK, TREK1 and TREK2 in the neuronal cytoplasm (Lafrenière et al. 2010; Pettingill et al. 2019; Royal et al. 2019).

Single amino acids substitutions in crucial domains of the TRESK channel have also been related to alteration of various nervous system functions. For example, the mutation W101R, which is near the selectivity filter of TRESK and impairs the channel function, has been related with intellectual disability and migraine with aura with a dominant negative inheritance (Han et al. 2018; Imbrici et al. 2020). On the other side, the biallelic missense variants Y163D and S252L, that affect the calcineurin-dependent modulation of the human TRESK, have been

related with intellectual disability, seizures and autism spectrum disorder (Pavinato et al. 2021).

Some drugs produce severe pain as a side effect through still unknown mechanisms. TRESK has been proposed as a possible secondary target for these drugs and, thus, as a possible mediator of the noxious side effects of the treatments.

On one side, the chemotherapeutic drug cisplatin can provoke the development of the cisplatin chemotherapy-induced peripheral neuropathy, which curses with chronic pain and thermal and tactile allodynia and hyperalgesia. Finno et al., 2022 propose that the neuropathic effects of the drug might be mediated by TRESK in the TH population of C-low threshold mechanoreceptors of DRG, where the channel is expressed (Usoskin et al. 2015; Weir et al. 2019), as they found that the drug effects are carried by targeting outward potassium currents.

On the other side, calcineurin inhibitors such as cyclosporine A and Tacrolimus (FK506) are immunomodulatory drugs used after organ transplantations and to treat atopic dermatitis, autoimmune and inflammatory diseases. A rarely secondary complication of these drugs is the development of the Cacineurin-Inhibitor Pain Syndrome (CIPS), which is characterized by severe pain in the lower limbs and bone affectation, and that can be reversed by stopping the treatment with the calcineurin inhibitor or by using calcium channels blockers (Grotz et al. 2001; Wei et al. 2018). It is proposed that CIPS effects are mediated by the dysregulation of the calcineurin effects in the neuronal excitability and the vascular tone regulation (Prommer 2012). As TRESK is activated in a calcium-dependent manner by calcineurin, is expressed in nociceptors, and reduction of its currents result in nociceptors' increased excitability, some authors have hypothesised that the infrequent effects of calcineurin inhibitors in sensitivity might be mediated in part by TRESK inactivation (Y. Huang et al. 2020; Prommer 2012; Smith 2009).

Some studies in mice report that cyclosporine A or Tacrolimus intraperitoneal treatment induces heat and mechanical hyperalgesia (Y. Huang et al. 2020; Sato et al. 2007; Yang et al. 2018) and that intraplantar injection of Tacrolimus induces nocifensive behaviours in mice (Kita et al. 2019). However, systemic Tacrolimus is also used as a neuroenhancing therapy that accelerates axon growth and improve functional recovery after neuropathic injury. Some

authors found that Tacrolimus treatment in different models of neuropathic pain in rat ameliorates the mechanical, heat and cold hypersensitivity characteristic of the models in a dose-dependent manner (Muthuraman and Sood 2014; Voda, Hama, and Sagen 2007). Jo et al. 2019, however, found that subcutaneous Tacrolimus injections in rats after tibial nerve transection do not ameliorate their cold allodynia.

Arcas et al., 2019 and Kita et al., 2019 found that the calcineurin inhibitor Tacrolimus activates some $TRPM8^{+}$ and almost a half of $TRPA1^{+}$ DRG primary sensory neurons and that $TRPA1^{-/-}$ mice show no Tacrolimus-induced nocifensive behaviours. On the other side, preliminary results in our laboratory show that Tacrolimus at lower concentrations does not activate DRG primary sensory neurons *per se* and that preincubation of these neurons with the calcineurin inhibitor does not modify the number of $TRPA1^{+}$ and $TRPV1^{+}$ neurons that respond to the specific receptors' agonists. However, there is a tendence for more DRG neurons to respond to β-alanine after preincubation with Tacrolimus (Eriksson and Gasull Casanova 2019). The effects of Tacrolimus on the DRG neurons that potentially express TRESK (Usoskin et al. 2015) leaves a door open for studying possible TRESK-mediated effects in CIPS.

The role of TRESK in other systems apart from the somatosensory system is a field lowly explored. Recent studies, however, have revealed TRESK as a mechanism activated in the neurons of the CNS to compensate for hyperexcitation induced by pathological conditions. Thus, it has been shown that epileptic seizures result in increased TRESK transcript expression, which has been proposed as an intrinsic protective mechanism to avoid seizures' aggravation (W. Huang et al. 2021).

TRESK has also been revealed as a potent mechanism to prevent photophobia in people suffering from migraine (Weir et al. 2019) and to prevent from excitotoxic-induced brain damage and neuroinflammation in a model of neonatal brain injury in rats (Dilek et al. 2021).

TRESK in somatosensation

Due to the expression of TRESK in primary sensory neurons and other neurons of the somatosensory system, its effects in regulating their neuronal excitability, and its relationship with different pain-related models and diseases, several studies have focused on studying the function of TRESK in sensory perception, especially in pain and nociception. Using animal

models, several studies found that TRESK is involved in chemical, mechanical, thermal (both heat and cold) and itch sensing.

Treating mice with the inhibitor of TREK1, TREK2 and TRESK isobutylalkenyl amide result in nocifensive behaviours and increased plantar mechanical sensitivity in mice (Tulleuda et al. 2011). In a similar way, decreased TRESK expression in a rat model with bone metastasis or in TRESK knock-down rats directly correlate with increase in spontaneous pain, that is recovered after TRESK overexpression (Yang et al. 2018). TRESK KO studies also allowed to discard a role for TRESK in the prevention of visceral pain (Guo et al. 2019) but showed that the channel prevents from hypertonic stimuli-induced pain (Castellanos et al. 2020).

To study the role of TRESK in the sensory perception mediated by different groups of primary sensory neurons, different studies injected the TRPA1 and TRPV1 specific agonists AITC and capsaicin to the paw or check of WT and TRESK KO mice and evaluated their responses. The previously presented study from Castellanos et al., 2020 described that TRESK does not modify the number of DRG and TG neurons responsive to capsaicin and of the TG neurons responsive to AITC but that, contrary to what would be expected, the channel activity increases the number of DRG neurons responding to AITC. At the behavioural level, it was found that TRESK protects from mice's nociception induced by capsaicin injection to the cheek or paw but decreases the nociception induced by AITC injection to the paw (Castellanos et al. 2020; Guo et al. 2019).

Different studies using murine models present opposite results regarding the role of TRESK in preventing punctate mechanical and heat hypersensitivity or allodynia (**Table 2**). Most of the studies agree on the role of TRESK in preventing mechanical punctate allodynia, which is more related to nociception than other stimuli, in both the DRG- and TG-mediated sensitivities. Some of the differences between studies might be explained by the role of TRESK in preventing mice responses to light touch and dynamic mechanical stimuli (Weir et al. 2019), as some punctate mechanical stimuli can activate the C-low threshold mechanoreceptors involved in tactile sensitivity and that also express TRESK (Deuis, Dvorakova, and Vetter 2017; Usoskin et al. 2015). There is more controverse regarding the effects of TRESK in heat sensitivity. Some authors argue that the channel protects mice from heat sensitivity while others show that is only involved in TG-mediated heat sensitivity in female mice (Guo et al. 2019), in noxious heat sensitivity (Weir et al. 2019), or is no involved in the murine animals'

heat sensitivity. Differences between the results regarding the role of TRESK in punctate mechanical and heat sensitivity may also be explained by differences in the specie, strain, sex or age of the animals used, by different housing and environmental conditions, by variability between researchers' performing, by limitations of the techniques used, or by other possible uncontrolled factors (Mogil 2017; Sadler, Mogil, and Stucky 2022).

Recent studies show that TRESK prevents mice from cold hypersensitivity. While Guo et al., 2019 showed that TRESK expression did not modify mice plantar but increased facial cold sensitivity, Castellanos et al., 2020 found that that TRESK depletion result in an increase in the DRG-mediated cold sensitivity of mice. Nevertheless, the number of saphenous C-fibres responsive to cold and the temperature threshold at which they are activated does not depend on TRESK expression, although the responsiveness of the cold-sensitive fibres to other stimuli changes depending on TRESK (Castellanos et al. 2020).

Pain and itch share transduction pathways. Non-peptidergic subpopulations of nociceptors NP1 and NP2 are involved in itch sensation (Usoskin et al. 2015). A recent study in a process of review shows that TRESK is involved in the non-histaminergic itch mediated by NP1 and NP2 populations of nociceptors and that the activation of the channel using cloxyquin reduces both acute and chronic itch in mice (Llimós-Aubach et al. n.d.).

Among the studies on TRESK function in nociception, only Guo et al., 2019 and Castellanos et al., 2020 compared the effects of TRESK on the sensitivity of males and females. In these studies, no differences in the role of TRESK in mechanical, heat and cold sensitivity were detected between males and females except for the selective effects of TRESK in preventing eye heat sensitivity only in female mice.

Study	Animals	TRESK model	Punctate mechanical sensitivity	Heat sensitivity
(Chae et al. 2010)	Mice (sex not specified)	TRESK$^{-/-}$		**Increased** heat sensitivity
(Tulleuda et al. 2011)	Rats ♂	TRESK siRNA	**Increased** plantar sensitivity (♂)	**No effects** in heat sensitivity (♂)
(Zhou et al. 2013)	Rats ♂	Overexpression of TRESK to compensate the reduction by spared nerve injury	**Alleviation** of increased plantar sensitivity	TRESK expression **can not ameliorate** the increased heat sensitivity
(Zhou et al. 2017)	Rats ♂			
(Yang et al. 2018)	Rats (sex not specified)	Reduced TRESK expression due to bone metastasis	**Increased** plantar sensitivity	**Increased** heat sensitivity
		Overexpression of TRESK to compensate the reduction by bone metastasis	**Alleviation** of increased plantar sensitivity	TRESK expression **can not ameliorate** the increased heat sensitivity
		TRESK siRNA	**Increased** plantar sensitivity	**Increased** heat sensitivity
(Guo et al. 2019)	Mice ♂♀	TRESK$^{-/-}$	**No effects** in plantar sensitivity **Increased** facial sensitivity (more exaggerated in ♀)	**No effects** in infrared heat and noxious temperatures sensitivity **Increased** eye sensitivity (only ♀)
(Pettingill et al. 2019)	Mice (sex not specified)	TRESK$^{-/-}$	**No effects** in plantar sensitivity	**No effects** in heat sensitivity
		Cloxyquin treatment in a model of migraine	**Alleviation** of plantar hypersensitivity	TRESK expression **can not ameliorate** heat hypersensitivity
(Weir et al. 2019)	Mice ♂♀	TRESK$^{-/-}$	**No effects** in plantar sensitivity	**No effects** to infrared heat sensitivity **Increased** sensitivity to noxious temperatures
(Kim et al. 2020)	Mice ♂♀	Trasgenic overexpression of TRESK in a model of spinal cord injury	**Alleviation** of increased plantar sensitivity	
(Castellanos et al. 2020)	Mice ♂	TRESK$^{-/-}$	**Increase** in the number of saphenous C-fibers activated at lower thresholds (♂)	**No effects** in the number of saphenous C-fibers activated or the threshold for activation (♂)
	Mice ♂♀	TRESK$^{-/-}$	**Increased** plantar sensitivity (♂ and ♀)	**No effects** in infrared heat and noxious temperatures sensitivity (♂ and ♀)
		Model of neuropathic pain	TRESK expression **can not ameliorate** the increased plantar sensitivity	TRESK expression **can not ameliorate** the increased heat sensitivity

Table 2. Role of TRESK in the mechanical and thermal sensitivity of rodents. *Results of behavioural studies in rodents with increased, decreased or depleted TRESK expression.*

Hypothesis

The role of TRESK in chronic pain and in the modulation of mechanical, thermal and pruritic sensitivity, together with its selective expression in nociceptors and low-threshold mechanoreceptors, leads to the **hypothesis that TRESK regulates the activation and excitability of specific populations of nociceptors, which results in the modulation of pain and cold sensitivities.**

Objectives

From this hypothesis, we proposed to study the participation of TRESK in the regulation of the excitability and responsiveness of specific populations of nociceptors and cold-sensitive primary sensory neurons and its function in mechanical and thermal sensitivity of mice through the following specific objectives:

1. Validation of TRESK effects in physiological mechanical and thermal sensitivities.
2. Determination of the TRESK role in mechanical and thermal sensitivities in models of inflammatory and calcineurin inhibitor-induced pain.
3. Study of the TRESK role in the modulation of the neuronal excitability and responsiveness of specific populations of nociceptors and cold-sensitive primary sensory neurons.
4. Identification of possible sex differences in TRESK-involving modulation of chemical, mechanical and thermal sensitivities of primary sensory neurons and mice.

Methods

Animals

All experimental procedures were conducted in strict adherence to the recommendations of the International Association for the Study of Pain (IASP) and were approved by the Animal Care Committee of the University of Barcelona and the Department of the Environment of the Generalitat de Catalunya, Catalonia, Spain.

Female and male C57BL/6N mice, aged between 8 and 20 weeks, were utilised in all experimental procedures. TRESK (*Kcnk18*) knockout mice (KO) and their wild-type (WT) littermates were sourced from the Knock-Out Mouse Project (KOMP) Repository at the University of California, Davis, USA. The TRESK KO mouse was engineered by replacing the complete Kcnk18 gene from chromosome 19 with a ZEN-UB1 cassette via homologous recombination following VelociGene's KOMP Definitive Null Allele Design. TRESK KO mice showed no significant neurological or physical alterations.

Mice were housed at temperatures between 20 and 24 ºC, maintained under a 12-hour alternating light and dark cycle, and provided with free access to food and water. Experimental procedures included behavioural studies and chronic pain induction, with efforts made to minimize animals' discomfort and stress-induced variability.

MrgprD-Cre TdTomato mouse line

The transgenic MrgprD$^{Cre/TdTomato}$ mice, in which MrgprD-expressing cells show red fluorescence, were obtained by crossing transgenic MrgprD^{Cre} animals (Mrgprd$^{tm1.1(Cre)And}$), kindly provided by Dr. Mark Zylka (University of North Carolina at Chapel Hill), with Cre-dependent TdTomato reporter line animals (B6.Cg-Gt*(ROSA)26Sor*$^{tm14(GAG-tdTomato)Hze}$/J, here named ROSA^{TdTomato}). MrgprD^{Cre} was generated by replacing the sequence of the *Mrgprd* gene by the sequence of the Cre recombinase gene after the Mrgprd promotor (Rau et al. 2009). The Cre-reporter line ROSA^{TdTomato} was obtained by inserting the TdTomato gene sequence preceded by a loxP-flanked STOP cassette in the *Gt(ROSA)26Sor* locus to prevent the constitutive expression of the fluorescent marker in absence of the Cre recombinase.

The MrgprD$^{Cre/TdTomato}$ mice line was then crossed with TRESK KO mice to obtain MrgprD$^{Cre/TdTomato/TRESK+/-}$ mice. We further crossed MrgprD$^{Cre/TdTomato/TRESK+/-}$ offspring to obtain MrgprD$^{Cre/TdTomato/TRESK-/-}$ mice without TRESK expression.

We used mice with MrgprD and Cre in heterozygosis to maintain MrgprD function and fluorescent marking of the MrgprD-expressing cells. Both animals with TdTomato gene in heterozygosis and homozygosis were used. We compared the electrophysiological recordings of fluorescent primary sensory neurons of primary cultures from MrgprD$^{Cre/TdTomato}$ and MrgprD$^{Cre/TdTomato/TRESK-/-}$ mice to understand the role of TRESK in MrgprD-expressing neurons.

Genotyping

Animals were weaned, separated, and identified by ear punching at 3 weeks of age. Genomic DNA was isolated from ear snip samples incubated in a solution containing 25mM NaOH and 0.2 mM EDTA (pH 12) at 95ºC during 30 minutes, following neutralization with 40 mM Tris-HCl solution at pH 5. The isolated DNA underwent Polymerase Chain Reaction (PCR) amplification with specific primers for the *Kcnk18* gene and the cassette sequence replacing the gene in KO mice (ZEN-UB1). For the MrgprD$^{Cre/TdTomato}$ mice, PCR was also done with specific primers for the Cre sequence, the ROSA site, and the modified ROSA site (TdTomato, **Table 3**). The PCR mixture consisted of 9 µL of DNA sample, 10 µL Master Mix (Thermo Scientific; Ref. K0171) and 0.5 µL forward and reverse primers (20 µM), obtaining a final volume of 20 µL.

Target sequence	**Primers** (5' – 3') Forward (F) and Reverse (R)	**Annealing step**	**Resulting band**
***Kcnk18* gene**	*Reg-Kcnk18-wt-F*: GGAGAACCCTGAGTTGAAGAAGTTCC *Reg-Kcnk18-wt-R*: GGCTCTAACTTTCCTCACTGCACC	57 ºC – 30 s	252 bp
ZEN-UB1 casette	*Reg-Neo-F*: GCAGCCTCTGTTCCACATACACTTCA *Gene-specific-R*: AGACTTCTCCCAGGTAACAACTCTGC	58 ºC – 1 min	625 bp
Cre	*Cre-F*: CAGAGACGGAAATCCATCGC *Cre-R*: GGTGCAAGTTGAATAACCGG	53 ºC – 30 s (extension 72 ºC 30 s)	500 bp
ROSA (WT)	*Gt(ROSA)-wt-F:* GGCATTAAAGCAGCGTATCC *Gt(ROSA)-wt-R:* CTGTTCCTGTACGGCATGG	58 ºC – 1 min	297 bp
Modified ROSA	*Gt(ROSA)-mut-F:* AAGGGAGCTGCAGTGGAGTA *Gt(ROSA)-mut-R:* CCGAAAATCTGTGGGAAGTC	58 ºC – 1 min	196 bp

Table 3. Characteristics of the PCR amplification of each target sequence. *Primers (forward – F, and reverse – R), temperature and time of the annealing step, and number of base pairs (bp) of the resulting band.*

PCR amplifications were obtained with the following program: initial denaturation of 3 minutes at 95 ºC, followed by 35 cycles of 95 ºC for 30 s, the annealing step (different for each sequence, **Table 3**), and 72 ºC for 40 s, with a final extension at 72ºC for 5 min.

PCR products were analysed by electrophoresis in 1% agarose gels and genotypes were identified by depending on the resulting bands size (**Table 3**).

Real-time quantitative PCR

Mouse tissue samples were collected and processed for RNA analysis. RNALater solution and storage at - 20 ºC was utilized for preservation of samples. Total RNA extraction was performed using the Nucleospin RNA kit and its quality and concentration was evaluated using a Nanodrop. Subsequently, first-strand cDNA synthesis was carried out with the SuperScript IV Reverse Transcriptase (Invitrogen, ThermoFisher Scientific).

Quantitative real-time PCR (qPCR) was conducted on an ABI Prism 7300 using the Fast SYBR Green Master mix or TaqMan Universal PCR MasterMix depending on the analysed genes. qPCR included the analysis of melting temperatures of the amplified fragments as a quality control measure for primers' selectivity.

SybrGreen

To evaluate the gene expression of K_{2P} and TRP channels in cDNA from DRGs obtained from all levels of the spinal cord, the qPCR was performed using SybrGreen with gene-specific primers for TRESK, TREK-1, TREK-2, TRAAK, TRPA1, TRPV1, and GAPDH. GAPDH transcripts served as a standard for normalization. The number of cycles to reach the Cycle threshold (Ct) for the target gene was compared with that of GAPDH to obtain ΔCT values.

TaqMan

To evaluate the gene expression of *Kcnk18* in cDNA from the DRGs, TG, spinal cord, cerebellum, brain cortex and hippocampus of WT mice, the qPCR was performed using TaqMan Universal PCR MasterMix with gene-specific primers *Kcnk18* and *Rlp19*. *Rlp19* transcripts served as a standard for normalization. The number of cycles to reach the Ct for *Kcnk18* was compared with that of *Rlp19* to obtain ΔCT values.

RNAscope *in situ* hybridization

To verify that MrgprD and MrgprA3 receptors and the TRESK channel are expressed in the same subpopulations of sensory neurons and to confirm their colocalization, as suggested by various single-cell sequencing studies (Chiu et al. 2014; Jung et al. 2023; Usoskin et al. 2015; Table 1), *in situ* hybridization was performed using the RNAscope technique on fresh frozen sections of TG and DRG. Tissue was extracted from WT mice, embedded in O.C.T. medium (Tissue Tek), rapidly frozen in liquid nitrogen and maintained at – 80 ºC to fix and prevent RNA degradation. Sections of 14 µm were obtained using a cryostat (Leica), placed in pre-labelled microscope slide (SuperFrost, Fisherbrand, Thermo Fisher Scientific) and stored at -80ºC until the *in situ* hybridisation procedure.

Multi-labelling *in situ* hybridization was performed with the RNAscope technology (Advanced Cell Diagnostics (ACD), Newark, CA) according to the manufacturer's instructions. Predesigned probes against *Mrgpra3*, *Mrgprd*, tubulin beta 3 (*Tubb3*), and *Kcnk18* (TRESK) were used. Images were obtained on a Zeiss LSM880 confocal laser-scanning microscope (Jena, Germany). ImageJ (NIH, Bethesda, MD) was used to analyse images and to determine soma size.

Primary cultures of DRG sensory neurons

Mice were euthanized under isoflurane anaesthesia, and sensory ganglia were dissected, including thoracic, lumbar, and cervical DRG. The dissection involved careful removal of DRG, which were then maintained in cold Mg^{2+}/Ca^{2+}-free PBS (Sigma, Madrid) supplemented with glucose, HEPES, penicillin, and streptomycin. Ganglia underwent chemical dissociation using collagenase CLS I, bovine serum albumin (BSA), and dispase II for 1h and 45 min, followed by mechanical dissociation using 1 mL pippetes.

The resulting cell suspensions were centrifuged, and neurons were resuspended in culture medium containing Dulbecco's Modified Eagle Medium (DMEM) with 10% fetal bovine serum (FBS), penicillin/streptomycin, and L-glutamine. The neurons were plated on glass coverslips pre-treated with poly-L-lysine/laminin and incubated for 1 day in a humidified 5% CO_2 atmosphere at 37ºC.

Electrophysiology (whole-cell recording)

Electrophysiological recordings of fluorescent-labelled MrgprD^{+} DRG neurons from MrgprD$^{Cre/TdTomato}$ mice were conducted, consistent with established protocols (Llimós-Aubach et al. n.d.). The patch-clamp technique was employed with an Axopatch 200B amplifier (Molecular Devices, Union City, CA) and acquired with pClamp 10 software. Patch electrodes, fabricated using a Flaming/Brown micropipette puller P-97 (Sutter Instruments, Novato, CA, USA), had a resistance of 2-3 MΩ when filled with an intracellular solution (in mM): 140 KCl, 2.1 $CaCl_2$, 2.5 $MgCl_2$, 5 EGTA, 10 Hepes, and 2 ATP (pH 7.3). The bath solution comprised (in mM): 145 NaCl, 5 KCl, 2 $CaCl_2$, 2 $MgCl_2$, 10 Hepes, and 5 glucose (pH 7.4). The isotonic solution's osmolality was 311.1 ± 0.9 mOsm kg^{-1}.

Recordings were conducted at room temperature (22-23ºC), 18-24 hours post-dissociation. Sensory neuron excitability was studied by switching the amplifier to current-clamp bridge mode after achieving the whole-cell configuration in the patch clamp technique. Parameters assessed included membrane capacitance (C_m), resting membrane potential (RMP), action potential (AP) rheobase, whole-cell input resistance (R_{in}), AP amplitude, AP duration at 50% of amplitude, and hyperpolarizing afterpotential (HAP). Rheobase was determined with ascending series of 100 ms depolarizing pulses, and neuronal excitability was assessed through various parameters, including the number of spikes during a 500 pA, 1s depolarizing ramp.

Data analysis was performed using Clampfit 10 (Molecular Devices) and Prism 8 (GraphPad Software, Inc., La Jolla, CA).

Intracellular calcium imaging

In this study, cultured DRG neurons from both WT and TRESK KO mice were utilised to investigate intracellular calcium dynamics. The experimental setup involved loading the neurons with 5 µM fura-2/AM for 20-40 minutes at 37ºC in culture medium. Subsequently, coverslips with fura-2/AM-loaded cells were placed in an open flow chamber (0.5 ml) on the stage of an inverted Olympus IX70 microscope equipped with a TILL monochromator for illumination. Imaging was performed using a cooled CCD camera (Orea II-ER, Hamamatsu Photonics, Shizuoka, Japan), and data were analysed with Aquacosmos software on a computer.

The fura-2/AM dye was excited at wavelengths of 340 nm (λ1) or 380 nm (λ2), capturing Ca^{2+}-bound and Ca^{2+}-free forms, respectively, with an emission wavelength of 510 nm. Images were captured every 2 seconds during drug application and calcium concentrations were calculated individually for each cell from the 340 nm to 380 nm fluorescence ratios at each time point. Neurons exhibiting a response >10% of the baseline value and responding to KCl-induced depolarization (50 mM) were included in the analysis. Experiments were conducted at room temperature.

The extracellular bath solution consisted of 140 mM NaCl, 4.3 mM KCl, 1.3 mM $CaCl_2$, 1 mM $MgCl_2$, 10 mM glucose, and 10 mM Hepes (pH 7.4 with NaOH).

Behavioural tests in mice

To mitigate stress-induced variability, mice underwent habituation to the experimental room, the experimenter and setup before testing. Behavioural measurements were conducted in a quiet environment with careful attention to minimizing animal discomfort. All experiments were systematically conducted from 9 am to 2 pm, further enhancing the reliability and reproducibility of the results.

Von Frey “up and down”

Mechanical sensitivity assessments in both WT and TRESK KO mice were conducted using the “up and down” method with calibrated von Frey filaments. Mice were acclimated to the experimental room and habituated to the von Frey setup. The setup included an elevated mesh platform with transparent enclosures and opaque dividers. A battery of 9 calibrated filaments, ranging from 0.04 to 4 grams, were perpendicularly applied to the hind paw, gently pushed to the bending point for 5 seconds. A withdrawal, licking, or flinching of the paw was considered a positive response. The mechanical sensitivity of each animal was expressed as the 50% withdrawal threshold in grams.

Dynamic aesthesiometer

A dynamic plantar aesthesiometer (Ugo Basile, Gemonio, Italy) was employed to evaluate mechanical sensitivity. A von Frey-type 0.5 mm filament was applied with a 10 s ramp (0-7.5 g), and the hind paw withdrawal threshold of mice was automatically recorded.

Von Frey “responses”

Another manual von Frey method to evaluate mechanical sensitivity and to better detect differences between allodynia and hyperalgesia in the plantar mechanical sensitivity of mice is the here called von Frey “responses” technique. In the same manner as in the von Frey “up and down” method, animals were separated in individual small cages in a wire mesh and calibrated von Frey filaments from 0.04 to 4 grams were applied perpendicularly in the centre of their plantar surface of the hind paws and gently pushed to bend for 5 seconds. Here, each filament was applied 5 times within 2 minutes period and mice’s responses were scored for each application following the criteria defined by (Ducourneau et al. 2014). Filaments of progressively incremental forces were applied sequentially.

The number of touch (score of “1”), withdrawal (score of “2”) and nocifensive (score over and including “2”) responses together with the mean score for each force applied were analysed. The mean score considered “noxious” was “1.2”, as filaments were applied 5 times and the first individual score over touch detection was “2”. To analyse the possible hypersensitivity and allodynia of mice, the area over the “1.2” score threshold and under the curve of the mean scores for each sensitivity was calculated for WT and TRESK KO animals, together with the percentage of each type of behaviour in response to each filament.

Hargreaves

In the evaluation of heat sensitivity in mice, the heat plantar test (Hargreaves method, Hargreaves et al., 1988; Ugo Basile, model 37370, Italy) was employed. Mice were individually placed on a glass surface separated by opaque dividers, and an infrared heat stimulus was directed at the plantar surface of the hind paw when all four paws were in contact with the glass surface. The latency time required to elicit nocifensive paw withdrawal was measured using an automatic stopwatch integrated into the apparatus. The infrared intensity was set to 30, with a 20-second cut-off time to prevent burn damage. Each animal's same hindpaw was tested two times, with a minimum of 15 minutes of rest between trials. The final pain parameter was determined as the mean of these measurements.

Plantar cold

To assess noxious cold sensitivity in TRESK KO mice, the cold plantar assay was employed, following the methodology outlined by (Castellanos et al. 2020; Deuis, Dvorakova, and Vetter 2017).

The setup involved placing mice on transparent boxes, separated by opaque dividers in a 1/8-inch thin glass or 1/4-inch thick glass plate. A cold probe, comprising a modified 3 ml syringe filled with freshly powdered dry ice, was used. The powdered dry ice was compressed into a pellet with a flattened surface. The dry ice pellet was applied beneath the glass, ensuring complete contact with the paw. This induced a cooling ramp, leading to withdrawal responses after a few seconds.

Withdrawal latency time was measured in a video using the Avidemus software. The final withdrawal latency time for each animal was the average of three trials, conducted at intervals of at least 15 minutes. A cut-off time of 20 seconds was implemented to prevent potential tissue damage. The methodology ensured a reliable assessment of cold sensitivity in TRESK KO mice, emphasizing the clear identification of withdrawal responses.

Knee-bending test

The knee joint dynamic mechanical sensitivity was evaluated using the Knee-bending test. Previously to experimental days, animals were habituated to manual retention and gently hind paw extension and flexion by the experimenter and experiments were not performed until the animals stayed restrained without struggling.

The experimental day, mice were gently restrained without anaesthesia. The experimenter extended and flexed the hind paws of the animals within physiological ranges and scored their struggling and vocalisation responses (Figure 22A) with a scale scoring with higher values the nocifensive behaviours of higher intensity (see Table methods B). Their responses to five cycles of extension and flexion were recorded and added. As for each cycle there was a process of extension and another of flexion, the maximum score possible adding the five cycles is 20.

Intraplantar β-alanine

To activate MrgprD-expressing DRG neurons innervating the hind paw of mice, 10 µL of β-alanine 50 mM diluted in PBS were injected subcutaneously in the plantar surface of one of their hind paws. Control animals were injected with 10 µL of PBS following the same procedure. Intraplantar injections were done under isoflurane anaesthesia with an insulin syringe of 30G (Becton-Dickinson). Animals' plantar cold and mechanical sensitivity were measured 10, 15 and 25 minutes after the injection.

CFA

Following baseline measurements and brief isoflurane anaesthesia, inflammatory localised pain was induced in mice through the subcutaneous injection 10 µl of Complete Freund's Adjuvant (CFA, Sigma-Aldrich, St Louis, MO, USA; 1 mg/mL) into the hind paw's glabrous skin. The mechanical von Frey threshold and heat withdrawal latency (radiant heat test) were evaluated 1 hour, 5 hours, 1 day, 3 days, 7 days, and 16 days post-injection. Prior to the CFA injection, animals were acclimated to the experimental room, von Frey setup, and the plantar apparatus. Throughout the experiment, inflammation remained localized to the injected paw, ensuring a consistent model for the assessment of inflammatory pain.

Tacrolimus

Immunosuppression in WT and TRESK KO mice was induced by administering a 40 mg of Tacrolimus in an intraperitoneal injection once daily for three consecutive days. Mechanical and thermal sensitivity were evaluated using the aforementioned tests for five consecutive days, commencing prior to the initial injection.

Drugs

Prograf® containing the active ingredient Tacrolimus (TAC) at a concentration of 5mg/1mL was acquired from the hospital pharmacy at Hospital Clinic (Barcelona, Catalonia, Spain). β-alanine (146064), Allyl isothiocyanate (AITC; 377430), and Capsaicin (M2028) were procured from Sigma-Aldrich (Madrid, Spain).

Statistics

Statistical analyses were conducted using GraphPad Prism software, with a significance level set at $p < 0.05$ for all tests. Results are presented as mean ± standard error of mean (SEM) unless otherwise specified.

Unless specified, for behaviour, patch-clamp and amplitude analysis in calcium imaging experiments, statistical differences between groups were assessed through paired or unpaired non-parametric tests (Student T-test). In calcium imaging and *in situ* hybridisation experiments, data was presented as a percentage, and Fisher's exact test was employed for comparisons, unless specified. The normal distribution of data was assessed with a Shapiro-Wilk test when comparing means.

Sample determination

Unless indicated, we used tissues and cells from, at least, 3 males and 3 females per group in expression and electrophysiological experiments. Following good practice guides, we compared the results obtained from males and females of the same experimental groups in these first prospective experiments. If results from males and females from the same group tended to differ, the sample size was increased until reaching, at least, data from 6 males and 6 females per group. If results from males and females were similar, data of animals from both sexes was analysed together and no further experiments were performed. In figures, data from males and females is plotted together unless indicated and the analysed number of cells and animals are indicated with a slash in between (n = cells / animals).

To determine sample size of behavioural experiments, we used previous baseline values for plantar cold, Hargreaves, dynamic aesthesiometer and von Frey “up and down” methods obtained in the laboratory. We extracted the mean and standard deviation from the data and, supposing a Gaussian distribution, we calculated the necessary sample size to obtain possible differences with a significance level of $\alpha = 0.05$ and a potency of $\beta = 0.20$ using the formula $\frac{(SD_1^2 + SD_2^2)(\frac{Z_1-\alpha}{2}+Z_1-\beta)^2}{(\bar{m}_1-\bar{m}_2)^2}$, where $\bar{m}$ are the means for each group (Dell, Holleran, and Ramakrishnan 2002). We had no previous data for the knee-bending test and based the group size in the recommendations of (Pitcher, Sousa-Valente, and Malcangio 2016), although we finally amplified the sample size to get to clearer conclusions from the baseline and

development of osteoarthritis data. Data from cold ramp and von Frey “responses” methods obtained in this Thesis may be used to calculate the sample size necessary to complete the analysis.

Since we did batteries of tests on animals and in all the experiments including treatment baseline values were recorded, we obtained higher sample sizes and baseline measurements for each test were added to the analysis to increase its statistical strength.

Following the good practice guides, first tests of each experiment were performed with half of the calculated sample size with animals of each sex and, as explained for the experiments with tissues and cells, only if tendencies to differ depending on sex were detected, the sample size was increased.

Results

TRESK ablation is not compensated by changes in the expression of other K_{2P} and TRP channels in DRG

TRESK has a prominent role in modulating primary sensory neurons' excitability and mice's mechanical and thermal sensitivity in both physiological conditions and pain models (see Chapter 4.5). However, TRESK is not the only channel regulating primary sensory neurons' excitability. TREK1, TREK2 and TRAAK, other members of the two-pore domain K^+ channels (K_{2P}) family, are also expressed in nociceptors, contribute to background potassium currents, modulate neuronal excitability and are involved in mechanical and heat sensitivity and spontaneous pain (Busserolles, Gasull, and Noël 2018; Enyedi and Czirják 2015).

As we study the role of TRESK using a TRESK knockout (KO) mouse model, we wanted to check whether TRESK deletion in this model is compensated by changes in the expression of the main K_{2P} channels involved in primary sensory neurons excitability and pain perception. Using Real-Time quantitative PCR, we found that the expression of messenger RNA (mRNA) of *Kcnk2* (codifying for TREK1), *Kcnk4* (for TRAAK) and *Kcnk10* (for TREK2) does not change between dorsal root ganglia (DRG) tissue from wild-type (WT) and TRESK KO animals. We also confirmed the absence of *Kcnk18* mRNA (codifying for TRESK) in DRGs from TRESK KO animals (**Figure 8**) and found no differences in the expression of the studied K_{2P} mRNAs between DRGs from males and females.

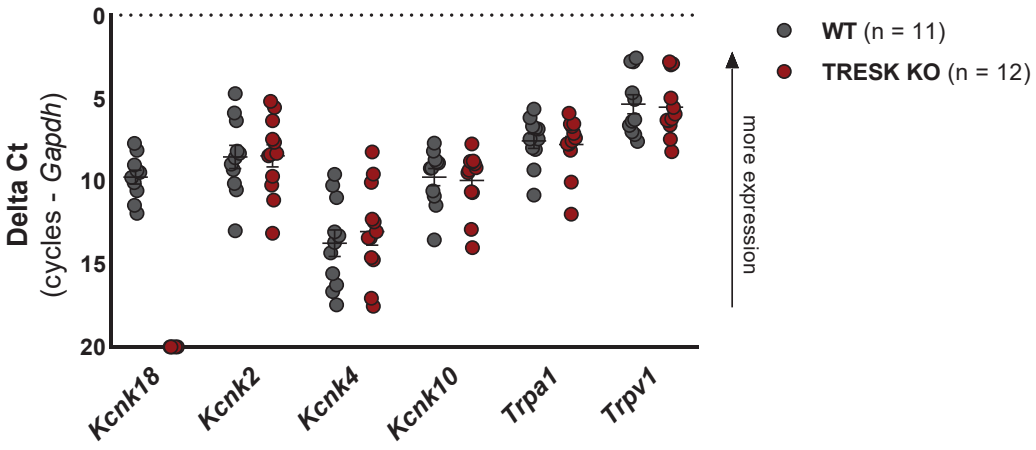

Figure 8. Loss of TRESK does not modify the expression of other K2P and TRP channels in DRGs. *Expression of mRNA coding for TRESK (Kcnk18), TREK1 (Kcnk2), TRAAK (Kcnk4), TREK2 (Kcnk10), TRPA1 and TRPV1 in relation to the reference gene Gapdh. Relative expression shown as Delta Ct, which corresponds to the difference between*

the Real-Time quantitative PCR number of cycles necessary to detect each RNA transcript and the number necessary to detect the Gapdh transcript. The lower the value of Delta Ct, the higher the transcript expression. Single points show relative expression of transcripts from DRGs of different animals (n = 8 WT males, 4 WT females, 8 TRESK KO males and 4 TRESK KO females), lines represent the mean with SEM of each group. As no differences were found between the gene expression in DRGs from males and females, data from animals of the two sexes is plotted together. When no transcript was detected, Delta Ct was arbitrarily assigned a value of 20 only for the purpose of graphing (data not considered for statistical analysis). Comparison of the levels of expression for each transcript between WT and TRESK KO tissues: Mann-Whitney test (p-values: 0.928 for Kcnk2, 0.525 for Kcnk4, 0.740 for Kcnk10, 0.880 for Trpa1, and 0.976 for Trpv1).

TRPA1 and TRPA1 are Transient Receptor Potential (TRP) channels involved in pain processing, and some populations of nociceptors expressing these channels also express TRESK (Chiu et al. 2014; Jung et al. 2023; Usoskin et al. 2015). We tested whether the deletion of the channel in TRESK KO animals induces compensatory changes in the mRNA expression of these TRP channels in DRG. We found no changes in the expression of *Trpa1* or *Trpv1* transcripts when comparing males' and females' or WT and TRESK KO animals' DRG tissues (**Figure 8**).

Kcnk18 is expressed in different tissues of the central and peripheral nervous system

As explained before (Chapter 1), pain sensation and perception are complex processes involving many structures from both the peripheral and central nervous systems (PNS and CNS, respectively). Knowing the expression of TRESK in those structures is important for understanding its role in the whole process of pain perception and predicting possible side effects of using TRESK as a therapeutic target for pain treatment. However, while TRESK expression and function in the DRG and trigeminal ganglia (TG) have been well described, its presence in structures of the CNS of mice such as the spinal cord, cerebellum, brain cortex and hippocampus, has not been well documented yet.

We examined *Kcnk18* transcript levels in the spinal cord, cerebellum, brain cortex and hippocampus without considering specific subregions of those areas. *Kcnk18* mRNA was found in these CNS tissues and confirmed in DRG and TG tissues from WT mice using Real-Time quantitative PCR (**Figure 9**). Expression levels of the gene tend to be higher in the sensory ganglia compared to the other tissues analysed. No differences in *Kcnk18* transcript levels were found between tissues from male and female mice, although the transcripts' expression tends to be lower in the spinal cord of females compared to the obtained from males (**Figure 9**).

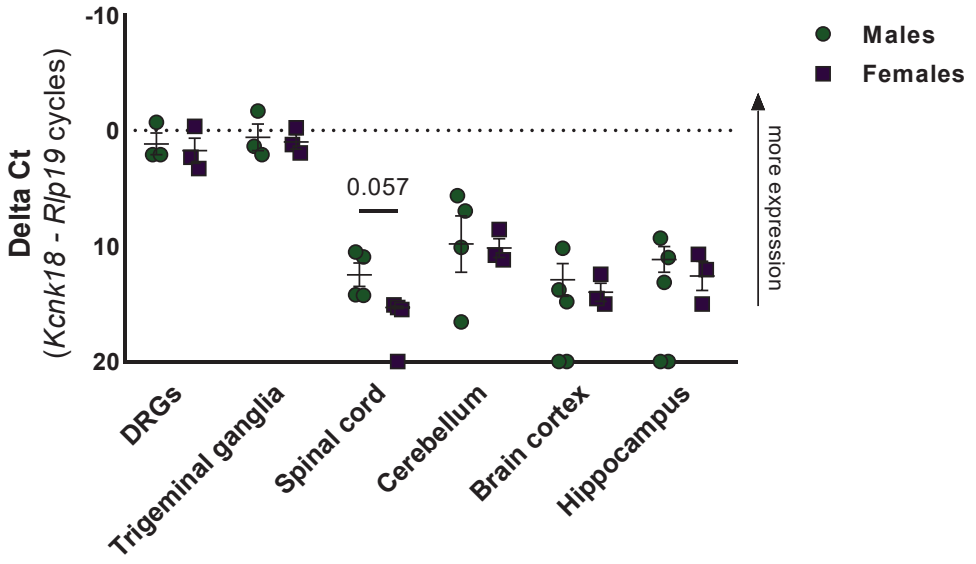

Figure 9. The Kcnk18 transcript is highly expressed in sensory ganglia and also expressed in different CNS structures. *Expression of Kcnk18 mRNA in relation to the expression levels of the reference gene Rlp19 in different PNS and CNS tissues from WT mice. Relative expression shown as Delta Ct, which corresponds to the difference between the Real-Time quantitative PCR number of cycles necessary to detect the Kcnk18 transcript and the number necessary to detect the Rlp19 transcript. The lower the value of Delta Ct, the higher the Kcnk18 expression. Single points show relative expression from tissues of different animals (n = 3 males and 3 females for DRG, TG and spinal cord; n = 4 males and 3 females for cerebellum; n = 5 males and 3 females for cortex and hippocampus), lines represent the mean with SEM of each group. When no Kcnk18 transcript was detected, Delta Ct was arbitrarily assigned a value of 20 only for the purpose of graphing (data not considered for statistical analysis). Comparison of the levels of Kcnk18 expression between tissues obtained from male and female animals: Mann-Whitney test (p-values: 0.057 for spinal cord, 0.400 for DRG, > 0.999 for TG, 0.063 for spinal cord, 0.629 for cerebellum, 0.700 for brain cortex and 0.700 for hippocampus). Comparison of mRNA levels between tissues: Kruskal-Wallis test p-value < 0.0001.*

Kcnk18 is expressed in primary sensory neurons expressing *Mrgprd*

As explained before (Chapter 2.1), single-cell sequencing of primary sensory neurons allowed their classification into different groups according to their gene expression patterns. Most of the defined groups have specific functions and sensitivities. *Kcnk18* transcript expression has been described at some subgroups of non-peptidergic nociceptors of DRG and TG characterized by their expression of the G protein coupled receptor MrgprD (Jung et al. 2023; Usoskin et al. 2015; Yang et al. 2018).

Once we had validated the high expression of *Kcnk18* transcript in sensory ganglia, we wanted to confirm its expression in *Mrgprd*-expressing primary sensory neurons of WT mice using *in situ* hybridization (**Figure 10**). The results shown here are only from tissues of female mice. *Kcnk18* mRNA was detected in 40.1 % of DRG neurons and in 39.3 % of TG neurons. *Mrgprd* transcript was found in 28.4 % of DRG neurons but only in 16 % of TG neurons. 72.1 % and 54.0 % of *Mrgprd*-expressing neurons of DRG and TG, respectively, also presented *Kcnk18*

expression. 48.5 % of *Kcnk18*- expressing DRG neurons and 20.9 % of TG *Kcnk18*- expressing neurons also expressed *Mrgprd* (**Figure 10**).

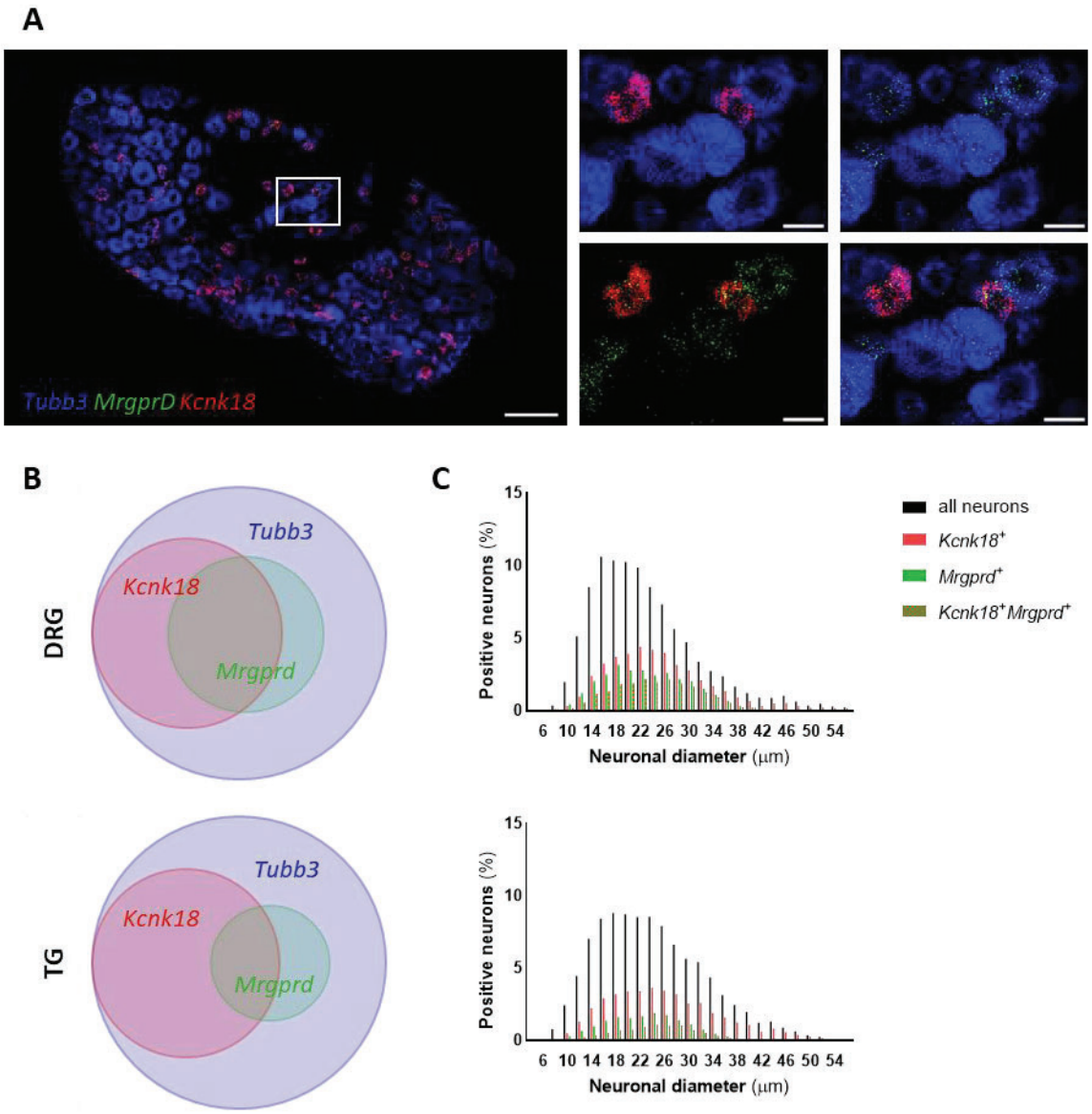

Figure 10. Kcnk18 and Mrgprd transcripts are co-expressed in a population of primary sensory neurons. *Expression of Kcnk18 and Mrgprd transcripts detected by in situ hybridization in DRG and TG tissues from WT mice (n = 5485 DRG neurons and 9378 TG neurons from 3 female mice).* ***(a)*** *Representative image of a DRG stack showing neurons marked with Tubb3 (blue), Kcnk18 (red) and Mrgprd (green). Scale bar of 100 µm in the whole ganglia image. Amplification of a selected area of the entire ganglia showing transcripts' expression in different combinations to facilitate its visualization. Scale bar of 20 µm in amplified images, maintained colour coding.* ***(b)*** *Venn diagrams showing Kcnk18 and Mrgprd co-expression in primary sensory neurons of the DRG (top diagram) and the TG (down diagram).* ***(c)*** *Histograms showing the neuronal size distribution of different subpopulations of sensory neurons, classified according to their expression of Kcnk18 and Mrgprd. Data from DRG neurons (top diagram) and TG neurons (bottom diagram).*

Primary sensory neurons are also classified according to their size and, as explained before (Chapter 2.1), neurons of different sizes have also been related to different sensory functions.

Here, following Herweijer et al. 2014's criteria, neurons with diameter smaller than 19.5 µm are considered small, neurons with diameter larger than 27.5 µm are considered large, and neurons sized in between are considered medium. In DRGs, 40.1 % of analysed neurons were small, 34.7 % medium and 25.2 % of large. In TGs, 34 % of neurons were small, 33.2 % medium and 32.8 % large.

Kcnk18 transcript was found in sensory neurons of all sizes and, compared to all neurons, they were slightly larger (Mann-Whitney test p-value < 0.0001). *Mrgprd* mRNA was also expressed in neurons of all sizes. In DRG, *Mrgprd*-expressing neurons were also slightly larger than the whole population of neurons of these ganglia (Mann-Whitney test p-value: 0.0004). In TG, however, *Mrgprd*-expressing neurons were slightly smaller than the entire population of neurons of the ganglia (Mann-Whitney test p-value: 0.0027). Although *Mrgprd*-expressing neurons of all sizes express *Kcnk18*, in both DRG and TG, neurons expressing both *Mrgprd* and *Kcnk18* transcripts were slightly larger than neurons that only express *Mrgprd* (Mann-Whitney test p-value < 0.0001; **Figure 10**, **Table 4**).

		Neuronal populations			
	neuronal size	**all**	***Mrpgrd*$^{+}$**	***Kcnk18*$^{+}$**	***Mrgprd*$^{+}$ *Kcnk18*$^{+}$**
DRG neurons	**Small**	40.05 %	35.02 %	27.07 %	26.25 %
	Medium	34.73 %	36.75 %	38.86 %	40.75 %
	Large	25.21 %	28.22 %	34.07 %	33 %
	diameter	23.05 ± 0.12 µm	23.17 ± 0.19 µm	25.26 ± 0.18 µm	27.37 ± 0.22 µm
TG neurons	**Small**	34.03 %	33.00 %	27.02 %	24.97 %
	Medium	33.19 %	42.55 %	33.23 %	44.50 %
	Large	32.78 %	24.45 %	39.75 %	30.53 %
	diameter	24.27 ± 0.09 µm	22.89 ± 0.17 µm	26.04 ± 0.15 µm	24.14 ± 0.23 µm

Table 4. Size of neurons expressing Kcnk18 and Mrgprd. *Percentage of small-sized (diameter ≤ 19.5 µm), medium-sized (diameter between 19.5 and 27.5 µm) and large-sized neurons (diameter ≥ 27.5 µm, according to* Herweijer et al. 2014*) and mean ± SEM neuronal diameter of each subpopulation of neurons according to their Kcnk18 and Mrgprd transcripts expression.*

Kcnk18 is expressed in primary sensory neurons expressing *Mrgpra3*

Expression of MrgprA3, another G protein coupled receptor, is also characteristic of different subgroups of non-peptidergic nociceptors involved in pain and itch sensation. Single-cell sequencing studies of DRG neurons identified *Kcnk18* mRNA expression in some of those subpopulations (Jung et al. 2023; Usoskin et al. 2015; Yang et al. 2018). To verify that *Kcnk18* transcripts are found in *Mrgpra3*-expressing neurons, we used *in situ* hybridization in DRG and TG tissues from WT female mice.

Signal corresponding to the *Mrgpra3* transcript detected in the *in situ* hybridization of DRG and TG was less abundant and defined than those corresponding to *Kcnk18* and *Mrgprd* transcripts (**Figure 11**). 4.6 % of DRG neurons and 5.2 % of TG neurons express *Mrgpra3* mRNA (**Figure 11**). 58.6 % and 61.8 % of *Mrgpra3*-expressing neurons of DRG and TG, respectively, also express *Kcnk18* mRNA.

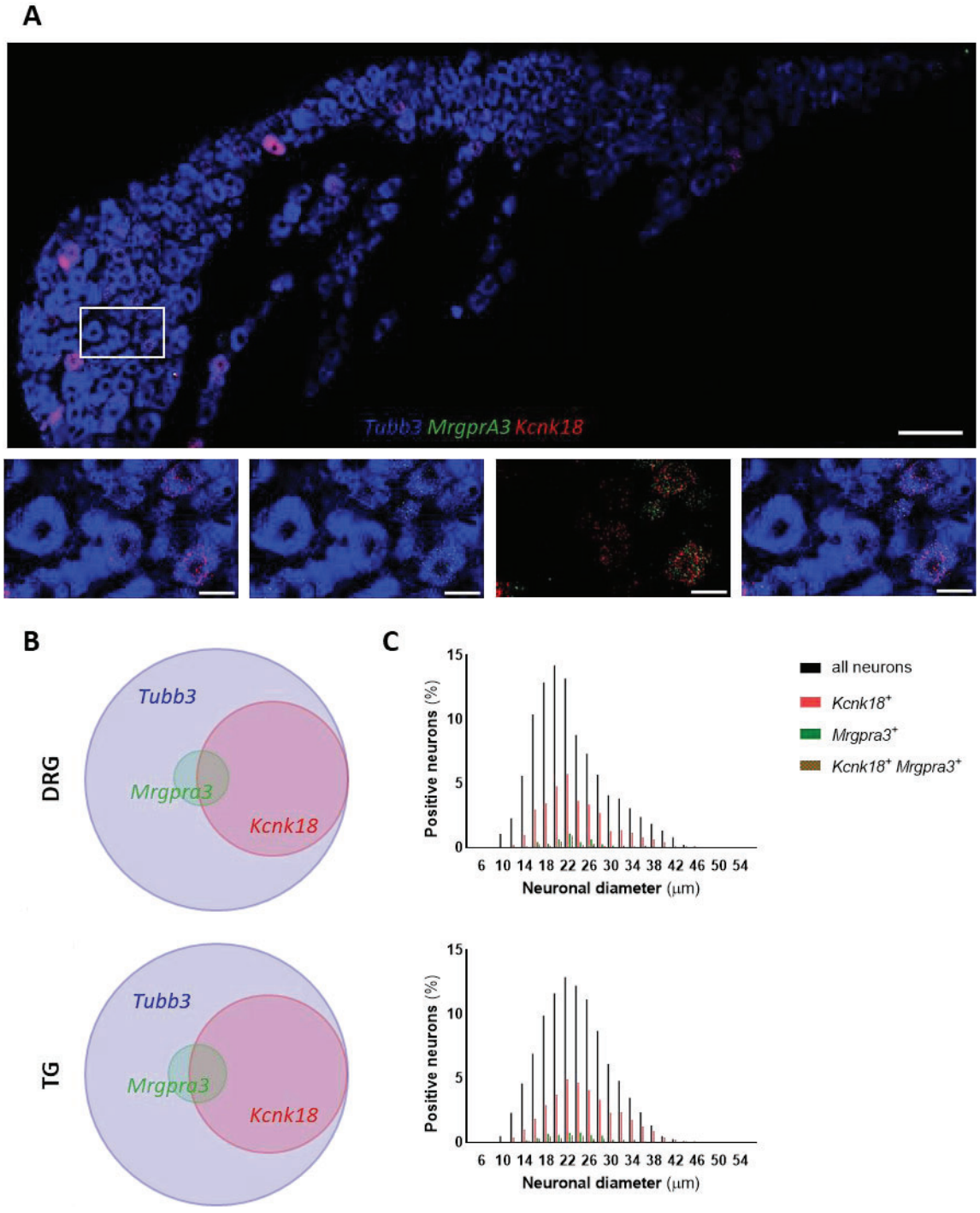

Figure 11. Kcnk18 and Mrgpra3 transcripts are co-expressed in a population of primary sensory neurons. *Expression of Kcnk18 and Mrgpra3 transcripts detected by in situ hybridization in DRG and TG tissues from WT*

mice (n = 1879 DRG neurons and 5854 TG neurons from 3 female mice). ***(a)*** *Representative image of a DRG stack showing neurons marked with Tubb3 (blue), Kcnk18 (red), and Mrgpra3 (green). Scale bar of 100 µm in the whole ganglia image. Amplification of a selected area from the entire ganglia, showing transcripts' expression in different combinations to facilitate its visualization. Scale bar of 20 µm in amplified images, maintained colour coding.* ***(b)*** *Venn diagrams showing Kcnk18 and Mrgpra3 co-expression in primary sensory neurons of DRG (top diagram) and TG (down diagram).* ***(c)*** *Histograms the showing neuronal size distribution of different subpopulations of sensory neurons, classified according to their expression of Kcnk18 and Mrgpra3. Data from DRG neurons (top diagram) and TG neurons (down diagram).*

The Mrgpra3 transcript is expressed in neurons of all sizes. When comparing to the size distribution of all neurons, *MrgprA3*-expressing neurons of TG follow the same pattern while there are less large and small and more medium-sized *MgrprA3*-expressing neurons in DRG (*Mrgpra3*-expressing neurons diameter mean of 25.26 ± 0.18 µm in DRG and 23.62 ± 0.08 µm in TG, Mann-Whitney test p-values of 0.032 in DRG and of 0.613 in TG). Neurons co-expressing *Mrgpra3* and *Kcnk18* follow a size distribution similar to the one of *Mrgpra3*-expressing neurons in both DRG and TG (*Mrgpra3*- and *Kcnk18*- expressing neurons diameter mean of 22.47 ± 0.58 µm in DRG and 23.8 ± 0.56 µm in TG, Mann-Whitney test p-values 0.051 and 0.275, respectively, **Figure 11**).

TRESK modulates the excitability of MrgprD^{+} neurons

Several studies have concluded that TRESK modulates primary sensory neurons excitability and that its depletion increases animals' sensitivity to different physical and chemical stimuli (see Chapter 4.5). After validating that most of the DRG *Mrgprd*-expressing neurons also express the *Kcnk18* transcript, we wondered whether the expression of this K_{2P} channel is modulating the excitability of this specific population of neurons.

To solve this question, cultured MrgprD-expressing neurons' action potential (AP) firing properties were studied using whole-cell current-clamp electrophysiological recordings. Neurons were obtained from DRG of TRESK$^{+/+}$ and TRESK$^{-/-}$ lines of mice that have one allele of MrgprD replaced by a sequence containing the Cre recombinase gene (Rau et al. 2009) and an inserted construct in the ROSA26 locus consistent on a stop cassette flanked by loxP sequences followed by the red fluorescent protein TdTomato gene sequence (Madisen et al. 2010). In these transgenic lines, cells expressing MrgprD also express the Cre recombinase that, in turn, deletes the loxP-flanked stop codon preceding TdTomato gene and, therefore, allows this red fluorescent protein expression and MrgprD-expressing neurons identification. TRESK WT and TRESK KO sequences are not altered by these transgenic changes and, thus, although the mouse lines used in these experiments contain more transgenic modifications

than the ones used for expression and behavioural experiments, they are also referred to as WT (for TRESK$^{+/+}$) and TRESK KO (for TRESK$^{-/-}$).

In electrophysiological recordings, neuronal size can also be determined by the neuronal membrane capacitance (C_m) recorded in voltage-clamp configuration, as the charge that neurons can accumulate at a given potential (C_m) depends on the extension of the neuronal membrane surface that, in turn, is conditioned by neuronal size. 60.6 % of the recorded red neurons were small-sized (≥ 20 pF), 36.4 % were medium-sized (20 – 35 pF) and just 1 out of the 33 recorded neurons was large-sized (≥ 35 pF). We found that recorded red neurons from WT and TRESK KO animals had similar sizes (C_m 19.83 ± 1.21 pF for neurons from WT animals and 22.20 ± 4.14 pF for neurons from TRESK KO animals, Mann-Whitney test p-value 0.969, **Figure 12**).

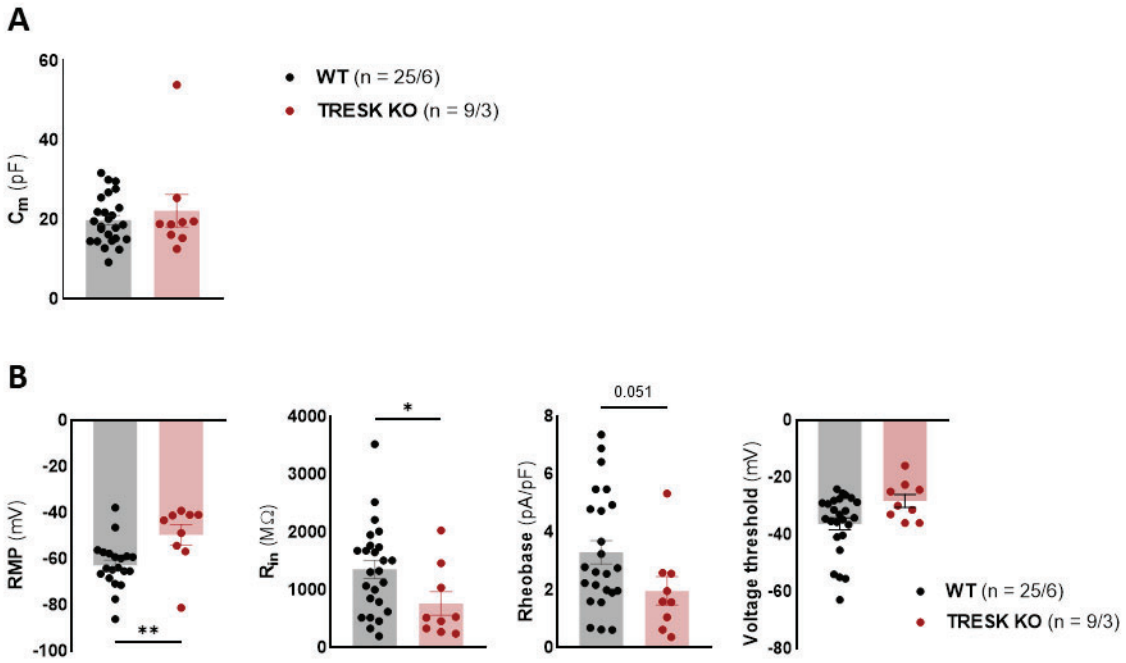

Figure 12. MrgprD-expressing sensory neurons from TRESK KO animals show alterations in neuronal excitability*. Data of red neurons from 6 WT (3 males and 3 females) and 3 TRESK KO males. The total number of neurons and the animals from which they come from are indicated in parentheses and separated with a slash in each graph. Dots indicate measures from single cells, bars and lines the mean and SEM of studied neurons.* ***(a)*** *Comparison of membrane capacitances measured in a voltage clamp configuration used as indicator of neuronal size.* ***(b)*** *Comparison of cell membrane electrical characteristics (RMP and Rin measured at -20 pA, left figures) and cell excitability parameters (rheobase and voltage to elicit APs, right figures) of red neurons from WT and TRESK KO animals measured in whole-cell current clamp configuration. Mann-Whitney test: * indicates p-value < 0.05, ** indicates p-value < 0.01.*

Neuronal excitability determines the neuronal capacity to elicit APs and, thus, to transmit information. APs initiate when membrane voltage reaches a depolarized threshold level that

allows voltage-dependent channels opening and, thus, sodium influx. The distance of this threshold from resting membrane potential (RMP) and the membrane capacity to retain charges and, thus, maintain differences in voltage (input resistance – R_{in}) condition neuronal excitability. Previous studies showed that, in DRG small and medium neurons, TRESK depletion does not affect RMP but results in an increase in neuronal R_{in} and, thus, in an increase in neuronal excitability (Castellanos et al. 2020; Guo et al. 2019).

Here, taking advantage of the mouse line expressing TdTomato in MrgprD-expressing cells, we could study the effects of TRESK depletion in the excitability of MrgprD-expressing neurons specifically. Compared to the red neurons from WT animals, red neurons lacking TRESK presented depolarized RMP (-62.8 ± 2.30 mV in neurons from WT animals and -49.6 ± 4.5 mV in neurons from TRESK KO animals, Mann-Whitney test p-value 0.004, **Figure 12**), which could be explained by the reduction of potassium outflow due to the channel depletion. Reduction of membrane capacity to allow charges to flow results in an increase in its capacity to maintain charges and, thus, membrane potential. However, we found that red neurons from TRESK KO animals had lower R_{in} than those from WT animals (1357 ± 153.8 MΩ and 767.2 ± 206.4 MΩ for neurons from WT and TRESK KO animals, respectively, Mann-Whitney test p-value 0.036, **Figure 12**). A possible explanation for the lower R_{in} in cells lacking TRESK might be the opening of voltage-gated channels due to the slightly depolarized RMP.

In whole-cell registers, it is possible to measure the minimum current injected necessary to elicit an AP (rheobase). We found that neurons from TRESK KO animals had lower rheobases than those from WT animals (71.1 ± 10.0 pA/pF in neurons from WT animals and 37.8 ± 9.1 pA/pF in neurons from TRESK KO animals, Mann-Whitney test 0.040, **Figure 12**), which could be explained by their depolarized RMP, closer to the membrane potential threshold for AP firing, and the reduction of the potassium outflux counteracting membrane depolarization. In relation to this, we observed that neurons lacking TRESK tend to fire APs at more depolarized membrane potentials than neurons with the channel (-36.3 ± 2.1 mV for neurons from WT animals and -28.2 ± 2.3 mV for neurons from TRESK KO animals, Mann-Whitney test p-value 0.071). This increase in the voltage threshold for AP firing in neurons lacking TRESK might be explained by precocious inactivation of small amounts of sodium voltage-gated channels (Na_V) previously activated at slightly depolarized membrane potentials, or due to expression changes in Na_V channels due to neurons' constant depolarized state. These situations might

result in the need of recruiting more voltage-gated channels to fire APs and, thus, in the increase in the voltage threshold (**Figure 12**).

To test whether the variation of these neuronal excitability parameters also resulted in a change in the neuronal response to depolarizing stimuli, DRG red neurons were challenged with depolarizing currents of increasing intensity: a current ramp from 0 to +500 pA in 1 second, a pulse of 1 second at neurons' own rheobase current, a pulse of 1 second at 2.5 times each neuron's rheobase current, and a train of 5 pulses of 500 milliseconds from +50 to +550 pA with an increase of +100 pA between pulses. Red neurons lacking TRESK tended to elicit more APs than neurons with the channel in response to most of the depolarizing stimuli, which is consistent with the RMP and R_{in} parameters indicating an increase in neuronal excitability. This difference was only significant in the response to the +50 pA, +150 pA and +550 pulses of 500 ms (**Figure 13**, **Table 5**).

When depolarized, especially in response to high intensity stimuli, some neurons showed irregular membrane voltage waves (**Figure 13**). This type of wave was often related to a reduction of AP firing, and we defined them as "saturated" responses, which might be due to Na_V channels inactivation after previous activation. As a response to the protocol of pulses increasing from +50 to +550 pA with intervals of +100 pA, red neurons from WT mice showed increasing number of APs in response to depolarizing pulses of increasing amplitude and only showed saturated responses in response to depolarizing steps equal or higher than +350 pA, while red neurons from TRESK KO mice showed saturated responses even when stimulated with a +50 pA step and fired fewer APs at higher intensity steps. Compared to neurons from WT animals, red neurons lacking TRESK tended to show more saturated responses in response to +50 pA depolarizing current and showed more saturated responses in response to +150 pA, +250 pA and +350 pA current pulses (**Figure 13**, **Table 5**). Similarly, red neurons lacking TRESK showed more saturated responses in response to the current ramp than neurons with the channel. Responses to current pulses at rheobase or 2.5 times the rheobase intensities showed similar tendencies that can not be confirmed statistically (**Figure 13**, **Table 5**).

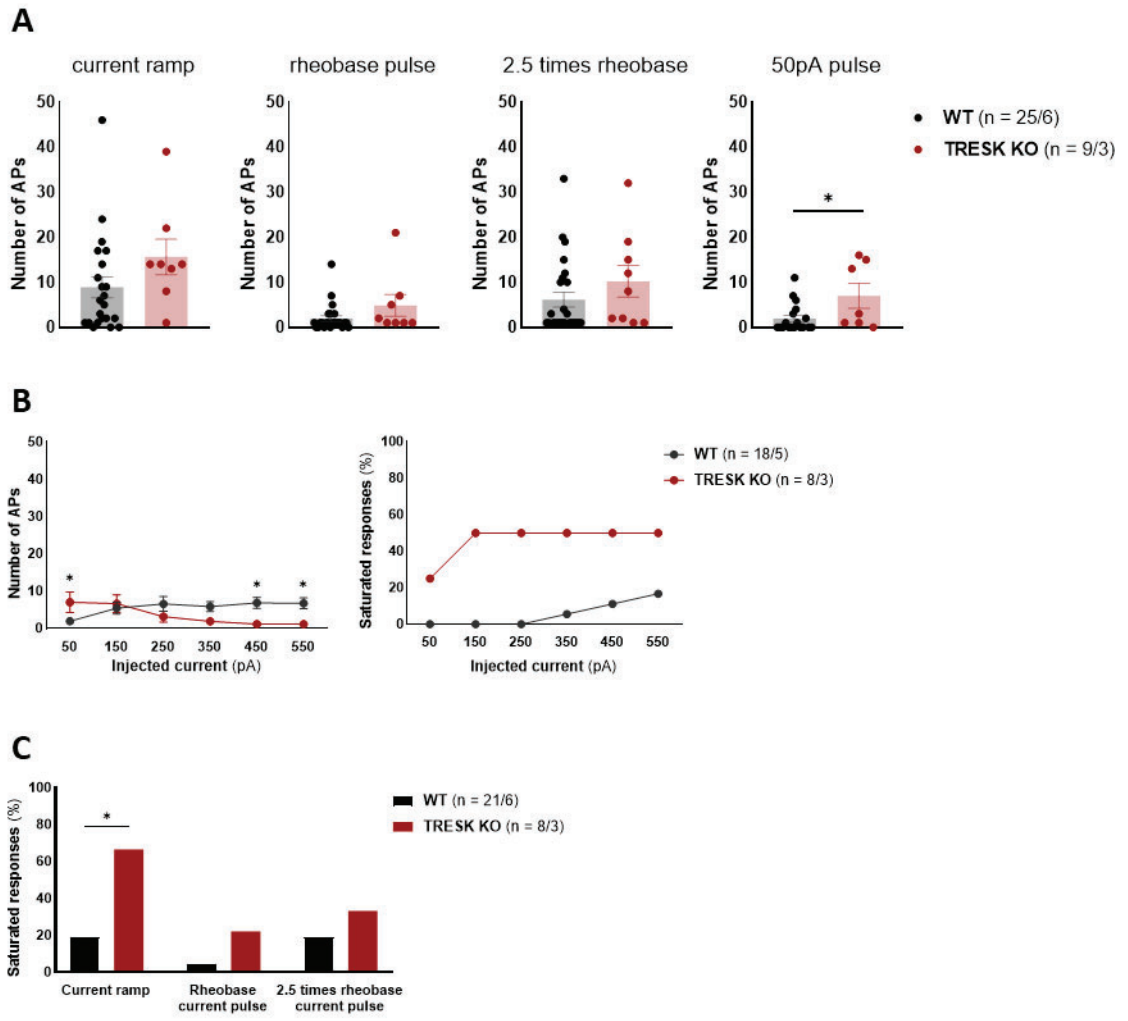

Figure 13. MrgprD-expressing sensory neurons from WT and TRESK KO animals elicit different changes in voltage in response to depolarizing stimuli. *The total number of neurons and animals from where they were obtained indicated in parentheses in each graph as: number of cells / number of animals.* ***(a)*** *Number of APs elicited by red neurons from WT and TRESK KO animals in response to depolarizing currents. From left to right: quantification of APs fired in response to a depolarizing current ramp (from 0 to +500 pA in 1 second), a current pulse of one second at each cell's own rheobase, a current pulse of one second at 2.5 times each cell's own rheobase and a 500 ms pulse of +50 pA. Dots indicate measures from single cells, bars and lines the mean and SEM of each group.* ***(b)*** *Quantification of neuronal excitability as the number of APs fired and percentage of neurons showing "saturated" signals in response to depolarizing current pulses of 500 ms from +50 pA with +100 pA increments. From left to right: Whole-cell current-clamp recording of a MrgprD-expressing neuron from a TRESK KO animal: APs fired and appearance of "saturated" responses in response to injection of currents of increasing intensity can be observed. Comparison of the number of APs fired by neurons from WT and TRESK KO animals in response to current pulses of increasing intensities. Comparison of the percentage of neurons from WT and TRESK KO animals showing "saturated" responses to current pulses of increasing intensities.* ***(c)*** *Comparison of the percentage of neurons from WT and TRESK KO animals showing "saturated" responses to depolarizing stimuli: current ramp (from 0 to +500 pA in 1 second), current pulse of 1 second at each cell's own rheobase, current*

Changes in potassium current and in activation and inactivation of voltage-gated channels can also modulate AP characteristics. Previous studies in our laboratory indicated that DRG small and medium neurons lacking TRESK fired wider APs with reduced APH compared with those

fired by neurons with the channel, probably as a result of the decrease in potassium current (Castellanos et al. 2020). To check the effect of TRESK on the characteristics of APs fired by MrgprD-expressing neurons, we analysed the AP amplitude, AP duration and AP afterpotential hyperpolarisation (APH) in red-marked neurons from both WT and TRESK KO animals.

		Summary data		$TRESK^{+/+}$ *vs.* $TRESK^{-/-}$
		$TRESK^{+/+}$	$TRESK^{-/-}$	p-value
Number of APs (mean ± SEM) Mann-Whithey test	**Current ramp**	8.9 ± 2.3	15.6 ± 4	*0.093*
	Pulse rheobase	2 ± 0.6	4.9 ± 2.4	*0.086*
	Pulse 2.5 rheobase	6.2 ± 1.7	10.2 ± 3.5	*0.155*
	Pulse +50 pA	1.94 ± 0.74	7 ± 2.75	***0.046***
	Pulse +150 pA	5.4 ± 1.6	6.6 ± 2.4	*0.561*
	Pulse +250 pA	6.6 ± 1.9	3.1 ± 1.5	*0.301*
	Pulse +350 pA	5.8 ± 1.4	1.9 ± 0.5	*0.137*
	Pulse +450 pA	6.8 ± 1.5	1.1 ± 0.1	***0.024***
	Pulse +550 pA	6.7 ± 1.5	1.1 ± 0.1	***0.023***
Saturated responses (%) Fisher's exact test	**Current ramp**	19	66.7	***0.030***
	Pulse rheobase	4.3	22.2	*0.184*
	Pulse 2.5 rheobase	19	33.3	*0.640*
	Pulse +50 pA	0	25	*0.086*
	Pulse +150 pA	0	50	***0.005***
	Pulse +250 pA	0	50	***0.005***
	Pulse +350 pA	5.6	50	***0.020***
	Pulse +450 pA	11.1	50	*0.051*
	Pulse +550 pA	16.7	50	*0.149*
AP characteristics (mean ± SEM) Welch's T-test	**AP amplitude** (mV)	♂: 135.7 ± 7.3 ♀: 110.2 ± 7.7	♂: 88.7 ± 9.8	♂ $TRESK^{+/+}$ *vs.* $^{-/-}$: ***0.002*** ($TRESK^{+/+}$: ♂ *vs.* ♀: ***0.025***)
	AP width (ms)	♂: 2.04 ± 0.20 ♀: 3.09 ± 0.40	♂: 2.18 ± 0.34	♂ $TRESK^{+/+}$ *vs.* $^{-/-}$: *0.473* ($TRESK^{+/+}$: ♂ *vs.* ♀: ***0.028***)
	APH (mV)	♂: -59.4 ± 2.32 ♀: -48.7 ± 3.4	♂: -50 ± 2	♂ $TRESK^{+/+}$ vs. $^{-/-}$: ***0.007*** ($TRESK^{+/+}$ ♂ *vs.* ♀: ***0.015***)

Table 5. Representative values and statistical analysis of the neuronal excitability parameters of DRG MrgprD-expressing neurons from WT and TRESK KO animals.

In contrast with the excitability parameters studied in red neurons, we found differences in the AP characteristics of neurons from WT male and WT female animals. For this reason, while the excitability parameters of neurons from both males and females have been analysed together, animals' sex variable has been considered in AP characteristics' analysis. APs of red neurons from WT female mice showed less amplitude, longer duration and smaller APH compared to APs elicited by neurons from WT male mice (**Figure 14**, **Table 5**).

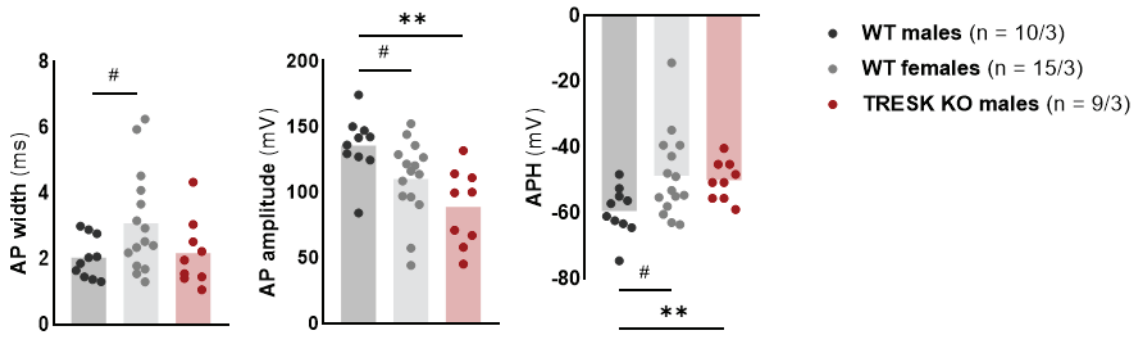

Figure 14. Characterisation of the APs fired by MrgprD-expressing neurons. *Comparison of AP amplitude, duration, and APH of red neurons from WT males, WT females and TRESK KO males. The total number of neurons analysed and the number of animals from which they come from are indicated in parentheses and separated with a slash next to the figures. Statistical analysis detailed in Table 2. * indicates p-value < 0.05, ** indicates p-value < 0.01.*

AP characteristics were studied only in neurons from male animals as, due to animals' availability, we could not record red neurons from TRESK KO females. APs fired by neurons lacking TRESK had the same duration but smaller amplitude and APH than those fired by neurons with the channel (**Figure 14**, **Table 5**). Reduction of potassium outflow due to TRESK ablation may result in the observed reduction of the APH magnitude, which, in turn, may difficult the transition of inactivated Na_V channels to deactivated states. Precocious or maintained inactivation of Na_V channels or changes in the expression of different subtypes of channels may also explain the reduction of the AP magnitude.

MrgprD activation increases MrgprD$^+$ neurons' excitability similarly to knocking out TRESK

As seen, TRESK deletion induces a pre-activated state in MrgprD-expressing neurons, which respond easier and with more intensity to depolarizing stimuli until reaching "saturated" states. By its side, MrgprD activation also induces increases in the neuronal excitability of the MrgprD-expressing neurons (Crozier et al. 2007; Rau et al. 2009). As detailed previously (Chapter 4.4), TRESK is the only K_{2P} channel activated in response to increases in intracellular calcium in a process mediated by the phosphatase calcineurin that allows the restoring of membrane potential to negative values when neurons are activated (Czirják and Enyedi 2010; Czirják, Tóth, and Enyedi 2004). As the activation of the G protein coupled receptor MrgprD results in an increase in the intracellular calcium levels, we wondered whether the calcium-induced activation of TRESK may modulate the effects of the receptor activation in the excitability of MrgprD-expressing neurons. To answer this question, we treated the recorded

MrgprD-expressing neurons from WT and TRESK KO mice with the MrgprD agonist β-alanine and studied their excitability and AP characteristics.

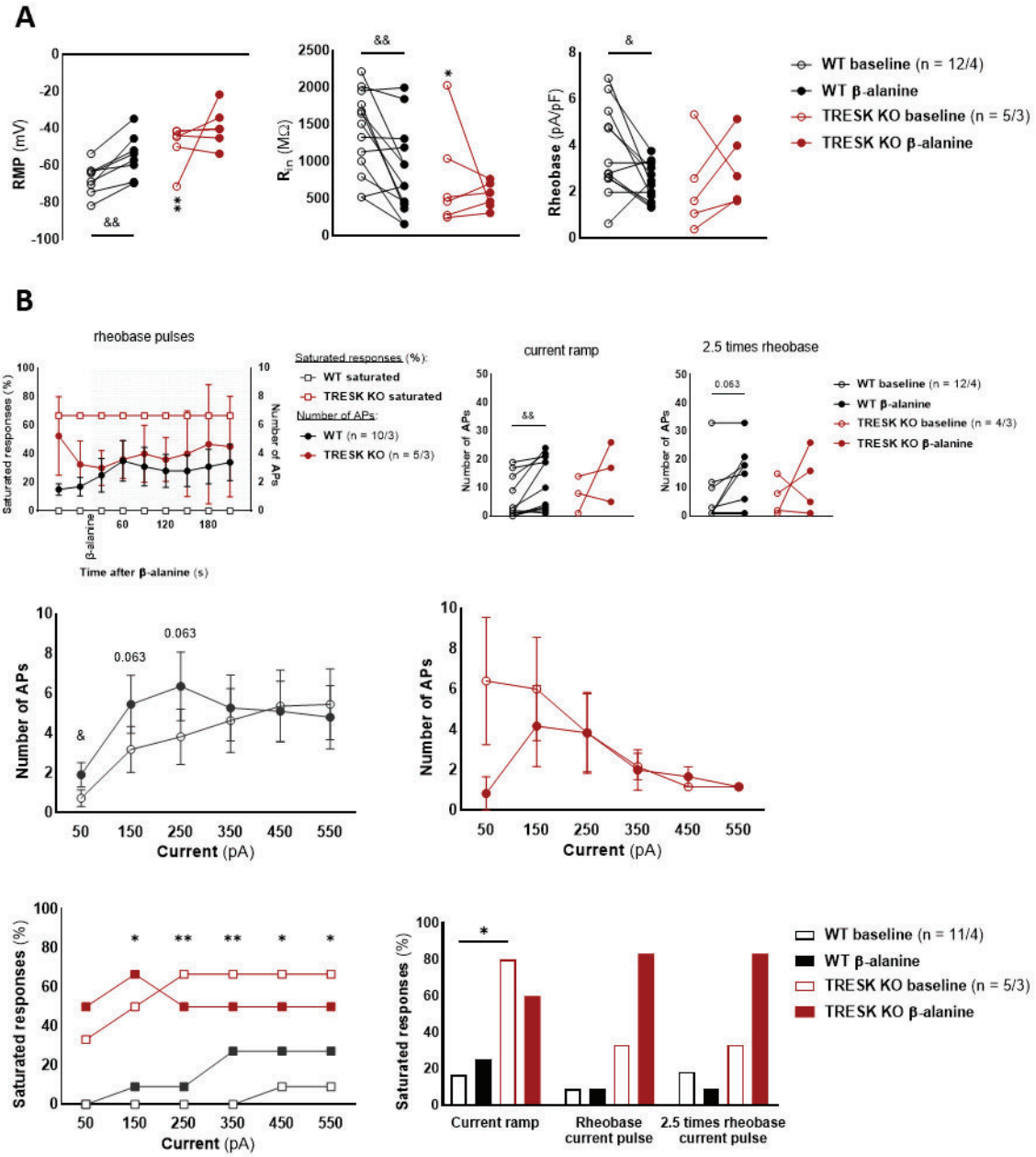

Figure 15. β-alanine treatment and TRESK depletion modify MrgprD-expressing neurons' excitability similarly. *Effects of challenging cultured DRG red neurons from the transgenic mouse line expressing TdTomato in potentially MrgprD-expressing neurons with β-alanine 500 μM. Measures obtained from whole-cell current clamp electrophysiological registers before and after red neurons' treatment with β-alanine for 5 minutes, unless indicated.* ***(a)*** *Comparison of cell membrane electrical characteristics (RMP and Rin measured at -20 pA, left figures) and rheobase (right figure) of red neurons from WT and TRESK KO animals before and after β-alanine treatment. Single dots connected with lines represent data from individual cells before and after β-alanine treatment. Comparison of baseline values of WT and TRESK KO animals: Welch's T-test for RMP (p-value 0.009); unpaired T-test for Rin (p-value 0.048), and Welch's T-test for rheobase (p-value 0.170).* ***(b)*** *Number of APs fired and percentage of neurons showing "saturated" signals in response to different depolarizing stimuli. Upper left: Responses to pulses of one second at each cell's own rheobase. Timeline: 30 seconds and just before β-alanine addition and each 30 seconds after β-alanine addition until 210 seconds after. Shaded area indicates time after*

*β-alanine addition. The number of APs is shown as connected dots indicating the mean, with error bars indicating the SEM at each time point. The percentage of the total number of neurons showing "saturated" responses is indicated as connected squares. Upper right: Number of APs fired in response to depolarizing current ramp (0 to +500 pA in 1 second) and current pulse of one second at 2.5 times each cell's own rheobase. Middle line from left to right: Number of APs fired in response to depolarizing pulses from +50 to +550 pA with increments of +100 pA between pulses before and after β-alanine treatment. The number of APs shown as connected dots indicating the mean, with error bars indicating the SEM of APs fired in response to each current pulse. Data of red neurons from WT (left) and TRESK KO (right) animals. Lower left: Percentage of red neurons showing "saturated" responses to depolarizing pulses from +50 to +550 pA. The Percentage of the total number of red neurons showing "saturated" responses indicated as connected dots. Lower right: Percentage of the total number of red neurons showing "saturated" responses to depolarizing current ramps (from 0 to +500 pA in 1 second), current pulses of one second at each cell's own rheobase and current pulses of one second at 2.5 times each cell's own rheobase. Bars indicate the percentage of all neurons showing this kind of response before and after β-alanine treatment. The total number of neurons and animals from where they were obtained are indicated in parentheses in each subsection or graph as: number of cells / number of animals. Samples from subsection (b – middle) are the same of the subsection (b – bottom). Data analysis is detailed in Table 3. Asterisks indicate statistically significant differences between data obtained from WT and TRESK KO animals: * indicate p-value < 0.05, ** p-value < 0.01. Ampersands indicate statistically significant differences between data obtained before and after β-alanine treatment of neurons: & indicate p-value < 0.05, && p-value < 0.01. Not statistically significant comparisons between untreated and treated neurons showing clear tendencies are indicated with numbers above dots.*

β-alanine application to DRG red neurons did not induce AP firing or changes in membrane currents measured in current-clamp and voltage-clamp configuration, respectively (data not shown). However, the RMP of red neurons from WT mice was depolarized after β-alanine treatment, reaching similar levels to those of TRESK KO mice (-67.5 ± 3 mV for WT baseline, -55.2 ± 4.1 mV after β-alanine treatment and -48.8 ± 4.7 mV of TRESK KO baseline, paired T-test p-value 0.002 for neurons of WT animals before and after β-alanine treatment, unpaired T-test p-value 0.329 for treated neurons from WT animals *vs.* untreated neurons from TRESK KO animals, **Figure 15**). This depolarization may be explained by the increase in positive charges of the free calcium cations in the intracellular medium or the effects of MrgprD downstream pathways on other channels, that, apparently, can not be compensated by the potassium outflow through the activated TRESK. β-alanine application to red neurons of TRESK KO animals, however, did not change their RMP (-39.2 ± 4.4 mV after β-alanine treatment, paired T-test p-value 0.298, **Figure 15**). The incapacity of MrgprD activation to change RMP of MrgprD-expressing neurons from TRESK KO animals might be due to limited action of MrgprD downstream pathways in depolarised ranges of voltage or due to compensating activity of other channels, although we found no differences in the expression of the main K_{2P} channels in DRGs from TRESK KO animals compared to those from WT (**Figure 8**).

Although we could not detect membrane currents in response to β-alanine application, effects of MrgprD activation in the R_{in} of red neurons from WT animals were similar to those on RMP: β-alanine application induces a reduction of the R_{in} of red neurons from WT animals to similar levels to those of neurons lacking TRESK, while it has no effect on the R_{in} of red neurons from TRESK KO animals (baseline of 1392 ± 155.8 MΩ for neurons from WT animals and of 761.7 ± 279.2 MΩ for neurons of TRESK KO animals, 858.8 ± 165.3 MΩ for treated neurons from WT animals and 536.7 ± 72.2 MΩ for treated from TRESK KO animals; paired T-test p-values of 0.005 in baseline *vs.* β-alanine treated neurons from WT animals and of 0.471 in baseline *vs.* β-alanine treated neurons from TRESK KO animals; unpaired T-test p-value of 0.756 for β-alanine treated neurons from WT animals *vs.* untreated neurons from TRESK KO animals, **Figure 15**). The increase in potassium outflow through activated TRESK in response to increased intracellular calcium together with the activation of some voltage-dependent channels due to depolarized RMP in neurons from WT animals treated with β-alanine might have a role in the reduction of membrane capacity to retain charges (R_{in}), which is consistent with the lack of effect of β-alanine in the R_{in} of neurons from TRESK KO animals.

In concordance with previous studies (Rau et al. 2009), we confirmed that β-alanine application to MrgprD-expressing neurons from WT mice reduces their rheobase and increases the number of APs they fire in response to depolarizing stimuli (rheobase of 3.74 ± 0.55 pA/pF for untreated neurons and 2.41 ± 0.24 pA/pF after treatment, paired T-test p-value of 0.027, **Figure 15**, **Table 6**). Moreover, β-alanine-treated red neurons from WT animals fire similar number of APs than untreated neurons of TRESK KO animals when challenged with depolarising currents (**Figure 15**, **Table 6**). The increase in the number of APs fired by red neurons from WT mice in response to 1 second current pulses at their own rheobase appear progressively and differences in these values are not statistically significant during the 4 first minutes after β-alanine treatment (number of APs on relation to β-alanine addition point: 1.5 ± 0.4 30 seconds before, 1.7 ± 0.7 just before the addition, 2.5 ± 1.2 30 seconds after, 3.5 ± 1.4 60 seconds after, 3.1 ± 1.3 90 seconds after, 2.8 ± 1.2 120 seconds after, 2.8 ± 1.1 150 seconds after, 3.1 ± 1.2 180 seconds after and 3.4 ± 1.3 210 seconds after, Dunn's multiple comparisons test comparing each time to 30 seconds before addition number of APs p-values: > 0.999 until 180 seconds after and 0.537 for 210 seconds after β-alanine application, **Figure 15**).

		Summary data				Comparisons (p-value)			
		TRESK$^{+/+}$		TRESK$^{-/-}$		baseline *vs.* β-alanine		TRESK$^{+/+}$ β-alanine *vs.* $^{-/-}$ baseline	baseline TRESK $^{+/+}$ *vs.* $^{-/-}$
		baseline	β-alanine	baseline	β-alanine	TRESK$^{+/+}$	TRESK$^{-/-}$		
Number of APs (mean ± SEM)	**Current ramp**	6.09 ± 2.21	11.64 ± 2.82	7.67 ± 3.76	16 ± 6.08	***0.003***	*0.750*	*0.470*	*0.739*
	Pulse rheobase	1.3 ± 0.65	5.2 ± 1.51	2.33 ± 1.33	5.67 ± 4.7	***0.016***	*0.750*	*0.322*	*0.511*
	Pulse 2.5 rheobase	5.5 ± 2.73	9.75 ± 3.14	6.5 ± 3.23	12 ± 5.64	*0.063*	*0.875*	*0.989*	*0.319*
	Pulse +50 pA	0.73 ± 0.43	1.91 ± 0.61	6.4 ± 3.16	0.83 ± 0.83	***0.039***	*0.375*	*0.327*	*0.056*
	Pulse +150 pA	3.18 ± 1.16	5.46 ± 1.46	6 ± 2.56	4.17 ± 2.01	*0.063*	*0.813*	*0.976*	*0.294*
	Pulse +250 pA	3.82 ± 1.39	6.36 ± 1.72	3.83 ± 1.94	3.83 ± 2.01	*0.063*	*> 0.999*	*0.615*	*0.959*
	Pulse +350 pA	4.64 ± 1.61	5.27 ± 1.66	2.17 ± 0.65	2 ± 1	*0.438*	*0.875*	*0.635*	*0.652*
	Pulse +450 pA	5.36 ± 1.82	5.1 ± 1.52	1.17 ± 0.17	1.67 ± 0.49	*0.438*	*> 0.999*	*0.127*	*0.160*
	Pulse +550 pA	5.46 ± 1.78	4.8 ± 1.6	1.17 ± 0.17	1.17 ± 0.17	*0.563*		*0.275*	*0.160*
Saturated responses (%)	**Current ramp**	16.67	25	80	60	*> 0.999*	*> 0.999*	*0.101*	***0.028***
	Pulse rheobase	9.09	9.09	33.33	83.33	*> 0.999*	*0.242*	*0.515*	*0.515*
	Pulse 2.5 rheobase	18.18	9.09	33.33	83.33	*> 0.999*	*0.242*	*0.515*	*0.584*
	Pulse +50 pA	0	33.33	0	50	*> 0.999*	*> 0.999*	*0.110*	*0.110*
	Pulse +150 pA	0	50	9.09	66.67	*> 0.999*	*> 0.999*	*0.099*	***0.029***
	Pulse +250 pA	0	66.67	9.09	50	*> 0.999*	*> 0.999*	***0.028***	***0.006***
	Pulse +350 pA	0	66.67	27.27	50	*0.214*	*> 0.999*	*0.162*	***0.006***
	Pulse +450 pA	9.09	66.67	27.27	50	*0.587*	*> 0.999*	*0.162*	***0.028***
	Pulse +550 pA	9.09	66.67	27.27	50	*0.587*	*> 0.999*	*0.162*	***0.028***
AP characteristics (mean ± SEM)	**AP amplitude** (mV)	♂: 145.1 ± 5.8	♂: 129.2 ± 11	♂:	♂:	♂: *0.091*	♂: *0.200*	♂: ***0.045***	♂: ***0.003***
		♀: 94.7 ± 14.1	♀: 70.4 ± 13	86.9 ± 15.7	57.8 ± 12.9	♀: *0.158*			
	AP width (ms)	♂: 1.83 ± 0.21	♂: 1.62 ± 0.25	♂:	♂:	♂: *0.566*	♂: *0.592*	♂: *0.514*	♂: *0.806*
		♀: 3.37 ± 0.67	♀: 2.69 ± 0.36	1.94 ± 0.44	2.30 ± 0.30	♀: *0.420*			
	APH (mV)	♂: -61.8 ± 2.7	♂: -60.4 ± 3.8	♂:	♂:	♂: *0.788*	♂: *0.103*	♂: *0.082*	♂: ***0.018***
		♀: -46.4 ± 7.5	♀: -47.8 ± 6.8	-49.3 ± 3.2	-32.4 ± 4.5	♀: *0.899*			

Statistics tests:
baseline *vs.* β-alanine: Wilcoxon test (number of APs), Fisher's exact test (saturated responses), paired T-test (AP characteristics)
TRESK $^{+/+}$ vs. $^{-/-}$: Mann-Whithey test (number of APs), Fisher's exact test (saturated responses), unpaired T-test (AP characteristics)

Table 6. Representative values and statistical analysis of the effects of MrgprD activation in DRG MrgprD-expressing neurons from WT and TRESK KO animals .

The increase in the excitability of treated neurons from WT mice also results in the appearance of “saturated” responses. Although the percentage of neurons from WT mice showing saturated responses when stimulated with a current ramp from 0 to +500 pA in 1 second, a pulse of 1 second at neurons’ own rheobase current or a pulse of 1 second at 2.5 times their own rheobase current do not change between pre- and post-β-alanine treatment, neurons that did not show “saturated” responses to pulses of 500 milliseconds from +150 to +550 pA with an increase of +100 pA between pulses, started showing those oscillations in response to the same stimuli after β-alanine treatment. The increase of those percentages, however, did not reach statistically significant levels, neither similar levels to those of untreated neurons from TRESK KO mice (**Figure 15**, **Table 6**). The increase in calcium intracellular levels due to MrgprD activation in MrgprD-expressing neurons from WT mice is probably activating TRESK (Czirják and Enyedi 2014; Czirják, Tóth, and Enyedi 2004) which, in turn, may be compensating neuronal excitation, preventing the appearance of “saturated” responses.

In red neurons from TRESK KO mice, β-alanine treatment had entirely different effects. Neurons’ treatment with the agonist had variable effects on their rheobase, which tended to increase in most of the neurons, although the change did not reach significant levels (rheobase of 2.18 ± 0.86 pA/pF for untreated neurons and 3 ± 0.68 pA/pF after treatment, paired T-test p-value of 0.434, **Figure 15**). Moreover, β-alanine treatment does not affect the number of APs fired by neurons from TRESK KO animals in response to most of the applied depolarizing stimuli (**Figure 15**, **Table 6**). Changes in the number of APs fired by red neurons of TRESK KO mice before and after β-alanine treatment only appear when neurons are stimulated by pulses of 500 ms at +50 and +150 pA. In response to those pulses, red neurons from TRESK KO mice tend to fire less APs after treatment, probably due to changes in neuronal responses from AP firing to “saturated” responses. β-alanine treatment of neurons from TRESK KO animals tends to increase the percentage of neurons showing “saturated” responses after stimulation with current pulses at each neuron’s own rheobase or at 2.5 times the rheobase, although those changes can not be confirmed by significant statistical levels (**Figure 15**, **Table 6**). The reduction of potassium outflow through TRESK, may difficult the recovery of the physiological activity of the neuronal channels, thus potentiating these β-alanine effects.

Presented results confirm that MrgprD activation in MrgprD-expressing neurons increases their excitability, which can not be compensated by TRESK activity. Moreover, the already hyperexcitable state of MrgprD-expressing neurons from TRESK KO animals can not be further increased by the activation of the G protein coupled receptor. However, as just a few neurons from TRESK KO animals could be registered after β-alanine treatment, more experiments need to be performed to confirm these findings. According to the preliminary results, however, we might hypothesize that the hyperexcitable state of TRESK KO neurons may activate compensatory mechanisms such as other potassium channels activation or the inactivation of sodium voltage-gated channels, that do not allow further increase in neuronal excitability through MrgprD activation.

As mentioned before, changes in the activity of channels and other regulating mechanisms may modify AP characteristics. Moreover, considering that TRESK depletion reduced the amplitude and APH of APs fired by DRG neurons (**Figure 14**), we wanted to investigate the effects of TRESK calcium-mediated activation after MrgprD activation in the characteristics of APs fired by MrgprD-expressing neurons. Here, as we showed differences in the baseline characteristics of APs fired by neurons from male and female mice, we also analysed the effects of β-alanine considering the sex variable. Although it is not statistically significant, MrgprD-activation seems to cause a decrease in the amplitude of APs fired by most of the red neurons from WT males, WT females and TRESK KO animals (**Figure 16**, **Table 6**). These changes might be due to the increased number of inactivated Na_V channels before the AP initiation or to mechanisms that potentiate cations outflow activated by depolarized voltages or pathways downstream MrgprD activation. The role of activated TRESK in reducing the amplitude of APs fired by WT animals is negligible, as changes in the AP amplitude are also present and more pronounced in treated neurons from TRESK KO animals.

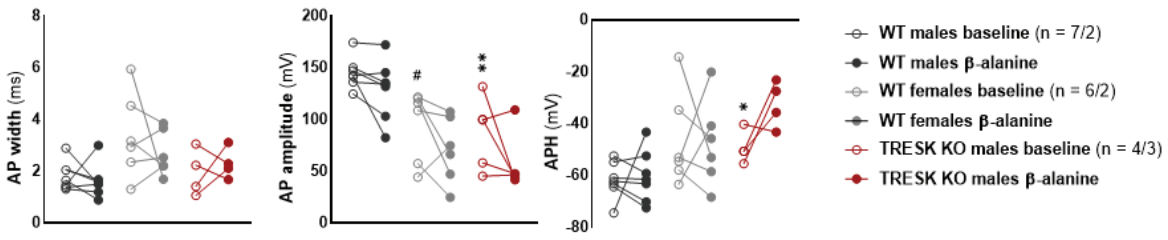

Figure 16. β-alanine treatment modifies the characteristics of the APs fired by MrgprD-expressing neurons from WT males, WT females and TRESK KO males. *Comparison of AP duration, amplitude, and APH of β-alanine 500 μM treated and untreated red neurons from WT males, WT females and TRESK KO males. Characteristics measured from APs elicited in response to rheobase current pulses of 200 ms in whole-cell current clamp*

*registers. Single dots connected with lines represent data from individual cells before and after treatment. The total number of neurons analysed and the number of animals from which they come from are indicated in parentheses and separated with a slash. In the comparison of baselines of different groups with baseline values of neurons from WT males: * indicates p-value < 0.05, ** indicates p-value < 0.01 and numbers above dots indicate not statistically significant comparisons (> 5 %) showing clear tendencies. Data analysis detailed in Table 3 except for Mann-Whitney tests comparing baseline values of WT males and females (p-values: 0.001 for AP amplitude, 0.073 for AP duration and 0.101 for APH).*

MrgprD activation has no effects on the duration of the APs fired by MrgprD-expressing neurons from WT males, WT females or TRESK KO males, while tends to reduce the APH only of neurons from TRESK KO mice (**Figure 16**, **Table 6**). Although more registers are necessary to validate these results, we hypothesize that the maintenance of APH of neurons from WT males after β-alanine treatment might be due to TRESK activity, as the agonist has no effects on the APH of TRESK KO males.

Knocking out TRESK increases the activation of DRG neurons by β-alanine and different TRP agonists

Single cell-sequencing experiments indicate that DRG primary sensory neurons that express the *Kcnk18* transcript are mainly non-peptidergic nociceptors that also express *Trpa1* and *Trpv1* transcripts and, as confirmed in this work, *Mrgprd* mRNA (**Figure 10**). By its side, *Trpm8* transcript is mainly expressed in peptidergic nociceptors that do not show *Kcnk18* expression (**Table 1**), (Jung et al. 2023; Usoskin et al. 2015). As TRESK is involved in the modulation of DRG neurons' excitability (Castellanos et al. 2020; Guo et al. 2019), we wondered whether its expression in populations of neurons expressing TRPA1, TRPV1, TRPM8 or MrgprD, caused changes in their activation. To answer this question, we measured changes in intracellular calcium of cultured DRG primary sensory neurons from WT and TRESK KO (without further genomic changes) males and females after stimulating them with 1 mM β-alanine (MrgprD agonist), 100 µM menthol (TRPM8 agonist), 100 µM AITC (TRPA1 agonist) and 100nM and/or 1 µM capsaicin (TRPV1 agonist) (**Figure 17**).

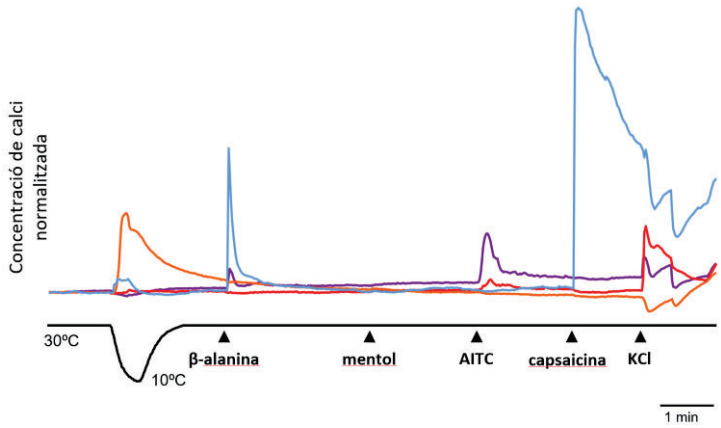

Figure 17. DRG neurons are activated by cold, β-alanine, menthol, AITC and capsaicin. *Top: Example traces of the relative intracellular calcium levels of single neurons responding to a cold ramp from 31.0 ± 0.1 °C to 11.6 ± 0.2 °C and to β-alanine, menthol, AITC, capsaicin 100 nM, capsaicin 1 µM and saturated potassium chloride (KCl 50 mM) application. Different calcium peak types are shown. Bottom: Trace showing registered solution temperature during the intracellular calcium register and arrows indicating time points of drugs addition. Scale bar of 1 minute.*

DRG cultures presented neurons of all sizes. Of neurons from WT males, 40.7 % were small-sized, 38.3 % medium-sized and 21 % large-sized; of neurons from TRESK KO males, 29.6 % were small-sized, 51.9 % were medium-sized and 18.5 % were large-sized; of neurons of WT females, 22.8 % were small-sized, 43.1 % were medium-sized and 34.1 % were large-sized, and of neurons from TRESK KO females, 24.7 % were small-sized, 41.7 % medium-sized and 33.6 % large-sized. Neurons from females were larger than those from males (Mann-Whitney test p-values: < 0.0001 for neurons from both WT and TRESK KO animals) and neurons from TRESK KO males were also larger than those from WT males, while there were no differences in the sizes of the neurons from WT and TRESK KO females (Mann-Whitney test p-values: < 0.0001 for neurons from males and 0.235 for those from females, **Figure 18**).

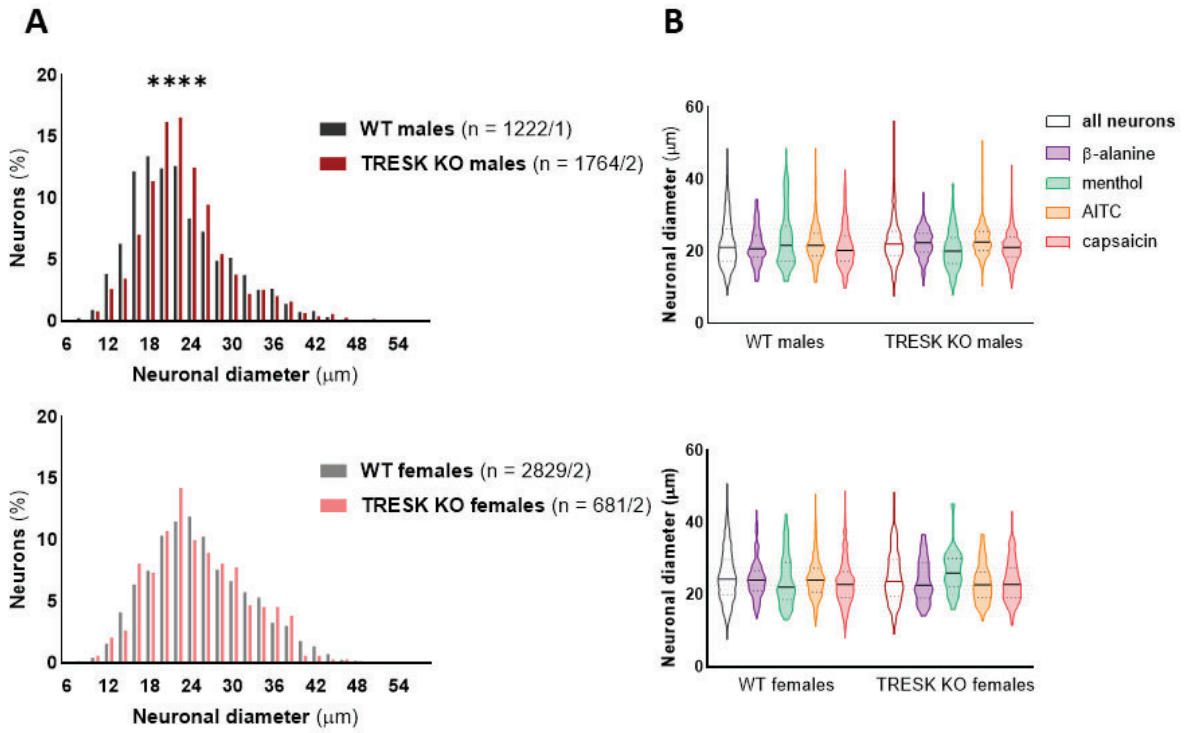

Figure 18. Size of neurons from WT and TRESK KO animals responding to MrgprD and TRPs agonists. (a) *Histograms showing the quantification and distribution of soma size of the cultured DRG neurons analysed. Top: neurons from male mice. Bottom: neurons from female mice. In the comparison of the distribution of the soma sizes of neurons from WT and TRESK KO animals using the Mann-Whitney test, **** indicate p-values < 0.0001. The total number of neurons and animals from which they were obtained are indicated in parentheses in the graph as: number of cells / number of animals.* ***(b)*** *Violin plots showing the distribution of soma sizes of neurons responding to the different agonists applied. The continuous and discontinuous lines on each violin plot indicate the median and quartiles of each analysed groups, respectively. The number of neurons analysed are indicated in the legends of section (a) of this figure. The shaded area corresponds to the neuronal diameter of the neurons classified as medium-sized (diameter between 19.5 and 27.5 µm).*

Different populations of neurons showed increases in intracellular calcium in response to one or more of the agonists applied. Although we had described that 28.4 % of neurons from WT females expressed the *Mrgprd* transcript (**Figure 10**), only a 10.5 % and an 8.9 % of WT neurons of males and females, respectively, responded to the MrgprD agonist β-alanine. However, in neurons lacking TRESK, the percentages of cells responding to the agonist increase, reaching levels of 18.9 % and 14.4 % for neurons from males and females, respectively (comparison of neurons from WT and TRESK KO animals; Fisher's exact test p-values: < 0.0001 for neurons from both males and females, **Figure 19**). Both in the case of neurons from WT and TRESK KO animals, the percentage of neurons from female animals that responded to β-alanine tended to be smaller than the one from male animals, although differences are only statistically significant in the case of TRESK KO animals (Fisher's exact test

p-values: 0.062 and < 0.003 for neurons from WT and TRESK KO animals, respectively, **Figure 19**).

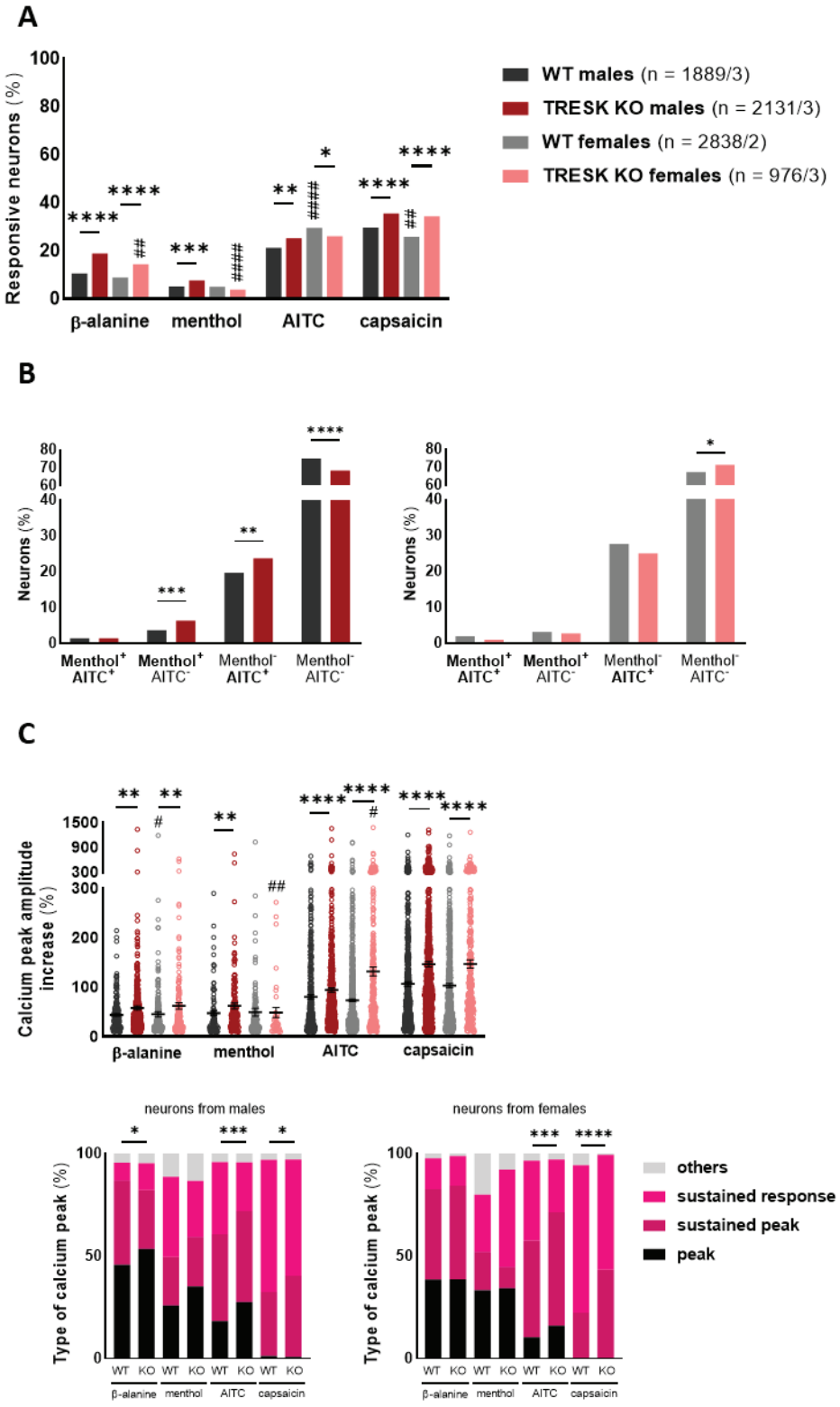

Figure 19. Neurons lacking TRESK show increased responsiveness to most of the agonists tested. (a) *Percentage of neurons from male and female mice responding with intracellular calcium increases to β-alanine 1mM,*

menthol 100 µM, AITC 100 µM, and capsaicin 100 nM and/or 1 µM. ***(b)*** *Percentage of neurons responding with intracellular calcium increases to menthol and AITC classified according to their coresponsiveness to both agonists.* ***(c)*** *Characteristics of the intracellular calcium peaks induced by each of the agonists tested. Top: Peak amplitudes shown as the relative increment of intracellular calcium in relation to baseline levels in each neuron. Bottom: Distribution of peaks according to their shape (see peak shapes in Figure 10B). The total number of neurons and animals from where they were obtained are indicated in parentheses in section (a) of the figure: number of cells / number of animals. Dots indicate values of single cells, bars and lines the mean and SEM for each group. Differences between groups are analysed using the Fisher's exact test (a and b) or Mann-Whitney test (c) and are shown with asterisks in comparisons of WT vs. TRESK KO (* indicates p-value < 0.05, ** p-value < 0.01, *** p-value < 0.001, and **** p-value < 0.0001) and with pads in comparisons of males vs. females (# indicates p-value < 0.05, ## p-value < 0.01 and #### p-value < 0.0001).*

Consistent with the findings supporting a TRESK role in the modulation of MrgprD-expressing neurons excitability (**Figure 12**, **Figure 13**), neurons from TRESK KO males and females showed higher relative calcium peak amplitudes than neurons from WT animals in response to β-alanine (+44.1 ± 2.4 % for neurons from WT males, +45.5 ± 5.2 % for neurons from WT females, 58.1 ± 4.3 % for neurons from TRESK KO males and +62.6 ± 6.5 % for neurons from TRESK KO females; Mann-Whitney test p-values: 0.006 and 0.009 for neurons from males and females, respectively). Calcium peak amplitudes presented by neurons from WT females in response to β-alanine were smaller than those presented by neurons from WT males (Mann-Whitney test p-value: 0.038), while neurons from TRESK KO males and females presented similar intracellular calcium peak amplitudes (Mann-Whitney test p-value 0.307, **Figure 19**).

TRESK depletion in neurons from male animals also resulted in an increase in the percentage of them that responded AITC, capsaicin and, surprisingly, menthol (percentage of neurons from WT and TRESK KO males responding to agonists and Fisher's exact test p-values resulting of the comparison for menthol: 5.1 % *vs.* 7.7 %, p-value of 0.0009; AITC: 21.2 % *vs.* 25.2 %, p-value 0.003; and capsaicin 29.7 % and 35.5 %, p-value < 0.0001). Moreover, neurons from male animals also showed higher amplitude of calcium peaks in response to those agonists (relative calcium peak amplitude and Mann-Whitney test p-values resulting of comparing responses of neurons from WT and TRESK KO males to different agonists: +47.9 ± 5.3 % and 62.4 ± 6.1 % of neurons from WT and TRESK KO males, respectively, in response to menthol, p-value of 0.0011; +80.7 ± 4.5 % and 94.7 ± 4.7 % in response to AITC, p-value < 0.0001; and +106.8 ± 4.9 % and 146.5 ± 5.5 % in response to capsaicin, p-value < 0.0001, **Figure 19**).

TRESK depletion in neurons from female mice, however, only increased the percentage of them that respond to β-alanine and capsaicin, while had no effect in the percentage of neurons responding to menthol, and resulted in a decrease in the percentage of neurons

responding to AITC (percentage of neurons from WT and TRESK KO females responding to agonists and Fisher's exact test p-values resulting of the comparison for menthol: 5.1 % *vs.* 3.8 %, p-value of 0.116; AITC: 29.6 % *vs.* 26 %, p-value 0.036; and capsaicin 25.8 % and 34.3 %, p-value < 0.0001). Similarly, neurons from WT and TRESK KO females showed calcium peaks of similar amplitudes in response to menthol (+49.8 ± 7.8 % for neurons from WT females, +62.4 ± 6.1 % for neurons from TRESK KO females, Mann-Witney test p-value: 0.466). In response to AITC and capsaicin, neurons from TRESK KO females showed peaks of higher amplitude than those of neurons from WT females (+103.7 ± 4 % for neurons from WT females, +146.5 ± 5.5 % for neurons from TRESK KO females, Mann-Witney test p-value < 0.0001; +73.8 ± 2.9 % for neurons from WT females, +94.7 ± 4.7 % for neurons from TRESK KO females, Mann-Witney test p-value < 0.0001, **Figure 19**).

The sex of the animals from which the DRG neurons were obtained modified their sensitivity to the nociceptor-activating compounds AITC and capsaicin, but not to menthol (Fishers' exact test p-value resulting from comparing percentage of neurons from WT males and females: 0.946). Thus, a higher percentage of neurons from WT females responded to AITC compared to neurons from WT males (Fishers' exact test p-value < 0.0001), while this relation was switched in the responsiveness to capsaicin, where more neurons of WT males responded to the agonist compared to neurons from WT females (Fishers' exact test p-value of 0.0003). However, the amplitude of calcium peaks in response to the TRP agonists applied did not change between neurons from WT males and females (Mann-Whitney test p-values: 0.782 for menthol, 0.680 for AITC and 0.721 for capsaicin, **Figure 19**).

Moreover, the sex of the animals from which the DRG neurons were obtained also modified the weight of the role of TRESK in neuronal sensitivity to the tested TRP agonists. Thus, while we found no differences in the percentage of neurons from TRESK KO males and females responding to capsaicin or in the amplitude of calcium responses they elicited in response to the agonist (neurons from TRESK KO males *vs.* females: comparison of the percentage of response, Fisher's exact p-value: 0.527; comparison of calcium amplitude, Mann-Whitney test p-value: 0.755), we found that, compared to the responsiveness of neurons from TRESK KO males, a higher percentage of neurons from TRESK KO females responded to menthol and with a higher calcium peak amplitude (comparison of percentage of neurons of TRESK KO males and females responding to menthol: Fisher's exact test p-value < 0.0001; comparison

of the amplitude of calcium peaks in response to menthol of TRESK KO males and females: Mann-Whitney test p-value of 0.003). By its side, the percentage of neurons from TRESK KO males and females responding to AITC is similar (Fisher's exact test p-value: 0.626) but calcium peaks of neurons from TRESK KO females responding to the agonist showed higher amplitude than those of neurons from TRESK KO males (Mann-Whitney test p-value: 0.015, **Figure 19**).

Although menthol has always been known as a TRPM8 agonist, it can also modulate TRPA1 activity, activating the channel at low concentrations and blocking it at higher concentrations (Karashima et al. 2007). As the percentage of neurons responding to menthol was increased in neurons from males lacking TRESK compared to those of WT males, we wondered whether this effect was mediated by TRPA1 activation. To answer this question, we classified neurons according to their responsiveness to menthol and AITC, and evaluated the role of TRESK in each of the resulting populations. Although both TRP channels are expressed in the same population of peptidergic nociceptors (Jung et al. 2023; Usoskin et al. 2015), (**Table 1**), previously studies indicated that there was little overlap of TRPM8 and TRPA1 expression in DRG neurons (Pogorzala, Mishra, and Hoon 2013). This way, if the increase in the percentage of neurons of TRESK KO mice that responded to menthol compared to the ones from WT mice was mediated by TRPA1 activation, we expected an increase in the percentage of neurons responding to both TRP agonists and no changes in the percentage of neurons responding to menthol alone in neurons from TRESK KO animals compared to neurons from WT animals. On the contrary, we found that just a few neurons responded to both menthol and AITC and that there were no differences in the percentage of neurons from WT and TRESK KO animals responding to both agonists (1.5 %, 1.4 %, 1.9 % and 1 % in neurons from WT males, TRESK KO males, WT females and TRESK KO females, respectively; comparison of percentage of responses using Fisher's exact test, p-values of 0.895 for males and 0.062 for females). Moreover, we saw that the increases in the percentage of neurons from TRESK KO males responding to menthol or AITC, compared to those from WT males described previously, were a result of the increase in neurons responding to just one of the agonists (3.7 % *vs.* 6.3 % of neurons from WT or TRESK KO males responded to menthol but not to AITC, Fisher's exact test p-value of 0.0001; 19.7 % *vs.* 23.8 % neurons from WT or TRESK KO males responded to AITC but not to menthol, Fisher's exact test p-value of 0.0002). In neurons from females, however, we found no differences in the percentage of neurons from WT and TRESK KO

animals responding to just one of the agonists (3.1 % *vs.* 2.8 % of neurons from WT or TRESK KO females responded to menthol but not to AITC, Fisher's exact test p-value of 0.666; 27.6 % *vs.* 25 % neurons from WT or TRESK KO females responded to AITC but not to menthol, Fisher's exact test p-value of 0.112, **Figure 19**). Thus, we can conclude that the role of TRPA1 in the increase in neuronal responses to menthol in TRESK KO animals is negligible.

Variations in the intracellular calcium signal were classified into different subgroups according to their shape. Responses with a fast increase followed with a fast decrease in calcium signal were classified as "peak" responses; responses with a fast increase followed by the maintenance or slow decrease in calcium signal were classified as "sustained" responses; combination of "peak" and "sustained" responses resulting in a fast increase and decrease in calcium signal with a reduced slope before reaching baseline signal levels were classified as "sustained peak" responses; responses with a slow and progressive increase followed by a slow decrease in calcium signal were classified as "rounded" responses; and, finally, "multiple peak" responses, consistent on sequenced "peak" responses, were also detected (see example traces in **Figure 17**). Neurons showed different types of responses depending on the agonist that activated them. Neurons from WT and TRESK KO mice responded similarly to each agonist, although differences between neurons of different genotypes were found (comparison of responses distribution of neurons from WT and TRESK KO animals, Chi-square tests p-values: β-alanine 0.015 and 0.876 for males and females, respectively; menthol 0.201 and 0.061 for males and females, respectively; AITC 0.0003 and 0.0003 for males and females, respectively, and capsaicin 0.018 and < 0.0001 for males and females, respectively, **Figure 19**). Those differences in intracellular calcium changes, including differences in calcium peak amplitude, might be explained by different effects of TRPs and MrgprD activation and, also, due to different composition of channels on different populations of neurons. The effect of TRESK in the shape of calcium responses to β-alanine is further described in the next chapter.

Finally, we observed that subgroups of neurons classified according to their responsiveness to single agonists presented different size distributions, except for the case of neurons from TRESK KO females, that followed similar size distributions independently of their responsiveness (in neurons from TRESK KO females, out of β-alanine-responsive neurons: 25.8 %, 45.5 % and 28.8 % were small-, medium- and large-sized, respectively; out of menthol-responsive: 12.5 % were small-sized, 45.8 % were medium-sized and 41.7 % were large-size;

out of AITC-responsive neurons: 28.2 %, 50.4 % and 21.4 % were small, medium- and large-sized neurons, respectively; and, out of capsaicin-responsive neurons: 27.2 % were small-sized, 47.6 % were medium-sized and 25.1 % were large-sized, Kruskal-Wallis test comparing neuronal sizes of different populations of neurons p-values < 0.0001 for groups of neurons from WT males, WT females, TRESK KO males and 0.233 for groups of neurons from TRESK KO females). In neurons from other mice, capsaicin-responsive neurons had the smallest diameter compared to other groups (out of capsaicin-responsive neurons, 44.4 % were small-sized and 41.4 % were medium-sized in neurons of WT males, 26.9 % were small-sized and 51.7 % were medium-sized in neurons of WT females, and 36.4 % were small-sized and 55.9 % were medium-sized in neurons of TRESK KO males). Menthol-responsive neurons' diameters where the more distributed among the whole range of sizes (40.5 % small-sized, 35.7 % medium-sized and 23.8 % large-sized neurons in WT males, 29.2 % small-sized, 4 1 % medium-sized and 29.9 % large-sized neurons in WT females, and 47.9 % small-sized, 40.8 % medium-sized and 11.3 % large-sized neurons in TRESK KO males) and AITC and β-alanine responsive neurons showed similar distributions to the whole population of neurons (β-alanine-responsive neurons: 38.6 %, 48.2 % and 13.2 % of small, medium- and large-sized neurons of WT males, respectively, 16.3 %, 61.5 % and 22.2 % of small, medium- and large-sized neurons of WT females, respectively, and 23.3 %, 67.5 % and 9.2 % of small, medium- and large-sized neurons of TRESK KO males, respectively; AITC-responsive neurons: 30.3 %, 56.3 % and 13.4 % of small, medium- and large-sized neurons of WT males, respectively, 17.3 %, 58.2 % and 24.6 % of small, medium- and large-sized neurons of WT females, respectively, 19.1 %, and 68.1 % and 12.8 % of small, medium- and large-sized neurons of TRESK KO males, respectively, **Figure 18**).

As shown previously, we found differences in the neuronal sizes of neurons from WT and TRESK KO animals (**Figure 18**). However, both for neurons from male and female animals, TRESK presence did not alter the size of neurons responding to each agonist (comparison of the size of neurons from WT and TRESK KO males depending on their responsiveness to TRP agonists: Kruskal-Wallis multiple comparisons' test p-values: 0.193 and > 0.999 for β-alanine-responsive neurons from males and females, respectively; 0.057 and 0.252 for menthol-responsive neurons from males and females, respectively; 0.073 and 0.053 for AITC-responsive neurons from males and females, respectively, and 0.931 and > 0.999 for

capsaicin-responsive neurons from males and females, respectively). In concordance with the larger diameters of the whole population of analysed neurons from females compared to those from males, we found that neurons from WT females responding to β-alanine, AITC and capsaicin but not to menthol had larger diameters than those of WT males (comparison of the size of neurons from WT males and females depending on their responsiveness: Kruskal-Wallis multiple comparisons' test: < 0.0001 for β-alanine-, AITC- and capsaicin-responsive neurons and > 0.999 for menthol-responsive neurons), while menthol and capsaicin-responsive but not β-alanine and AITC-responsive neurons from TRESK KO females had also larger diameters than those from TRESK KO males (comparison of the size of neurons from TRESK KO males and females depending on their responsiveness: Kruskal-Wallis multiple comparisons' test: 0.812 for β-alanine-responsive, 0.0003 for menthol-responsive, > 0.999 for AITC-responsive and < 0.0001 for capsaicin-responsive, **Figure 18**).

As a summary, our findings indicate that TRESK depletion induces an increase in neuronal responsiveness to β-alanine and capsaicin, both in the percentage of responsive neurons and the intensity of calcium responses. TRESK depletion also increased neuronal responsiveness to menthol and AITC in neurons from males but not from females. These findings indicate that TRESK may have a role in the modulation of non-peptidergic and peptidergic nociceptors chemical sensitivity. Moreover, we identified that neurons showed different patterns and intensities of calcium responses to each of the agonists, being these more intense and sustained in response to the irritant compounds AITC and capsaicin. We also showed differences in the sizes of neurons responding to each agonist and low differences in the size of those groups of neurons depending on their TRESK expression.

Knocking out TRESK increases the β-alanine-responsiveness of populations of neurons responsive to menthol, AITC and capsaicin

As seen, the *Kcnk18* transcript is expressed in 72.1 % of DRG *Mrgprd*-expressing neurons (**Figure 10**) and its depletion in those neurons increases their excitability similarly as treating them with β-alanine (**Figure 13**, **Figure 15**). Moreover, we identified that, compared to neurons from WT animals, more neurons lacking TRESK responded to the MrgprD agonist β-alanine (10.5 % *vs.* 18.9 % of neurons from males, and 8.9 % *vs.* 14.4 % of neurons from females) and with higher calcium increases (increases of +44 ± 4.4 % *vs.* 58.1 ± 4.3 % in

neurons from males, and 45.5 ± 5.2 % *vs.* 62.6 ± 6.5 % in neurons from females, **Figure 19**). As MrgprD-expressing neurons participate in nociception and TRESK seems to modulate their excitability, we decided to characterise the role of TRESK in the β-alanine-responding population of neurons from males and females in more detail.

First, we analysed the calcium peaks induced by β-alanine in neurons from WT and TRESK KO animals. Most neurons from both WT and TRESK KO animals responded with "peak" or "sustained peak" responses to β-alanine. We found that TRESK had a low impact on the type of neuronal calcium responses to β-alanine (**Figure 20**). These results indicate that TRESK probably can not compensate for the activity of the pathways downstream MrgprD, which is in line with the results showing low effects of TRESK on the excitability of MrgprD-expressing neurons once they had been activated (**Figure 15**).

The only TRESK-mediated effects detected were the decrease of "sustained peak" responses of neurons from TRESK KO males compared to those of WT males, probably compensated by increases of the percentage of "peak" and "sustained" responses that do not reach statistical significant levels (comparison of neurons from WT and TRESK KO males, Fisher's exact test: 45.7 % *vs.* 53.5 % of "peak" responses, p-value of 0.083; 41.2 % *vs.* 28.6 % of "sustained peak" responses, p-value of 0.002; 8.5 % *vs.* 13.2 % of "sustained" responses, p-value of 0.106; 3.5 % *vs.* 4.5 % of "multiple peaks" responses, p-value of 0.669, and 1 % *vs.* 0.2 % of "rounded" responses, p-value of 0.256). In DRG neurons from females, types of calcium responses to β-alanine were not altered by TRESK expression (comparison of neurons from WT and TRESK KO females, Fisher's exact test: 38.5 % *vs.* 38.6 % of "peak" responses, p-value > 0.999; 44 % *vs.* 45.6 % of "sustained peak" responses, p-value of 0.838; 15.1 % *vs.* 14.6 % of "sustained" responses, p-value > 0.999; 2 % *vs.* 1.3 % of "multiple peaks" responses, p-value of 0.712, and 0.4 % *vs.* 0 % of "rounded" responses, p-value > 0.999, **Figure 20**).

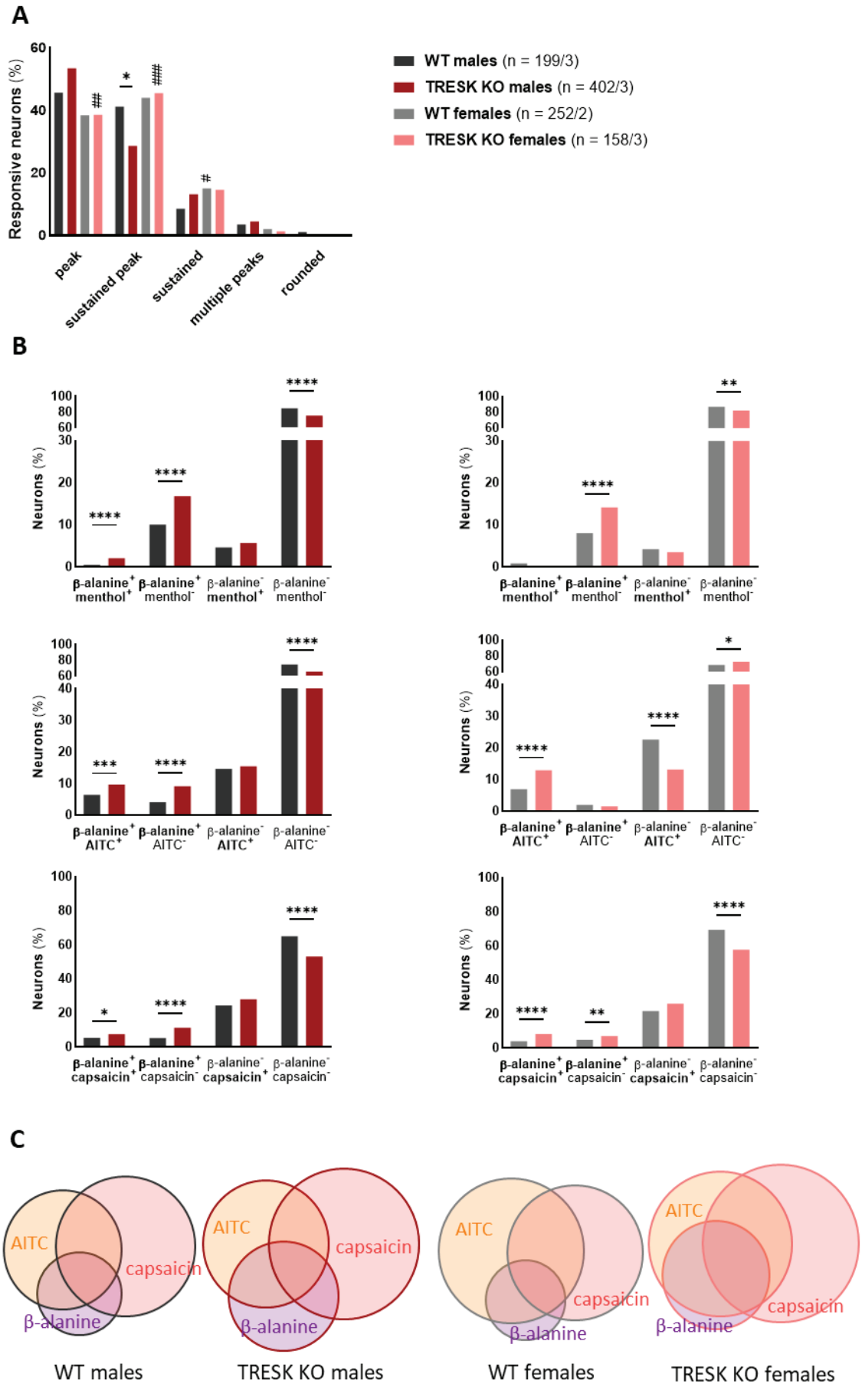
A
Responsive neurons (%)
WT males (n = 199/3)
TRESK KO males (n = 402/3)
WT females (n = 252/2)
TRESK KO females (n = 158/3)
peak
sustained peak
sustained
multiple peaks
rounded
B
Neurons (%)
β-alanine+ menthol+
β-alanine+ menthol-
β-alanine- menthol+
β-alanine- menthol-
β-alanine+ AITC+
β-alanine+ AITC-
β-alanine- AITC+
β-alanine- AITC-
β-alanine+ capsaicin+
β-alanine+ capsaicin-
β-alanine- capsaicin+
β-alanine- capsaicin-
C
AITC
capsaicin
β-alanine
WT males
TRESK KO males
WT females
TRESK KO females

Figure 20. Characterisation of β-alanine-responsive neurons. (a) *Distribution of the types of calcium peaks (shown in* ***Figure 17****) elicited by cultured neurons in response to β-alanine 1mM.* ***(b)*** *Percentage of neurons responding with intracellular calcium increases to β-alanine and another TRP agonist (menthol 100 µM – top, AITC 100 µM – medium or capsaicin 100 nM and/or 1 µM – bottom) classified according to their coresponsiveness.* ***(c)*** *Venn diagrams showing the coresponsiveness to β-alanine, AITC and capsaicin of DRG neurons. The total number of neurons and animals from where they were obtained are indicated in parentheses in section (a) of the figure as: number of cells / number of animals. Differences between groups are analysed using the Fisher's exact test and are shown with asterisks in comparisons of WT vs. TRESK KO (* indicates p-value < 0.05, ** p-value < 0.01, *** p-value < 0.001, and **** p-value < 0.0001) and with pads in comparisons of males vs. females (# indicates p-value < 0.05, ## p-value < 0.01 and ### p-value < 0.001). Statistics are not performed to compare the data from Venn diagrams (c).*

Comparing the responses to β-alanine of neurons from males and females, we observed that neurons from WT females showed more "sustained" responses than those from WT males (Fisher's exact test p-value of 0.042), and that neurons from TRESK KO females followed a similar tendency, with calcium responses more maintained in time (less "peak" responses *vs.* more "sustained peak" responses) compared to TRESK KO males (Fisher's exact test p-values of 0.0002 for "peak" responses and of 0.0002 for "sustained peak" responses).

As explained in Chapter 2.1, single-cell sequencing experiments identified *Mrgprd* expression in DRG specific populations of neurons that also expressed *Trpa1* and *Trpv1* but not *Trpm8* (Jung et al. 2023; Usoskin et al. 2015), (**Table 1**). However, not all neurons from each population show the same gene expression. Here, taking advantage of the experimental design that allowed the sequential exposure of neurons to different agonists (**Figure 17**), we analysed the responsiveness of β-alanine-responsive neurons to menthol, AITC and capsaicin.

As expected, we found only a few cells responding to both β-alanine and menthol (0.5 %, 2.1 %, 0.8 % and 0.3 % of neurons from WT males, TRESK KO males, WT females and TRESK KO females, respectively, **Figure 20**). However, the increase in menthol responsiveness of DRG neurons from TRESK KO males compared to those from WT males (**Figure 19**), was given mainly in the population of neurons responding to β-alanine, as the percentage of neurons responding to both agonists is increased in neurons from TRESK KO males compared to those of WT males, while the percentage of neurons responding to menthol but not β-alanine is maintained (Fisher's exact test p-value < 0.0001 for neurons responding to both agonists and 0.356 for neurons responding only to menthol, percentages of neurons responding only to menthol of 4.7 % and 5.7 % for WT and TRESK KO males, respectively). There were no differences in the percentage of neurons from WT and TRESK KO females responding to both agonists (Fisher's exact test p-value of 0.080). On the other way around, the increase in the

percentage of neurons from TRESK KO animals responding to β-alanine compared to those from WT animals is mainly in neurons that do not respond to menthol, except for the small percentage of neurons from TRESK KO males responding to both agonists commented above (**Figure 20**).

We also analysed the coresponsiveness of β-alanine with AITC and capsaicin, agonists of the nociceptor markers TRPA1 and TRPV1, respectively. We found that considerable numbers of β-alanine responsive cells also responded to one or both of these agonists. 61.3 %, 78.2 %, 51.5 % and 89.4 % of β-alanine responsive neurons from WT males, WT females, TRESK KO males and TRESK KO females, respectively, also responded to AITC while 50.8 %, 45.6 %, 39.8 % and 51.4 % of β-alanine responsive neurons from WT males, WT females, TRESK KO males and TRESK KO females, respectively, also responded to capsaicin (**Figure 20**).

In 2019, C. Wang et al. 2019 demonstrated that TRPA1 is the ion channel downstream MrgprD and that most of the β-alanine-induced calcium signal is mediated by TRPA1. In the previous chapter, we showed that TRESK depletion facilitated neuronal responses to both β-alanine and AITC (**Figure 19**). Here we found that, compared to neurons from WT animals, a higher percentage of neurons from TRESK KO males and females showed calcium increases in response to both β-alanine and AITC (6.5 % of neurons of WT males, 9.7 % of neurons of TRESK KO males, 6.9 % of neurons of WT females and 12.9 % of neurons of TRESK KO females, Fisher's exact test p-values of 0.0002 for neurons from males and <0.0001 for neurons from females), reaching high levels of AITC responsiveness in β-alanine responsive neurons. In fact, the role of TRESK in the increase in the percentage of neurons from TRESK KO females responding to β-alanine, compared to WT females, appeared only in AITC-responsive neurons (1.9 % and 1.5 % of neurons from WT and TRESK KO females responded to β-alanine but not AITC; Fisher's exact test p-value of 0.491). In neurons from male animals, however, TRESK depletion also resulted in an increase in the number of neurons responding to β-alanine but not AITC (4.1 % and 9.2 % of neurons from WT and TRESK KO males responded to both β-alanine and AITC ; Fisher's exact test p-value < 0.0001; Fisher's exact test comparing percentages of neurons from males and females p-values: 0.554 and 0.009 for TRESK KO; **Figure 20**).

Although *Trpv1* transcripts are identified in some subpopulations characterised by their *Mrgprd* expression (Jung et al. 2023; Usoskin et al. 2015), some studies indicated that there

is low or no coexpression of those proteins at the protein level (Rau et al. 2009; Zylka, Rice, and Anderson 2005). Here, we found that large percentages of β-alanine responsive cells also responded to the TRPV1 agonist capsaicin (50.8 %, 15.6 %, 39.8 % and 51.4 % of β-alanine-responsive neurons from WT males, TRESK KO males, WT females and TRESK KO females, respectively, respond to capsaicin). However, among all neurons, little percentages responded to both β-alanine and capsaicin. Only 5.3 %, 7.5 %, 4.1 % and 8.3 % of neurons from WT males, TRESK KO males, WT females and TRESK KO females, respectively, responded to both agonists (**Figure 20**). TRESK depletion, however, increased the percentage of neurons responding to both agonists (Fisher's exact test p-values of 0.035 for neurons from males and < 0.0001 for neurons from females). The increased percentages of neurons from TRESK KO animals responding to β-alanine compared to those from WT animals (**Figure 19**), however, can not be only attributed to the population of neurons responding to both agonists. In fact, the percentage of neurons lacking TRESK that respond to β-alanine but not to capsaicin is increased in both males and females, compared to neurons with the channel (4 %, 8.2 %, 3.8 % and 5.9 % in neurons from WT males, TRESK KO males, WT females and TRESK KO females, respectively, Fisher's exact test p-value < 0.0001 and of 0.004 for males and females, respectively). On the other side, TRESK did not alter the percentages of neurons from males and females responding to capsaicin but not β-alanine (18.8 %, 20 %, 17.2 % and 19.4 % of capsaicin- but not β-alanine responsive neurons of WT males, TRESK KO males, WT females and TRESK KO females, respectively, Fisher's exact test p-values of 0.242 for neurons from males and 0.085 for neurons from females, **Figure 20**).

We also found that some of β-alanine-responsive neurons responded to both AITC and capsaicin (**Figure 20**). Considering single-cell sequencing studies' classification of DRG neuronal populations, those neurons are likely to be non-peptidergic nociceptors expressing TRESK (NP1 and NP2 populations in Usoskin et al., although there is also coexpression of the three markers in PEP1 population of peptidergic nociceptors that do not express the K_{2P} channel, **Table 1**). Low number of DRG neurons responded to the three agonists: 3.4 %, 3.2 %, 3.3 % and 6.9 % of neurons from WT males, TRESK KO males, WT females and TRESK KO females. While, in neurons from male animals, TRESK depletion increased the responsiveness of β-alanine, AITC and capsaicin (**Figure 19**), and the number of neurons responding to both β-alanine and AITC and β-alanine and capsaicin (**Figure 20**), the channel had no effect on the

number of neurons responding to the three agonists (Fisher's exact test p-value of 0.790). Thus, the effects of TRESK in the responsiveness to β-alanine, AITC and capsaicin are not in the population of neurons from male animals responding to the three agonists. In the neurons from females, however, a higher percentage of neurons lacking TRESK responded to all β-alanine, AITC and capsaicin compared to those with the channel (Fisher's exact test p-value < 0.0001), pointing to an effect of the channel in the regulation of this population of neurons' responsiveness.

Knocking out TRESK increases the cold-responsiveness of neurons from female but not from male mice

As detailed in Chapter 2.1, TRPM8 and TRPA1 are known cold sensors. Moreover, different studies found that neurons expressing TRPA1, TRPV1 or MrgprD can mediate noxious cold sensing and that TRPM8-expressing neurons are responsible for mild-cold sensing. Castellanos et al. 2020 showed that mice lacking TRESK have increased sensitivity to mild and noxious cold, and that their cold-sensing fibres tend to be activated at higher temperatures compared to neurons from WT animals. As we already proved the role of TRESK in modulating the neuronal responsiveness to β-alanine, menthol, AITC and capsaicin (**Figure 19**), we wanted to unveil its role in the modulation of the cold sensitivity of the populations of DRG neurons responding to those agonists. To do so, we studied the calcium activity of cultured DRG neurons when challenging them with a temperature ramp from 31.0 ± 0.1 °C to 11.6 ± 0.2 °C in 40 seconds before the addition of MrgprD and TRPs agonists (**Figure 17**).

First, we saw that DRG neurons from WT females responded less to the cold ramp than those from WT males (15.6 % and 11.7 % of neurons from WT males and females, respectively, Fisher's exact p-value of 0.0002). A higher percentage of neurons from TRESK KO females responded to cold compared to neurons from WT females (20.7 % of neurons from TRESK KO males, Fisher's exact test p-value < 0.0001). Curiously, we found no effects of TRESK on the percentage of neurons from males responding to the cold ramp (14.5 % of neurons from TRESK KO males, Fisher's exact p-value of 0.350, **Figure 21**).

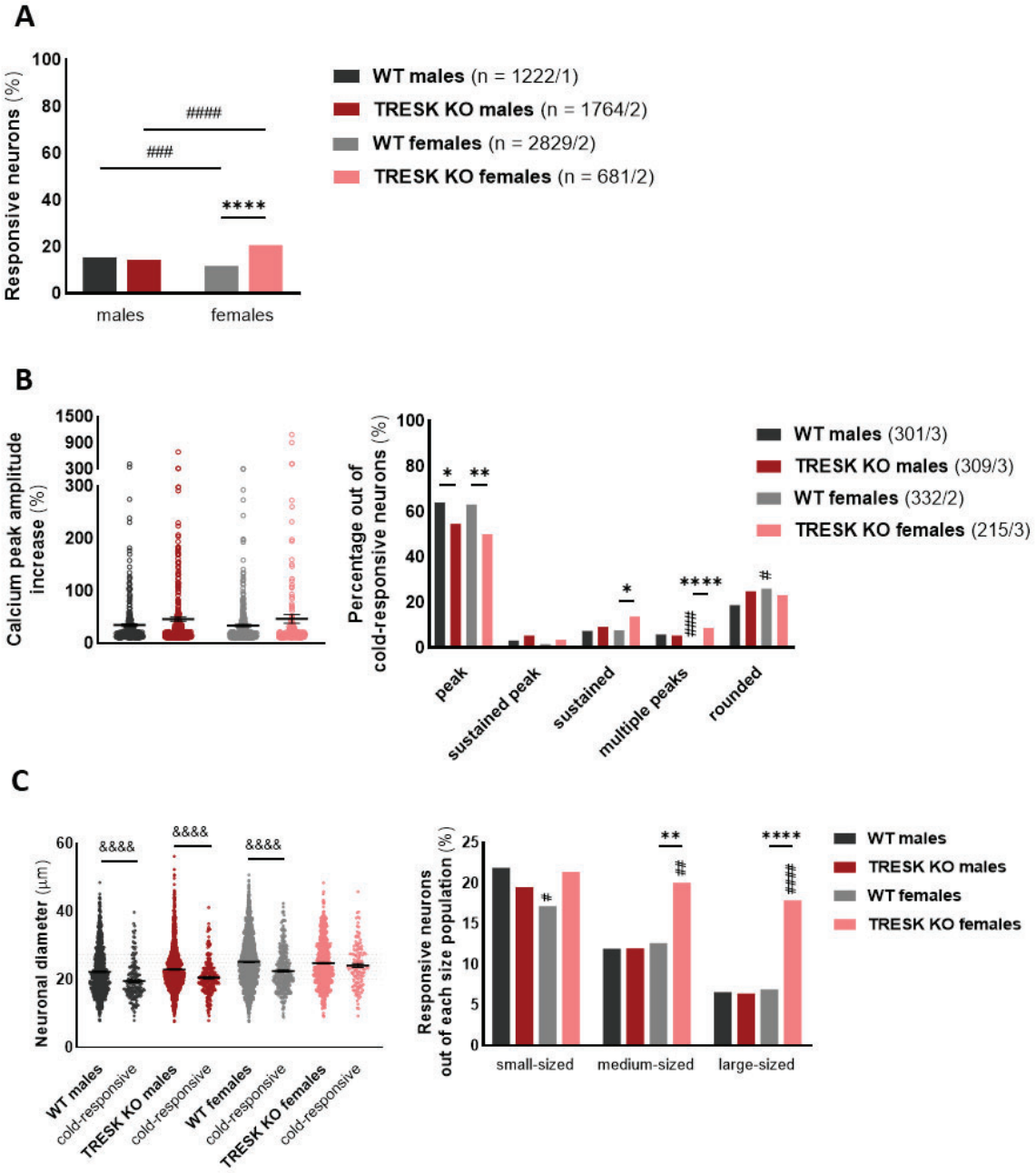

Figure 21. Primary sensory neurons' responsiveness to cold. Characteristics of the intracellular calcium increases detected using Fura-2 in response to a cold ramp from 31.0 ± 0.1 °C to 11.6 ± 0.2 °C. (a) *Top left: Percentage of neurons from WT and TRESK KO males and females responding to the cold ramp.* ***(b)*** *Characteristics of the calcium peak elicited by sensory neurons in response to the cold ramp. The number of cold-sensitive animals and the animals from which they come from are indicated in subsection b – right. Left: Increase in intracellular calcium levels in relation to baseline calcium levels. Single dots indicate the peak intensities of single cold-responding cells, and lines indicate the mean ± SEM. Right: Percentage of cold-responsive neurons of each group showing calcium peaks of different shapes (described in* ***Figure 17****) in response to the cold ramp.* ***(c)*** *Neuronal size of cold-responsive neurons in relation to the whole population of neurons analysed. Diameter of cold-sensitive neurons and all the neurons analysed by groups shown using individual dots for individual neurons and lines for mean ± SEM (left). Distribution of cold-responsive neurons grouped by ranges of sizes (defined by Herweijer G et al., 2014, right). The total number of neurons analysed is shown in section (a) and the number of cold-sensitive neurons is shown in section (b) together with the number of animals from which they come from in parentheses as: number of cells / number of animals. Statistical analysis using Fisher's exact tests (for percentages of neurons), Mann-Whitney test (for calcium peak amplitude), and Kolmogorov-Smirnov (for*

*neuronal diameter). P-values indicate the statistical significant differences between WT and KO: * for p-value < 0.05, ** for p-value < 0.01 and **** for p-value < 0.0001; between males and females: # for p-value < 0.05, ## for p-value < 0.01, ### for p-value < 0.001 and #### for p-value < 0.0001, and between the whole population of neurons analysed and the population of cold sensitive neurons: &&&& for p-value < 0.0001.*

Cold-sensitive DRG neurons responded with low calcium increases to the temperature ramp. Sensory neurons from TRESK KO animals tended to show higher calcium increases compared to those from WT animals, especially from males, although those differences did not reach statistically significant levels (calcium increase of +34.7 ± 2.7 % in neurons from WT males, 46 ± 3.8 % in neurons from TRESK KO males, 33.9 ± 2.4 % in neurons from WT females and 46.5 ± 8.3 % in neurons from TRESK KO females, Mann-Whitney test p-values of 0.076 for males and 0.422 for females, **Figure 21**). In concordance with a possible role of TRESK in modulating neuronal responses to cold, we found that neurons from TRESK KO males and females showed less "peak" responses and more responses maintained in time ("sustained peak" and "sustained" responses), especially in the case of neurons from female animals (for WT males, TRESK KO males, WT females and TRESK KO females: 64.1 %, 54.7 %, 63.3 % and 50.2 % of "peak" responses, 3.3 %, 5.5 %, 1.8 % and 3.7 % of "sustained peak" responses, 7.6 %, 9.4 %, 7.8 % and 14% of "sustained" responses, 6 %, 5.5 %, 0.9 % and 8.8 % of "multiple peaks" responses, and 18.9 %, 24.9 %, 26.2 % and 23.3 % of "rounded" responses; Fisher's exact test p-values: for "peak" responses: 0.021 and 0.003 for males and females, respectively, for "sustained peak" responses: 0.238 and 0.177 for males and females, respectively, for "sustained" responses: 0.471 and 0.030 for males and females, respectively, for "multiple peaks" responses: 0.863 and < 0.0001 for males and females, respectively, and for "rounded" responses: 0.079 and 0.480 for males and females, respectively, **Figure 21**).

Neurons responding to cold were mainly small- and medium-sized, except those obtained from TRESK KO females, that were distributed among the whole range of diameters (59.9 %, 30.8 % and 9.3 % of small-, medium- and large-sized neurons of WT males, respectively; 43.8 %, 47.2 % and 9 % of small-, medium- and large-sized neurons from TRESK KO males, respectively; 33.4 % of small, 46.4 % of medium and 20.2 % of large-sized and 26.9 % of small, 42.5 % of medium and 30.6 % of large-sized neurons from WT and TRESK KO females, respectively; comparison of cold-sensitive neurons diameters and the whole population of neurons diameters: Kolmogorov-Smirnov test p-values < 0.0001 for neurons from WT males, WT females and TRESK KO males and of 0.710 for neurons of TRESK KO females, **Figure 21**). TRESK depletion increased the percentage of medium- and large-neurons from females

responding to cold while, similarly to the effects on the whole population of neurons from males, it had no effect on the cold-responsiveness of different populations of neurons from males according to their size (comparison of WT *vs.* TRESK KO: 21.9 % *vs.* 19.5 % and 17.2 % *vs.* 21.4 % of small-sized neurons from WT males, TRESK KO males, WT females and TRESK KO females, respectively, responded to cold; 12 % *vs.* 12 % and 12.6 % *vs.* 20.1 % of medium-sized neurons from WT males, TRESK KO males, WT females and TRESK KO females, respectively, responded to cold, and 6.6 % *vs.* 6.4 % and 7 % *vs.* 17.9 % of large-sized neurons from WT males, TRESK KO males, WT females and TRESK KO females, respectively, responded to cold; Fisher's exact test p-values of small-, medium- and large-sized neurons of 0.354, > 0.999 and > 0.999 for males, and of 0.216, 0.002 and < 0.0001 for females; **Figure 21**).

Some cold-sensitive DRG neurons also respond to β-alanine, menthol, AITC and/or capsaicin. TRESK depletion had different effects on the proportion of cold-sensitive neurons responding to those agonists depending on the sex of the animals from where DRG neurons were obtained. 28.7 %, 22.4 %, 16.7 % and 39 % of β-alanine-responsive neurons from WT males, TRESK KO males, WT females and TRESK KO females, respectively, responded to the cold ramp. TRESK depletion resulted in an increase of the β-alanine-responsive neurons from females but not males that respond to cold (Fisher's exact test p-values of 0.104 and < 0.0001 for neurons from males and females, respectively; **Figure 22**). In neurons from both males and females, TRESK depletion resulted in an increase in the number of cold-sensitive neurons responding to β-alanine (19.6 % *vs.* 29.1 % and 12.7 % *vs.* 29.1 % of cold-sensitive neurons from WT males, TRESK KO males, WT females and TRESK KO females, respectively, responded to the MrgprD agonist, Fisher's exact test p-values: 0.008 and <0.0001 for neurons from males and females, respectively). TRESK depletion resulted in an increase in the neurons from both males and females responding to both stimuli (3.1 %, 4.2 %, 1.5 % and 5.6 % of neurons from WT males, TRESK KO males, WT females and TRESK KO females, respectively, Fisher's exact test p-values of 0.035 for males' neurons and < 0.0001 for females' neurons, **Figure 22**). In neurons from males, this effect seemed to come from an increase in the number of cold-responsive neurons that responded to β-alanine, as the number of neurons responding to cold but not to β-alanine tended to decrease in TRESK KO males compared to WT males (12.5 % of neurons from WT males and 10.3 % of neurons from TRESK KO males, Fisher's exact test of 0.057). In females, however, the number of cold-responsive neurons that do not respond

to β-alanine was increased in neurons from TRESK KO females in comparison to those from WT females (10.2 % of neurons from WT females and 15.1 % of neurons from TRESK KO females, Fisher's exact test p-value < 0.0001), indicating that β-alanine-responsive neurons are not the only population of neurons from female animals that increases its sensitivity to cold when TRESK lacks (**Figure 22**).

As expected, some cold-sensitive neurons also responded to the TRPM8 agonist menthol. 15.7 %, 26.5 %, 19.3 % and 8.4 % of cold-responsive neurons from WT males, TRESK KO males, WT females and TRESK KO females, respectively, to both cold temperatures and menthol. Although neurons from TRESK KO males do not respond more to the cold ramp than neurons from WT males (**Figure 21**), TRESK KO depletion in neurons from male animals resulted in an increase in the neurons responding to both cold and menthol (2.5 % of neurons from WT males *vs.* 3.8 % of neurons from TRESK KO males, Fisher's exact test p-value of 0.009, **Figure 22**). Similarly to the responsiveness to both cold and β-alanine, the increase in the number of neurons from male animals lacking TRESK responding to both cold and menthol seemed to be due to an increase in the menthol responsiveness of cold-responsive neurons, as the percentage of neurons of TRESK KO males responding to cold but not to menthol is lower than the one of neurons from WT males (12.8 % of neurons from WT males *vs.* 10.7 % of neurons from TRESK KO males, Fisher's exact test p-value of 0.039). TRESK expression did not change the percentage of neurons from females responding to both cold and menthol (2.3 % of neurons from WT animals and 1.7 % of neurons from TRESK KO animals, Fisher's exact test p-value of 0.370). These results are in concordance with the lack of TRESK effect in the menthol responsiveness of neurons from females and indicate that TRESK is not modifying the responsiveness of the population of neurons sensitive to cold and menthol (**Figure 19**, **Figure 22**). Although some cold-sensitive neurons respond to β-alanine or menthol, we found only a few cold-sensitive neurons responding to both β-alanine and menthol (2.8 %, 2.7 %, 9.1 % and 1 % of cold-sensitive neurons from WT males, WT females, TRESK KO males and TRESK KO females, respectively; **Figure 22**). Those results are consistent with previous studies defining MrgprD-expressing neurons and TRPM8-expressing neurons as two different populations of neurons showing different responses to different cold stimuli.

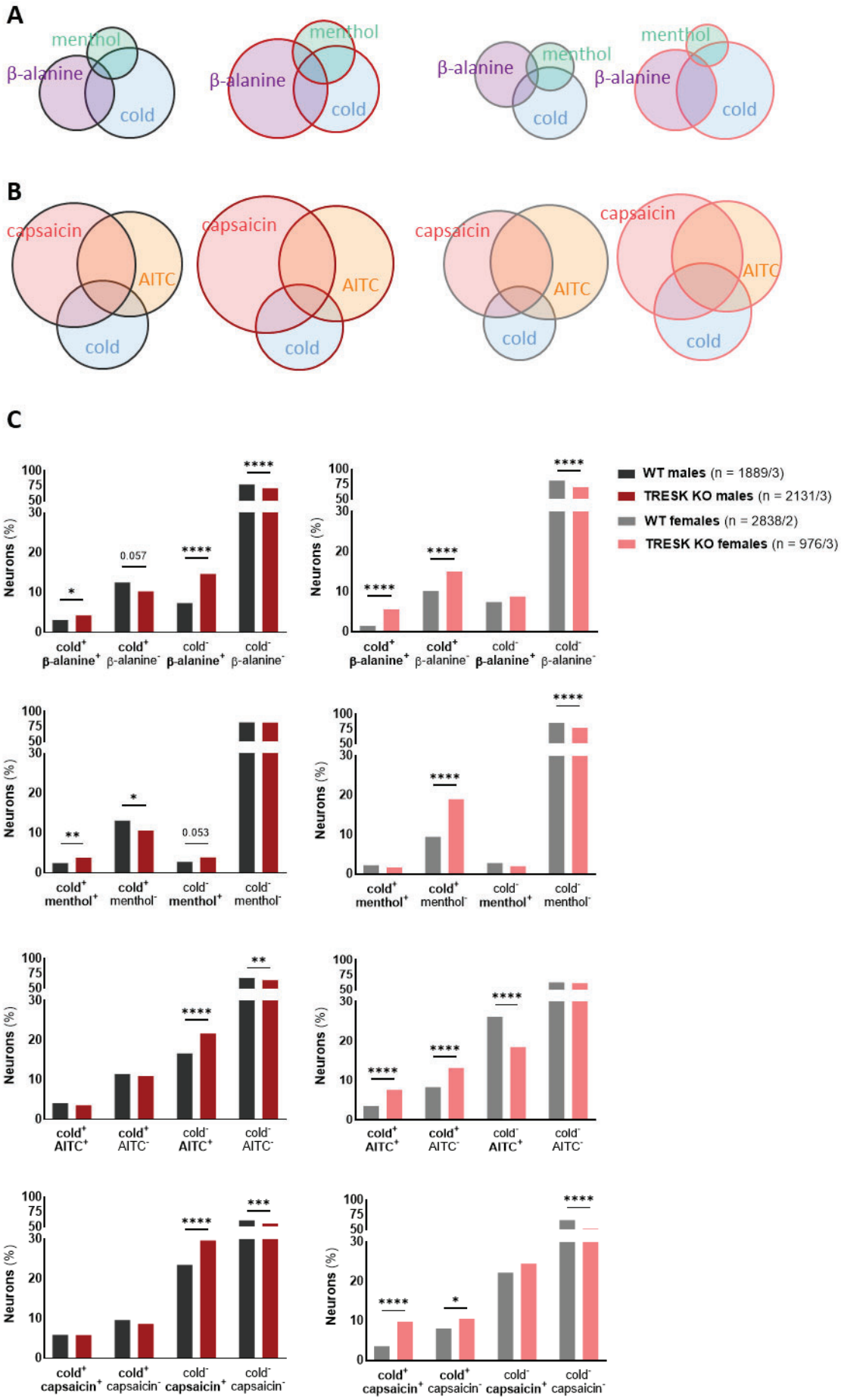
A
menthol
β-alanine
cold
B
capsaicin
AITC
cold
C
WT males (n = 1889/3)
TRESK KO males (n = 2131/3)
WT females (n = 2838/2)
TRESK KO females (n = 976/3)
Neurons (%)
cold+ β-alanine+
cold+ β-alanine-
cold- β-alanine+
cold- β-alanine-
cold+ menthol+
cold+ menthol-
cold- menthol+
cold- menthol-
cold+ AITC+
cold+ AITC-
cold- AITC+
cold- AITC-
cold+ capsaicin+
cold+ capsaicin-
cold- capsaicin+
cold- capsaicin-

Figure 22. Cold-responsive neurons' responsiveness to MrgprD and TRPs agonists. *Classification of the cold-responsive neurons (activated by a cold ramp from 31.0 ± 0.1 °C to 11.6 ± 0.2 °C) according to their responsiveness to β-alanine 1 mM, menthol 100 µM, AITC 100 µM and capsaicin 100 nM and/or 1 µM. Comparison of the coresponsiveness of neurons to different stimuli depending on the neuronal provenance from WT or TRESK KO animals. Venn diagrams showing populations of neurons according to their responsiveness to cold, menthol and β-alanine* ***(a)*** *or to cold, AITC and capsaicin* ***(b)****. Statistics are not performed to compare the data from Venn diagrams.* ***(c)*** *Percentage of neurons responding with intracellular calcium increases to the cold ramp, β-alanine, menthol, AITC or capsaicin classified according to their coresponsiveness. The total number of neurons and animals from where they were obtained are indicated in parentheses in the section (c) of the figure as: number of cells / number of animals. Differences between WT and TRESK KO are analysed using the Fisher's exact test and shown using asterisks (* indicates p-value < 0.05, ** p-value < 0.01, *** p-value < 0.001, and **** p-value < 0.0001), and numbers (p-values close to the established level of significance of 5 %).*

Thus, TRESK is involved in the modulation of the responsiveness of cold- and β-alanine-sensitive neurons from both males and females but only of the cold- and menthol-sensitive neurons from males. On the other side, the channel plays a role in the modulation of the responsiveness of cold- and AITC-sensitive neurons and of cold- and capsaicin-sensitive neurons only from females. Out of cold-responsive neurons from WT and TRESK KO males, 26.6 % and 24.3 % responded to AITC, and 38.1 % and 40.5 % responded to capsaicin, respectively. Out of cold-responsive neurons from WT and TRESK KO females, 29.5 % and 36.6 % responded to AITC, and 30.7 % and 45.2 % responded to capsaicin, respectively. Thus, a high proportion of cold-sensitive neurons responded to AITC and/or capsaicin, but only 13.6 %, 11 %, 15.7 % and 18.3 % of cold-responsive neurons from WT males, TRESK KO males, WT females and TRESK KO females responded to AITC and capsaicin (**Figure 22**). As said, we found the same proportion of neurons from WT and TRESK KO males responding to cold and AITC (4 % *vs.* 3.5 %, Fisher's exact test p-value of 0.407) and to cold and capsaicin (5.8 % *vs.* 5.9 %, Fisher's exact test p-value of 0.946), while more neurons from TRESK KO females responded to cold and AITC (3.5 % *vs.* 7.6 %, Fisher's exact test p-value < 0.0001) and to cold and capsaicin (3.6 % *vs.* 8.7 %, Fisher's exact test p-value < 0.0001), compared to those from WT females. As TRPA1 and TRPV1 are mostly expressed in nociceptors, the effect of TRESK in these neurons is likely to modulate noxious cold. However, the effect of TRESK on the cold responsiveness of females' neurons was not only in the AITC- or capsaicin-responsive populations, as we also saw increases in the proportion of neurons lacking TRESK responding to cold in neurons unresponsive to AITC or capsaicin (8.2 % of neurons from WT females and 13.1 % of neurons from TRESK KO females responded to cold but not to AITC, comparison with Fisher's exact test, p-value < 0.0001; 8.1 % of neurons from WT females and 10.6 % of

neurons from TRESK KO females responded to cold but not to capsaicin, comparison with Fisher's exact test, p-value of 0.021; **Figure 22**).

As neuronal responses to different agonists led to different types of calcium responses (**Figure 19**), we wondered whether responses to cold in the different populations of neurons were also different and whether TRESK influenced their amplitude and shape. First, we found that cold-induced calcium peaks showed smaller amplitudes than those generated by MrgprD and TRPs agonists on the same neurons, except in the case of cold responses to menthol-responsive neurons from WT males, WT females and TRESK KO males, which reached higher calcium amplitude levels compared to those induced by menthol (calcium increases in response to cold ramp: 25.9 ± 2.9 %, 67.6 ± 10 %, 37.3 ± 4.7 % and 37.8 ± 4.2 % in β-alanine-responsive, menthol-responsive, AITC-responsive and capsaicin-responsive neurons of WT males, respectively; 39.3 ± 9.4 %, 72.9 ± 9.3 %, 25.3 ± 3.1 % and 35.4 ± 4.5 % in β-alanine-responsive, menthol-responsive, AITC-responsive and capsaicin-responsive neurons of WT females, respectively; 44.7 ± 5.8 %, 83.6 ± 8.4 %, 41.1 ± 9.7 % and 46.4 ± 6.6 % in β-alanine-responsive, menthol-responsive, AITC-responsive and capsaicin-responsive neurons of TRESK KO males, respectively; 25.5 ± 3.6 %, 30 ± 7.1 %, 62.4 ± 20 % and 27.4 ± 4.1 % in β-alanine-responsive, menthol-responsive, AITC-responsive and capsaicin-responsive neurons of TRESK KO females, respectively; Mann-Whitney test p-values comparing peaks elicited by cold compared to those elicited by MrgprD or TRPs agonists activating the same set of neurons: < 0.0001, 0.0001, < 0.0001 and < 0.0001 for β-alanine-responsive neurons of WT males, WT females, TRESK KO males and TRESK KO females, respectively, 0.004, 0.006, 0.145 and 0.301 for menthol-responsive neurons of WT males, WT females, TRESK KO males and TRESK KO females, respectively, < 0.0001 for AITC-responsive and capsaicin-responsive neurons of all genotypes, **Figure 19**, **Figure 23**). As TRPM8 and TRPA1 are cold sensors, this may indicate that cold is activating more TRPM8 receptors than menthol while it is less capable to activate TRPA1 or downstream pathways than AITC, or that the stimuli that activates more each cell is doing it by recruiting more receptors. This indicates that cols temperatures and specific agonists may activate different receptors and downstream pathways in overlapping populations of neurons.

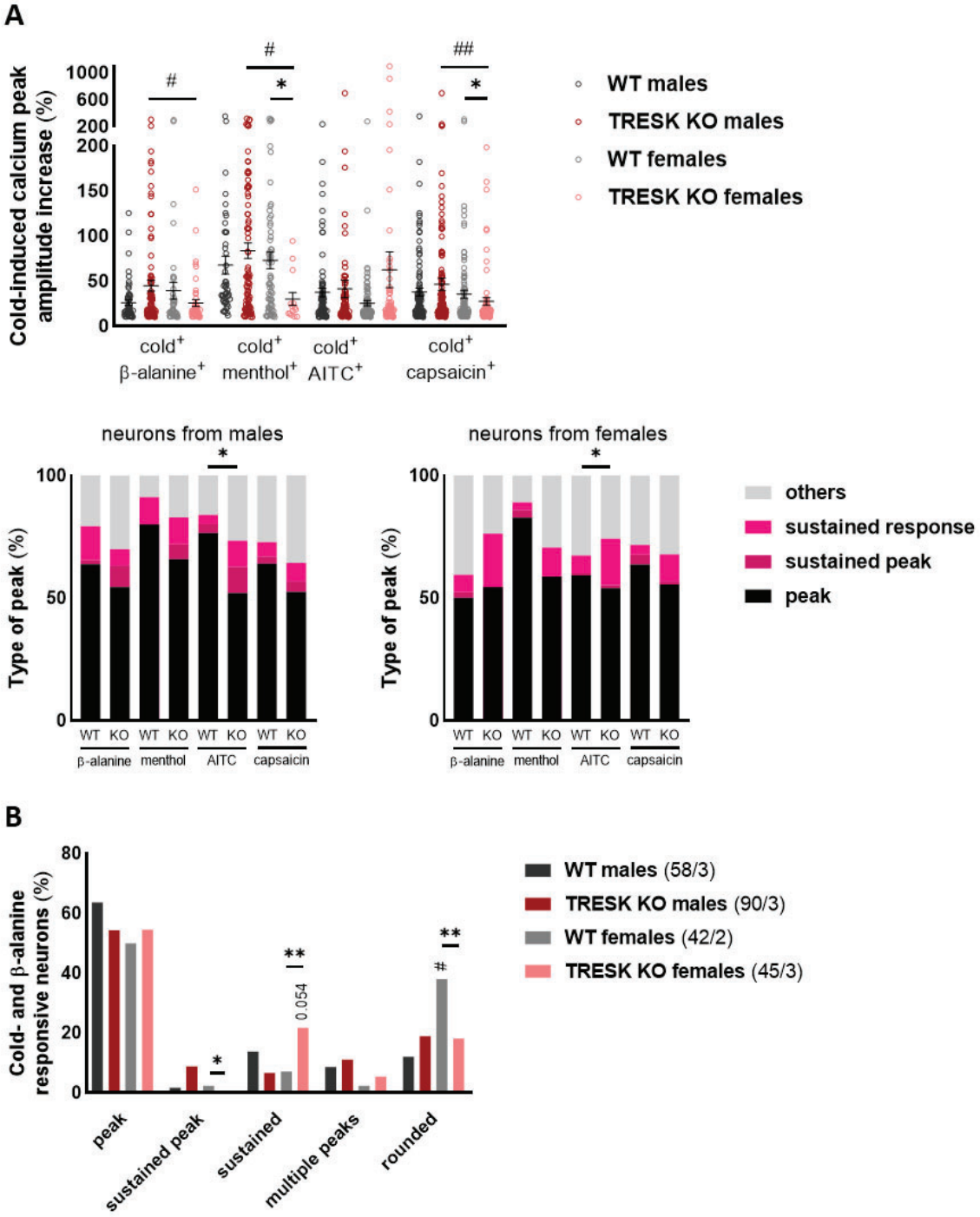

Figure 23. Characterisation of cold-responsive neurons populations classified according to their responsiveness to MrgprD and TRPs agonists. (a) *Characteristics of the intracellular calcium peaks in response to cold stimuli of populations of neurons responding to β-alanine 1 mM, menthol 100 µM, AITC 100 µM and capsaicin 100 nM or 1 µM. DRG neurons obtained from 3 WT males, 3 TRESK KO males, 2 WT females and 3 TRESK KO female mice. From each of these groups, 58, 90, 42 and 45 cold- and β-alanine-responsive neurons, 45, 82, 64 and 14 cold- and menthol-responsive, 81, 75, 98 and 62 cold- and AITC-responsive, and 112, 125, 102 and 52 cold- and capsaicin-responsive were analysed, respectively. Top: Peak amplitudes shown as the relative increment of intracellular calcium in relation to baseline levels of each neuron. Dots indicate values of single cells, lines the mean and SEM for each group. Bottom: Distribution of calcium peaks elicited by neurons in response to a cold ramp according to their shape (see peak shapes in Figure 10B).* ***(b)*** *Further detailed distribution of calcium peaks elicited by β-alanine-responsive neurons in response to a cold ramp according to their shape (see peak shapes in Figure 10B). The total number of neurons and animals from where they were obtained are indicated in*

parentheses as: number of cells / number of animals. Differences between groups are analysed using the Mann-Whitney test (to compare peak amplitudes), the Chi-square test (to compare the "simplified" distribution of peaks by shape in the subsection a) and the Fisher's exact test (to compare the distribution of peaks by shape in the subsection b). Differences of neurons from WT and TRESK KO animals are represented using asterisks (indicates p-value < 0.05 and ** p-value < 0.01), and differences between neurons from male and female mice using pads (# indicates p-value < 0.05, ## p-value < 0.01 and numbers for p-values close to the established level of significance of 5 %).*

We showed that, in response to cold, neurons responsive to β-alanine, AITC and capsaicin showed similar calcium peak amplitudes, which were smaller than those elicited by menthol-responsive neurons (Kruskal-Wallis multiple comparisons test p-values of < 0.0001, 0.0001 and 0.0001 when comparing the cold peaks of menthol-responsive neurons with β-alanine-responsive, AITC-responsive and capsaicin responsive neurons of WT males, respectively, and of 0.0006, < 0.0001 and 0.0002 when comparing the cold peaks of menthol-responsive neurons with β-alanine-responsive, AITC-responsive and capsaicin responsive neurons of WT males; **Figure 23**). Similarly, we found no differences in the patterns of calcium peak shapes of the different groups of cold-sensitive neurons of different genotypes (comparison of cold-induced peaks shape distribution of different neuronal populations: Chi-square test p-values of 0.199 for neurons from WT males, 0.084 for neurons from WT females, 0.198 for neurons from TRESK KO males and 0.849 for neurons from TRESK KO females, **Figure 23**).

Moreover, we found that TRESK expression did not modify the amplitude of calcium peaks in response to cold of the different populations of neurons of male animals (Mann-Whitney test p-values of 0.304, 0.321, 0.894 and 0.804 for β-alanine-responsive, menthol-responsive, AITC-responsive and capsaicin-responsive neurons from males, respectively). Surprisingly, in neurons from females, TRESK depletion resulted in a decrease in the amplitude of calcium responses to cold in menthol-responsive and capsaicin-responsive neurons, while it had no effects on β-alanine-responsive and AITC-responsive neurons (Mann-Whitney test p-values of 0.383, 0.016, 0.324 and 0.034 for β-alanine-responsive, menthol-responsive, AITC-responsive and capsaicin-responsive neurons from females, respectively, **Figure 23**). The distribution of the shapes of calcium responses to cold in the identified populations of neurons is similar in neurons with and without TRESK, except in the case of AITC-responsive neurons of males and females, where TRESK depletion increases the proportion of calcium maintained responses in detriment of "peak" responses (Chi-square test p-values: 0.157, 0.247, 0.018 and 0.173 for β-alanine-responsive, menthol-responsive, AITC-responsive and capsaicin-responsive neurons from males, respectively, and 0.067, 0.100, 0.048 and 0.121 for

β-alanine-responsive, menthol-responsive, AITC-responsive and capsaicin-responsive neurons from females, respectively, **Figure 23**). When analysing deeper the calcium responses to cold stimuli of β-alanine-responsive neurons, we found no effects of TRESK depletion in neurons from males but an increase in the percentage of "sustained" responses in detriment of "sustained peaks" and "rounded" responses, that decreased in neurons from TRESK KO females (Fisher's exact test p-values of 0.307, 0.090, 0.162, 0.783 and 0.362 for "peak", "sustained peak", "sustained", "multiple peaks" and "rounded" responses of neurons from male animals, respectively, and of 0.686, 0.433, 0.054, 0.631 and 0.038 for neurons from females, **Figure 23**).

To sum up, some DRG neurons responded to a cold ramp from 31.0 ± 0.1 °C to 11.6 ± 0.2 °C with small increases of intracellular calcium. TRESK depletion resulted in an increase in the number of neurons of different sizes from female animals responding to cold, although it had no effects on the percentage of cold-responding neurons from males, neither on the amplitude of calcium responses to cold of neurons from males and females. Some cold-sensitive neurons respond to β-alanine, menthol, AITC and capsaicin, which allows their classification into different subpopulations. Although their classification into different subpopulations, we found little differences in the patterns and amplitudes of their calcium responses to cold temperatures, which point to similar mechanisms being activated by cold in the different populations. TRESK had different effects on cold-sensitive populations of neurons depending on the sex of the animals from where they come from. TRESK depletion resulted in an increase in the number of neurons from males and females responding to both cold and β-alanine, while it had little effects on the characteristics of their calcium responses to cold. It also increased the number of neurons from male animals responding to both cold and menthol, and the number of neurons from females responding to both cold and AITC, and cold and capsaicin.

TRESK expression modifies the threshold temperatures to activate cold-sensing neurons

As explained, different populations of DRG neurons sense different ranges of temperatures and participate in different types of cold sensing, from unpleasant cool sensing (> 26.5 °C) to noxious cold (< 19 °C). In the previous chapter we have described our findings indicating that

some neurons from different populations classified according to their responsiveness to β-alanine, menthol, AITC and capsaicin, together with other populations unresponsive to those agonists, sense cold, and that TRESK had effects in the responsiveness of all the cold-sensitive populations responding to the agonists used. Taking this into account, we wondered whether TRESK is involved in the sensitivity of specific temperatures and whether it affects the neuronal sensitivity of the different DRG populations to different ranges of temperatures.

As we stimulated the cells with a cold ramp from 31.0 ± 0.1 °C to 11.6 ± 0.2 °C in 40 seconds (**Figure 17**), we could identify the temperature at which the calcium increases start. We observed some variability in the temperatures of stimulation depending on the flux of recording solution for each experiment. First, we found that neurons from WT and TRESK KO animals were activated by temperatures from 33 to 9.5 °C following different distributions of temperatures (Kolmogorov-Smirnov test p-value of 0.0001 for male neurons and of 0.0004 for female neurons, **Figure 24**). Most of the cold-sensitive neurons responded at the very beginning of the cold ramp, during the decrease from baseline temperature to the first following degree temperature (38.2, 40.1, 51.5 and 26.8 % out of cold-responsive neurons of WT males, TRESK KO males, WT females and TRESK KO females, respectively).

Following Madrid et al. 2009, we classified activating temperatures as low threshold (LT) temperatures when higher than 26.5 °C, high threshold (HT) temperatures when found between 26.5 and 19 °C, and very high threshold (vHT) temperatures when lower than 19 °C. Most of cold-responsive neurons showed calcium signals at LT temperatures (8.9, 8.6, 7.2 and 8.2 % out of the total number of neurons from WT males, TRESK KO males, WT females and TRESK KO females, respectively), but others also responded to HT (3.9, 4, 3.3 and 4.1 % out of the total number of neurons from WT males, TRESK KO males, WT females and TRESK KO females, respectively) and vHT temperatures (3.6, 1.9, 1.2 and 4.5 % out of the total number of neurons from WT males, TRESK KO males, WT females and TRESK KO females, respectively). While it had no effects on the percentage of neurons responding to low and high temperatures, TRESK depletion reduced the percentage of neurons of male animals and increased the percentage of neurons from female animals that responded to very high temperatures (comparison of WT *vs.* TRESK KO: Fisher's exact test p-values of 0.735, 0.870 and 0.002 for low threshold, high threshold and very high threshold responsive neurons from

males, respectively, and 0.322, 0.267 and < 0.0001 for low threshold, high threshold and very high threshold responsive neurons from females, respectively, **Figure 24**).

We also wondered whether different threshold temperatures resulted in different calcium peak characteristics and, although we only found a tendency for higher amplitudes of calcium peaks in response to cold (**Figure 21**), whether TRESK might have a role in the modulation of the calcium responses to specific temperatures. We tried to fit the relation of calcium peak amplitudes with threshold temperatures (ThT) using linear regression and found that different temperatures elicit calcium peaks of similar amplitude (calcium peak amplitude = 0.676 ThT + 17.5 % for neurons from WT males, 0.178 ThT + 41.4 % for neurons from TRESK KO males, 0.082 ThT + 31.7 % for neurons from WT females, and 0.167 ThT + 40.6 % for neurons from TRESK KO females; differences to slope of "0: p-values of 0.112 for neurons of WT males, 0.795 for neurons of TRESK KO males, 0.861 for neurons of WT females, and 0.879 for neurons of TRESK KO females). Comparing linear regressions, we found that neurons from TRESK KO animals showed higher calcium amplitudes than those from WT at all temperatures (p-value of 0.022, **Figure 24**).

Neurons with the same sex and genotype showed similar distributions of the shape of cold-induced calcium increases independently of the temperature at which they were activated, except for neurons from TRESK KO males, that showed more maintained responses and less "peak" responses in response to LT temperatures compared to vHT (comparison of the distribution of types of calcium peaks on different temperatures: Chi-square test p-values of 0.964 for WT males, 0.027 for TRESK KO males, 0.934 for WT females and 0.732 for TRESK KO females; comparison of distributions within different threshold groups of TRESK KO males: Fisher's exact test p-values of 0.107 comparing LT *vs.* HT, of 0.488 comparing HT *vs.* vHT, and of 0.017 comparing LT *vs.* vHT). TRESK depletion resulted in a change in the distribution of types of calcium responses only to LT temperatures in neurons from males, but had no effects on the shape of calcium peaks of neurons from females (comparisons of neurons from WT and TRESK KO animals: Chi-square test p-values of 0.019, 0.916 and 0.638 for LT, HT and vHT-responsive neurons from males, respectively, and of 0.483, 0.125, 0.232 for LT, HT and vHT-responsive neurons from females, **Figure 24**).

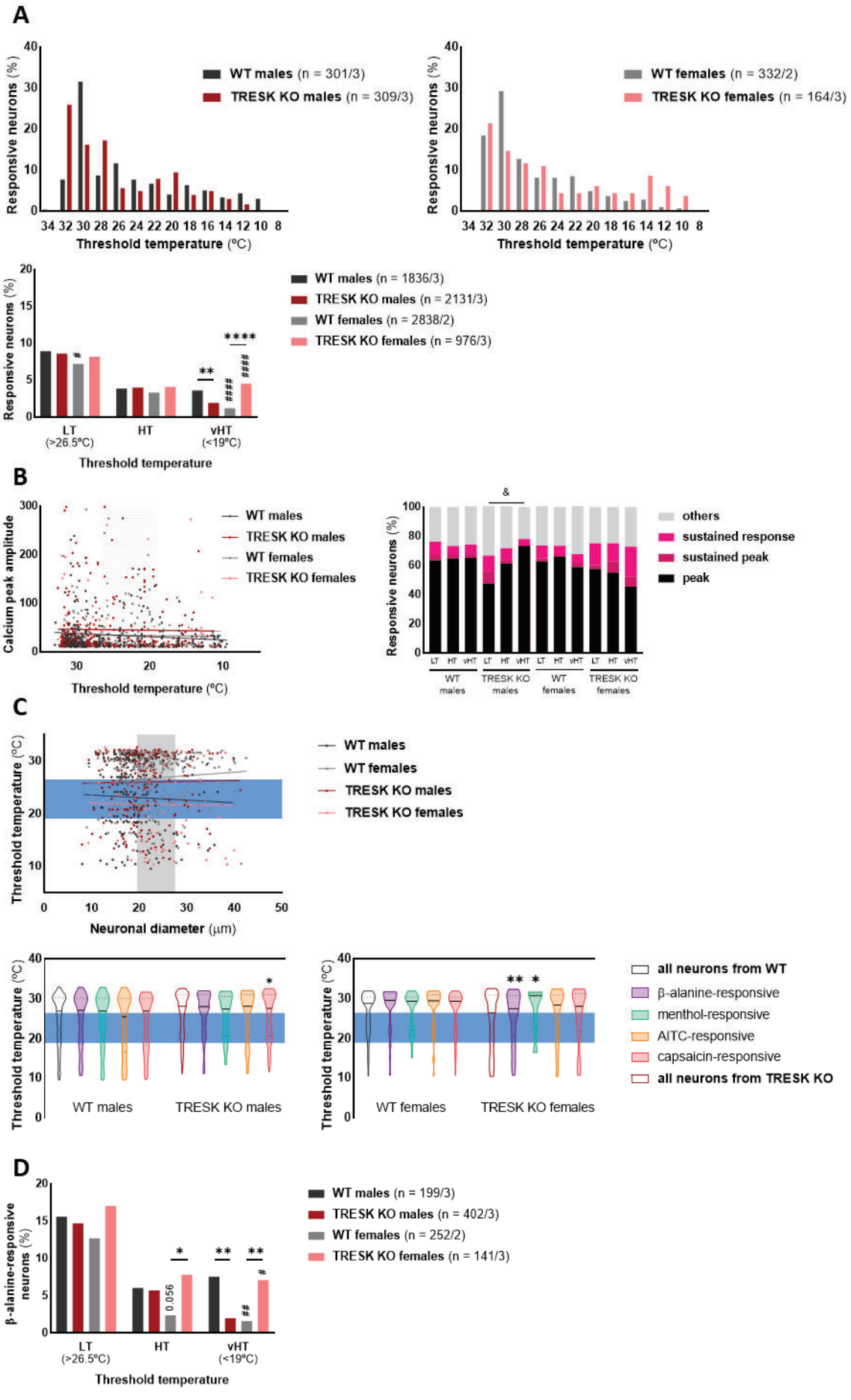
A
Responsive neurons (%)
WT males (n = 301/3)
TRESK KO males (n = 309/3)
Threshold temperature (°C)
WT females (n = 332/2)
TRESK KO females (n = 164/3)
WT males (n = 1836/3)
TRESK KO males (n = 2131/3)
WT females (n = 2838/2)
TRESK KO females (n = 976/3)
LT (>26.5°C)
HT
vHT (<19°C)
Threshold temperature
B
Calcium peak amplitude
Threshold temperature (°C)
others
sustained response
sustained peak
peak
WT males
TRESK KO males
WT females
TRESK KO females
C
Threshold temperature (°C)
Neuronal diameter (µm)
all neurons from WT
β-alanine-responsive
menthol-responsive
AITC-responsive
capsaicin-responsive
all neurons from TRESK KO
D
β-alanine-responsive neurons (%)
0.056

Figure 24. Cold-sensitive neurons respond to different ranges of temperatures. *Threshold temperatures identified as the temperature of the cold ramp applied to cultured DRG neurons (from 31.0 ± 0.1 °C to 11.6 ± 0.2 °C) at which cold-sensitive neurons start showing an increase in their intracellular calcium levels (see Figure 10B).* ***(a)*** *Distribution of cold-responsive neurons according to their threshold temperature. Top: histogram of cold-responsive neurons (number of analysed neurons and animals from which they come from indicated in parentheses as: number of cells / number of animals). Bottom: Percentage of neurons responding to different ranges of temperatures (LT: low-threshold, HT: high threshold and vHT: very high threshold according to Madrid 2009) out of the total number of neurons analysed (indicated in parentheses as number of cells / number of animals).* ***(b)*** *Characteristics of the calcium peaks elicited in response to different temperatures. Left: Relationship between calcium peak amplitude shown as increment from baseline intracellular calcium and threshold temperature of each cold-sensitive neuron. Single dots represent data from single cells and lines show the linear regression of the data from the cold-sensitive neurons of each group. Right: Distribution of shapes of the calcium peaks (described in Figure 10B) in response to different ranges of cold temperatures.* ***(c)*** *Characterisation of the population of neurons responding to different temperatures according to their neuronal size (top) and their responsiveness to β-alanine 1 mM, menthol 100 µM, AITC 100 µM and capsaicin 100 nM or 1 µM (bottom). Blue strips indicate the range of HT temperatures and the grey strip the range of medium-sized neurons (from 19.5 to 27.5 µm of diameter, according to Herweijer G et al., 2014). In the top graph, single dots represent data from single cells and lines show the linear regression of data from each group. In the bottom graph, the continuous and discontinuous lines on each violin plot indicate the median and quartiles of the analysed values, respectively.* ***(d)*** *Characterisation of the cold responsiveness of the β-alanine-responsive neurons: percentage of neurons responding to different ranges of temperatures out of the β-alanine-responsive neurons. The number of neurons analysed and the number of the animals from which they come indicated in parentheses as: number of cells / number of animals for each group. Numbers indicated in section (a) are valid for sections from a to c; numbers indicated in section (d) correspond to the β-alanine-responsive neurons and are valid only for section (d). Comparisons of percentages of responsive neurons analysed using the Fisher's exact test (subsection a – bottom and section d) or the Chi-square test (subsection b – right) and comparison of threshold temperatures analysed using the Kolmogorov-Smirnov test (subsection c – bottom). Statistical analysis shown indicating the p-values in asterisks for neurons from WT vs. TRESK KO (* < 0.05, ** < 0.01 and **** < 0.0001), in pads for neurons from males vs. females (# < 0.05, ## < 0.01, #### < 0.0001 and numbers for p-values close to the threshold for significance of 5 %), and in ampersands for comparisons of neurons from different populations (& < 0.05).*

Previously in this thesis, we showed that the percentage of neurons responding to cold stimuli was different in different groups of DRG neurons classified according to their neuronal size: we found more cold-responding neurons in the small-sized group, and less in the large-sized group. This distribution of cold-responsive neurons was not followed by neurons from TRESK KO females, which showed similar proportions of cold-sensitive neurons in different subpopulations (**Figure 21**). Thus, we inferred that the increase in the percentage of cold-responding neurons lacking TRESK was mainly due to more medium-sized and large-sized neurons responding to cold. Here, we wanted to check whether different populations of neurons classified according to their size also presented sensitivities to different temperatures, and whether the temperature sensitivities of each subpopulation was mediated by TRESK. Using linear regression (threshold temperature = 0.05 diameter + 24 °C for neurons from WT males, 0.02 diameter + 25.6 °C for neurons from TRESK KO males, 0.07 diameter + 25.2 °C for neurons from WT females, and -0.02 diameter + 22.1 °C for neurons from TRESK KO females), we found that neurons of different sizes responded to very similar

temperatures (comparison of the slope with slope = 0 p-values of 0.597 for neurons from WT males, of 0.830 for neurons from TRESK KO males, of 0.141 for neurons from WT females, and 0.903 for neurons from TRESK KO females) and confirmed that TRESK depletion influenced, as showed previously, the cold threshold temperature of activation of DRG cold-sensitive neurons from males and females (p-value < 0.0001, **Figure 24**).

As previously described, cold-responsive neurons can also be classified according to their responsiveness to MrgprD and TRP agonists and TRESK showed different effects on the cold-responsiveness of those subpopulations of neurons (**Figure 22**, **Figure 23**). Different subpopulations of neurons classified according to their responsiveness to β-alanine, menthol, AITC and capsaicin responded to similar temperatures (Kruskal-Wallis ANOVA test p-values of 0.518 for neuronal populations of WT males, of 0.796 for neuronal populations of TRESK KO males, of 0.242 for neuronal populations of WT females and of 0.265 for neuronal populations of TRESK KO females, **Figure 24**). TRESK depletion resulted in a shift of threshold temperature of capsaicin-responsive neurons from male animals to milder cold temperatures (mean and SEM of threshold temperatures: 23.8 ± 0.7 °C *vs.* 25.6 ± 0.5 °C for capsaicin-responsive neurons of WT and TRESK KO males, respectively, Kolmogorov-Smirnov test p-value of 0.015), in a shift of threshold temperature of β-alanine-responsive neurons from female animals to higher cold temperatures (27.7 ± 0.8 °C *vs.* 25 ± 1 °C for β-alanine-responsive neurons of WT and TRESK KO females, respectively, Kolmogorov-Smirnov test p-value of 0.007), and in a shift of threshold temperature of menthol-responsive neurons from female animals to milder cold temperatures (27 ± 0.6 °C *vs.* 27.3 ± 1.5 °C for menthol-responsive neurons of WT and TRESK KO females, respectively, Kolmogorov-Smirnov test p-value of 0.038). TRESK had no effects on the threshold temperatures of the other populations of neurons from male and female animals (24.7 ± 0.9 *vs.* 26.7 ± 0.6 °C for β-alanine-responsive neurons from WT and TRESK KO males, respectively, 24.5 ± 1 *vs.* 25.7 ± 0.6 for menthol-responsive neurons from WT and TRESK KO males, respectively, 23.5 ± 0.8 *vs.* 25.8 ± 0.7 °C and 27.7 ± 0.5 *vs.* 26 ± 0.8 °C for AITC-responsive neurons from WT males, TRESK KO males, WT females and TRESK KO females, respectively, and 27.1 ± 0.5 *vs.* 25.8 ± 0.9 °C for capsaicin-responsive neurons from WT and TRESK KO females, respectively; Kolmogorov-Smirnov test p-values of 0.110 for cold- and β-alanine-responsive neurons from males, of 0.719 for cold- and menthol-responsive neurons from males, 0.074 and 0.107 for cold- and AITC-responsive neurons from males and

females, respectively, and 0.101 for cold- and capsaicin-responsive neurons from females, **Figure 24**).

Looking deeper to the threshold temperatures of β-alanine responsive neurons, we found that TRESK depletion resulted in an increase in the percentage of neurons from female animals responding to HT and vHT temperatures, while it decreased the percentage of neurons from males responding to vHT (15.6, 14.7, 12.7 and 17 % of β-alanine-responsive neurons from WT males, TRESK KO males, WT females and TRESK KO females also responded to LT temperatures; 6, 5.7, 2.4 and 7.8 % of β-alanine-responsive neurons from WT males, TRESK KO males, WT females and TRESK KO females also responded to HT temperatures, and 7.5, 2, 1.6 and 7.1 % of β-alanine-responsive neurons from WT males, TRESK KO males, WT females and TRESK KO females also responded to vHT temperatures; Fisher's exact test p-values of 0.808 and 0.292 for LT-responsive from males and females, respectively, of 0.855 and 0.018 for HT-responsive from males and females, respectively, and of 0.002 and 0.008 for vHT-responsive from males and females, respectively, **Figure 24**). This might be explained by the increase of the β-alanine-responsiveness in cold-responsive neurons from males lacking TRESK (**Figure 22**), that appeared mainly in LT and HT-responsive neurons (percentage of neurons from male animals responding to β-alanine in different groups of cold-sensitive neurons: 18.9 *vs.* 32.2 % for LT-sensitive neurons of WT and TRESK KO, respectively, 16.9 *vs.* 27.1 % for HT-sensitive neurons of WT and TRESK KO, respectively, and 22.7 % *vs.* 19.5 % for vHT-sensitive neurons of WT and TRESK KO, respectively, Fisher's exact test of 0.005 for LT-responsive, of 0.177 for HT-responsive and 0.811 for vHT-responsive).

To summarize, the effects of TRESK depletion in cold sensing appeared mainly at extreme temperatures (< 19 °C). At these very high cold temperatures, TRESK had opposite effects on neurons from males and females: while it protected neurons from females from activation at very high temperatures, it increased the number of neurons from males responding to those temperatures. Neurons showed similar calcium responses to different temperatures, except for the reduction of "peak" responses in favour of more sustained responses to mild temperatures in neurons from males lacking TRESK, compared to those with the channel. When looking deeper at the effects of TRESK in the cold-sensing of different neuronal populations, we saw that neurons of different sizes or responding to different agonists showed similar cold temperature thresholds for neuronal activation, and that TRESK had

similar effects on the threshold temperature for calcium responses of DRG neurons of all sizes.

Among the different groups of cold-sensing neurons, in neurons from males, TRESK only affected the cold threshold of the population of capsaicin-responsive neurons, that moved to milder temperatures when the channel was depleted, although this did not result in an increase in the number of capsaicin-responsive neurons from TRESK KO males that responded to cold. Similarly, while the volume of the population of cold- and menthol-responsive neurons did not change depending on TRESK expression, the absence of the channel resulted in a shift of their threshold for cold-mediated activation to milder temperatures. Oppositely, TRESK depletion resulted in a decrease in the threshold temperature to activate β-alanine-responsive neurons from female animals.

TRESK has little impact on mice responses to innocuous and noxious cold

Here, using intracellular calcium recordings, we found that TRESK depletion resulted in an increase in the number of DRG neurons from female mice that responded to temperatures lower than 19 °C, while it had the opposite effect on DRG neurons from male mice (**Figure 24**). In more physiological conditions, previous studies in saphenous nerve skin preparations found similar percentages of cold-sensitive fibres from WT and TRESK KO males, although a tendency of more fibres from TRESK KO animals being activated at temperatures from 30 to 25 °C was observed (Castellanos et al. 2020). However, opposite effects of TRESK depletion were identified in different behavioural experiments evaluating hind paw plantar cold sensitivity in mice (Castellanos et al. 2020; Guo et al. 2019). As the role of TRESK in animals' cold sensitivity was not completely defined and, considering that the *Kcnk18* transcript is expressed in different structures of the CNS involved in cold perception (**Figure 9**), we decided to use a battery of behavioural test to evaluate the cold perception of male and female mice of WT and TRESK KO strains.

Using cold plantar assay, we could stimulate animals' hind paw plantar surface with a fast cold ramp and measure the latency time for WT and TRESK KO males and females to withdraw the paw. First, we used a thin glass (1/8'', temperature decrease of -1.3 °C in the first 4 s) to transmit cold from an ice pellet to the paw, and found no differences between the latency

times of WT and TRESK KO males and females (3.18 ± 0.16 s *vs.* 3.68 ± 0.14 s for WT and TRESK KO males and 3.71 ± 0.31 s *vs.* 4.23 ± 0.44 s for females, respectively; Mann-Whitney test p-values of 0.175 for males and of 0.357 for females). As we found no differences between males' and females' latency times (Mann-Whitney test p-values of 0.207 for WT animals and > 0.999 for TRESK KO animals, **Figure 25**), we analysed data from animals of the two sexes together. We found that TRESK KO animals tended to have longer latency times than WT animals, although those differences did not reach statistical significant values (3.5 ± 0.18 s *vs.* 4.09 ± 0.33 s for WT and TRESK KO animals, respectively; Mann-Whitney test p-value of 0.072). This pointed to lower sensitivity to cold in mice lacking TRESK.

Then, we decided to repeat the cold plantar assay with a wider glass (1/4'') to slow the cold ramp down to discriminate better between latency times (temperature decrease of -2 °C in the first 4 s). Here, we observed no differences in latency times for mice with and without TRESK (11.28 ± 0.64 s *vs.* 11.04 ± 0.62 s and 9.85 ± 0.99 s *vs.* 9.50 ± 0.55 s for WT males, TRESK KO males, WT females and TRESK KO females, respectively; Mann-Whitey test p-values of 0.896 and 0.779 for males and females, respectively; **Figure 25**). As we found no differences between latency times of males and females (Mann-Whitney test p-values of 0.485 and 0.075 for males and females, respectively), we also analysed the data together. Again, we found that there were no differences in the latency times between WT and TRESK KO animals (9.85 ± 0.99 s *vs.* 9.50 ± 0.55 s for WT and TRESK KO animals, respectively; Mann-Whitney test p-value of 0.619).

To better discriminate the temperatures at which animals started to react to cold stimuli, to cover a larger range of temperatures and to differentiate between cold allodynia and hyperalgesia, we studied animal reactions to a cold ramp from 30 °C to 0 °C with a decrease of 1 °C per minute. First, we observed typical behaviours that animals showed in the experimental set. They walked, jumped, licked their genitals, reared, avoided the touch of their tail with the cold surface, stood on their two hind paws to avoid body and front paws contact with the cold surface, and, rarely, shook, flinched and liked their front and hind paws. We counted the number of times they repeated those behaviours and the time they spent moving, rearing and avoiding tail contact on each temperature of the cold ramp, and measured the temperature at which they started to stand on their two hind paws. We found that only the number of jumps, the number of genital licks and the time spent moving

changed as temperatures got cooler (**Figure 25**). Therefore, we decided to pick those parameters to compare WT and TRESK KO animals' reactions to cold. Furthermore, we also studied the temperature at which animals started to stand on two paws.

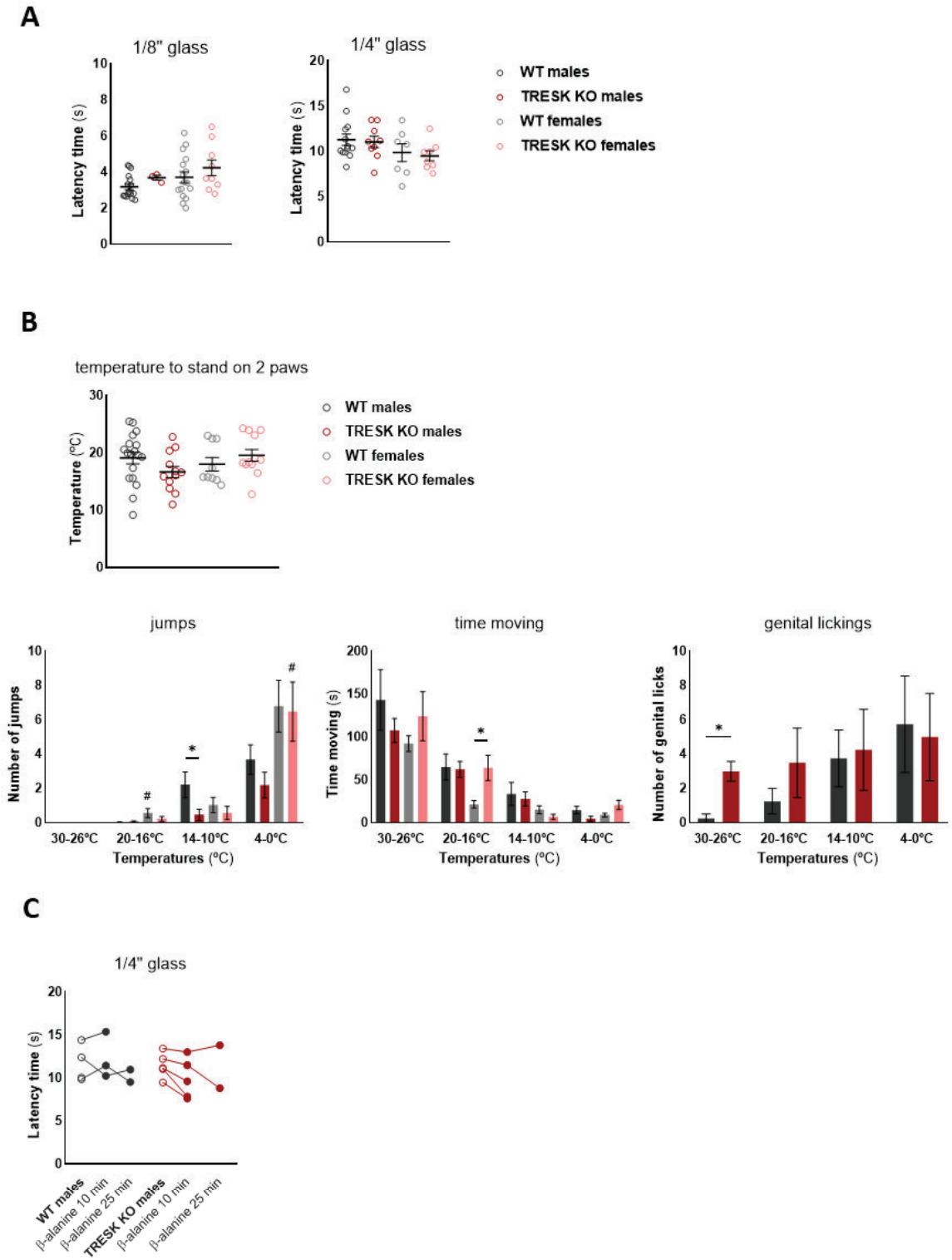

Figure 25. Cold sensitivity is not altered in mice lacking TRESK. *Approximations to measure the baseline cold sensitivity of WT and TRESK KO mice using:* ***(a)*** *the latency time to withdraw the paw from a dry ice cold*

*transferred fast through a thin glass of 1/8" (left, see schematic view on the left) or a thicker glass of 1/4" (right), or **(b)** the nocifensive behaviours shown in response to a slower ramp of decreasing temperatures from 30 °C to 0 °C at a speed of -1 °C / minute (see schematic view on the left. Temperatures are grouped in ranges and considered warm (from 30 to 26 °C), unpleasant cold (from 20 to 16 °C) and noxious cold (from 14 to 10 °C and from 4 to 0 °C). Comparison of the behavioural responses of WT males (n = 17, 13, 18, 32, 4 and 4), TRESK KO males (n = 3, 9, 12, 30, 4 and 4), WT females (n = 16, 7, 9, 30, 5 and 0), and TRESK KO females (n = 9, 8, 12, 35, 4 and 0 for cold plantar assay using a 1/8" glass, cold plantar assay using a 1/4" glass, temperature to stand up on the cold ramp, number of jumps, time moving, and number of genital lickings in the slow cold ramp, respectively). Single dots indicate the values obtained from single animals, bars or thick lines the means and thin lines the SEM of each measure. **(c)** Effects of an intraplantar injection of 10 µL of β-alanine 50 mM on the mice's cold sensitivity 10 and 25 minutes after the injection. Measurement of plantar cold sensitivity of 4 WT males and 5 TRESK KO males using the cold plantar assay with a 1/4" glass approach (see section a). Connected dots represent the sensitivity of single animals before and after β-alanine treatment. Comparison of different groups of data was performed using the Mann-Whitney test (for the cold plantar assay and the time moving and the number of genital lickings in the cold ramp), the unpaired T-test (for the temperature to stand on 2 paws in the cold ramp), the multiple T-test (for the number of jumps in the cold ramp) and the Wilcoxon test (for the different time points after β-alanine treatment) and are shown with asterisks in WT vs. TRESK KO comparisons (* for p-value < 0.05 and ** for p-value < 0.01), and with pads in male vs. female comparisons (# for p-value < 0.05).*

WT and TRESK KO animals started to stand on two paws at similar temperatures, although TRESK KO males showed a tendency to lower temperatures, compared to WT males (19.14 ± 1.04 *vs.* 16.69 ± 0.99 °C and 18.03 ± 1.19 *vs.* 19.60 ± 1.02 °C of threshold temperatures of WT males, TRESK KO males, WT females and TRESK KO females, respectively; unpaired T-test p-values of 0.116 and 0.330 for males and females, respectively, **Figure 25**). We did not analyse data from males and females together because TRESK KO males tended to show lower threshold temperatures than TRESK KO females, although these differences did not reach statistically significant values (unpaired T-test p-value of 0.054).

To analyse behaviours dependent on temperature, we chose different temperature ranges related to baseline or warm temperatures (30 – 26 °C), unpleasant cool temperatures (20 – 16 °C) and noxious cold temperatures (14 – 10 °C and 4 – 0 °C). We found that, as shown in Yalcin et al. 2009, animals tended to jump more as temperatures went colder (Friedman test p-values < 0.0001 for WT males, TRESK KO males, WT females and TRESK KO females), although these results varied among the different sets of experiments done. Unexpectedly, TRESK KO males tended to jump less at noxious cold temperatures, although those differences were only statistically significant for the range from 14 to 10 °C (for ranges of 30 – 26 °C, 20 – 16 °C, 14 – 10 °C and 4 – 0 °C, the number of jumps were: 0 ± 0, 0.03 ± 0.03, 2.22 ± 0.74 and 3.69 ± 0.86 for WT males, and 0 ± 0, 0.07 ± 0.05, 0.47 ± 0.32 and 2.2 ± 0.75 for TRESK KO males; Multiple T-test comparing WT *vs.* TRESK KO number of jumps: q-values of 0.118 and 0.300 for noxious ranges of males). We found no differences in the number of jumps that females did in each temperature range (for ranges of 30 – 26 °C, 20 – 16 °C, 14 – 10 °C and 4

– 0 °C, the number of jumps were: 0 ± 0, 0.57 ± 0.26, 1.03 ± 0.44 and 6.8 ± 1.5 for WT females, and 0 ± 0, 0.23 ± 0.14, 0.57 ± 0.38 and 6.49 ± 1.73; Multiple T-test comparing WT *vs.* TRESK KO number of jumps: q-values of 0.645, 0.645 and 0.902 for unpleasant and noxious ranges of females; **Figure 25**).

We only obtained data of the time moving from 4 WT males, 4 TRESK KO males, 5 WT females and 4 TRESK KO females and, of the number of genital licks, from 4 WT males and 4 TRESK KO males. Thus, the results presented here are very preliminary. We found that, as the temperature went down, animals tended to walk less around the set (Friedman test p-values of 0.033 for WT males, < 0.0001 for TRESK KO males, of 0.012 for WT females and 0.002 for TRESK KO females). TRESK KO females moved more than WT females at unpleasant cold temperatures, while the time moving at other ranges when comparing WT and TRESK KO animals was similar (for ranges of 30 – 26 °C, 20 – 16 °C, 14 – 10 °C and 4 – 0 °C, the times moving were of: 143.2 ± 35.35 s, 65.05 ± 15.13 s, 33.71 ± 13.48 s and 14.82 ± 4.46 s for WT males, 107.70 ± 13.95 s, 62.24 ± 9.25 s, 27.94 ± 8.27 s and 4.79 ± 2.85 s for TRESK KO males, 92.34 ± 9.09 s, 21.59 ± 4.26 s, 15.22 ± 4.60 s and 9.06 ± 2.13 s for WT females, and 124.24 ± 28.73 s, 64.02 ± 14.59 s, 6.84 ± 3.16 s and 20.79 ± 5.49 s for TRESK KO females; Mann-Whitney test comparing WT *vs.* TRESK KO time moving p-values of 0.343, 0.686, 0.686 and 0.114 for males and 0.556, 0.016, 0.286 and 0.111 for females; **Figure 25**). As when animals were standing on two paws, the genitals were in contact with the surface and animals tended to lick them often. We observed that at lower temperatures, WT males tended to lick their genitals more than at higher temperatures, while TRESK KO males did not change the number of lickings along temperatures (or ranges of 30 – 26 °C, 20 – 16 °C, 14 – 10 °C and 4 – 0 °C, the number of licks were: 0.25 ± 0.25, 1.25 ± 0.75, 3.75 ± 1.65 and 5.75 ± 2.81 for WT males, and 3 ± 0.58, 3.5 ± 2.02, 4.25 ± 2.36 and 5 ± 2.55 for TRESK KO males; Friedman test p-values of 0.073 for WT animals and of 0.931 for TRESK KO animals). We found that TRESK KO males licked their genitals more than WT males at baseline temperatures (30 – 26 °C), but found no differences between WT and TRESK KO animals at the other ranges of temperatures (Mann-Whitney test p-values of 0.029 for baseline temperatures, of 0.486 for unpleasant cold temperatures and > 0.999 and of 0.857 for noxious cold temperatures; **Figure 25**).

As a summary, although we found almost no effects of TRESK depletion on the cold sensitivity of mice, results pointed to a decrease in cold sensitivity of males lacking TRESK, which is

consistent with the decrease in the number of DRG neurons from TRESK KO males responding to temperatures lower than 19 °C (**Figure 24**).

As β-alanine increases MrgprD-expressing neurons excitability (Crozier et al. 2007; Rau et al. 2009), (**Figure 15**) and 28.7 %, 22.4 %, 16.7 % and 39 % of β-alanine-responsive neurons of WT and TRESK KO males and females, respectively, also respond to cold (**Figure 22**), we wondered whether the activation of β-alanine-sensitive neurons may modify the cold sensitivity of WT and TRESK KO animals. Here, we only show the preliminary results of the measurement of animals' cold sensitivity using the cold plantar assay in a 1/4'' glass before and 10 and 25 minutes after injecting their paw with β-alanine 50 mM. We found no effects of β-alanine treatment on the cold sensitivity of WT males (11.71 ± 1.08 s at baseline measures, 12.39 ± 1.55 s 10 minutes after β-alanine injection and 10.28 ± 0.72 25 minutes after β-alanine injection; Wilcoxon tests comparing baseline values to times post-injection p-value > 0.999 for 10 minutes, analysis not possible because of missing data at 25 minutes), but we observed a tendency of TRESK KO males 10 minutes after β-alanine injection to increase their sensitivity to cold (latency times of 11.49 ± 0.66 s at baseline, of 10.21 ± 0.89 s 10 after injection and of 11.34 ± 2.5 s 25 minutes after injection; Wilcoxon tests comparing baseline values to times post-injection p-value of 0.063 for 10 minutes, analysis not possible because of missing data at 25 minutes). Comparing the latency times of 4 WT males and 4 TRESK KO males after the treatment, we found no effects of TRESK depletion in their cold-sensitivity (Unpaired T-test p-values of 0.228 for 10 minutes after treatment and of 0.723 for 25 minutes; **Figure 25**). However, more experiments are needed to describe better the effects of MrgprD-expressing neurons on animals' cold sensitivity and the role of TRESK on its modulation in males and females.

Tacrolimus has almost no effects on cold perception

Tacrolimus is a Calcineurin inhibitor used as an immunosuppressant after transplantation. It can cause reversible severe pain as a side effect, and some authors hypothesised that these effects might be mediated by TRESK indirect inhibition in DRGs. On the other hand, some studies indicated that Tacrolimus treatment reduces mice's cold sensitivity in physiological conditions in a mechanism mediated mainly by TRPM8 (Arcas et al. 2019), and rats' cold hypersensitivity after spinal cord injury (Voda, Hama, and Sagen 2007).

Considering the bimodal effects of Tacrolimus on pain sensitivity, the recent findings indicating that most of Tacrolimus-responsive neurons are also cold-responsive (Arcas et al. 2019) and that TRESK modulates the neuronal responsiveness to cold and menthol differently in males and females (**Figure 19**, **Figure 21**, **Figure 22**), we wanted to elucidate the role of TRESK in the variation of effects of Tacrolimus in the cold-sensitivity of mice. Thus, we injected Tacrolimus and saline solution, as a negative control, intraperitoneally to WT and TRESK KO mice during three consecutive days and evaluated their responses to cold stimuli for four days.

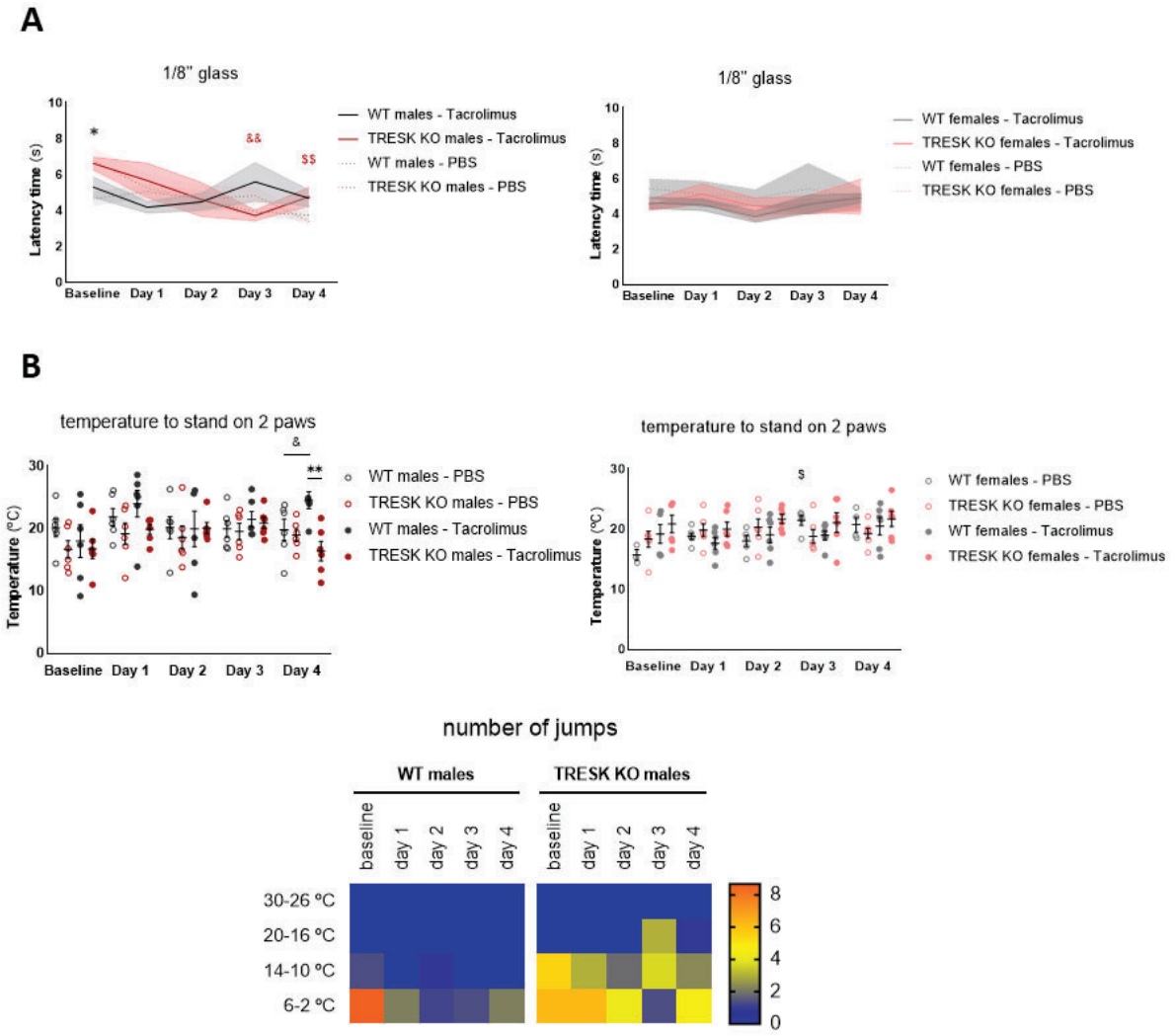

Figure 26. Tacrolimus increases the cold sensitivity of WT males. *6 WT males, 6 TRESK KO males, 6 WT females and 6 TRESK KO females were injected with 40 µg of Tacrolimus intraperitoneally during 3 consecutive days, while the same number of animals of the same groups were injected with saline solution (PBS) intraperitoneally, also during 3 consecutive days. Their cold sensitivity was evaluated using the cold plantar assay with a 1/8" glass and the quantification of the nocifensive behaviours in response to a cold ramp from 30 to 2 °C at -1 °C / min before the treatment (baseline) and during 4 consecutive days more (before the IP injections on baseline, 1 and 2 days). On section (a), lines and shadowed areas represent the mean and SEM, respectively. In subsection (b – middle), single dots represent values from single animals, while lines represent the mean and SEM of each group.*

In subsection (b – bottom), the colour scale represents the mean of the number of jumps for each group. For the analysis of the cold plantar assay, 1 WT female treated with Tacrolimus, 2 WT females and 1 TRESK KO female treated with PBS were discarded due to single characteristics not related to the experiment . Statistical analysis of the data is detailed in Table 4 and Table 5. Statistical significant differences between WT and TRESK KO animals are shown using asterisks (for p-value < 0.05 and ** for p-value < 0.01), between baseline values and each day after Tacrolimus treatment values using ampersands (& for p-value < 0.05 and && for p-value < 0.01), and between baseline values and each day after PBS treatment values using dollar/peso signs ($ for p-value < 0.05 and $$ for p-value < 0.01).*

First, in the cold plantar assay, we found that Tacrolimus and saline intraperitoneal (IP) injections had no effects on the latency times of WT males, WT females and TRESK KO females (**Table 7**, **Table 8**). TRESK KO male, however, showed a decreased latency time on day 3, that recovered to baseline values on day 4 after treatment with Tacrolimus (**Table 7**), and a decreased latency time on day 4 after saline solution injection (**Figure 26**, **Table 8**). Thus, we can not confirm that the increase in cold sensitivity of TRESK KO males after Tacrolimus injection is a consequence of the treatment. We could confirm that TRESK KO males showed higher latency times than WT males before treatments, although those results were only statistically significant for the saline-injected animals (Mann-Whitney test p-values of 0.065 and 0.041 for Tacrolimus and saline-injected animals).

To better discriminate possible Tacrolimus effects on the sensitivity to different cold temperatures, and to better discriminate possible effects of allodynia and hyperalgesia, we challenged WT and TRESK KO animals with a ramp from 30 °C to 2 °C with a speed of decrease of -1 °C per minute. Despite the considerable variability between animals, we found that the temperature at which animals started to maintain a stand-up position tended to increase in WT males on the first and fourth day after Tacrolimus injection and in TRESK KO males the third day after Tacrolimus injection, compared to baseline measures, although those differences did not reach statistically significant levels (**Table 7**) and the increase was not maintained in time. On the fourth day after Tacrolimus treatment, TRESK KO males recovered their baseline temperatures for standing on two paws, and, compared to them, WT males started to stand on two paws at warmer temperatures (comparison of WT and TRESK KO males 4 days after the beginning of Tacrolimus treatment: Mann-Whitney test p-value of 0.004). Threshold temperatures to stand on two paws maintained stable in males injected with saline solution (**Figure 26**, **Table 8**). As a measure of possible allodynia or hypersensitivity, we counted the number of jumps that male animals did at every range of temperatures. We found that Tacrolimus had no effects on the number of jumps that both

WT and TRESK KO males did at every range of temperatures (**Table 7**). Moreover, although graphs seem to point to a different direction (**Figure 26**), we found no differences between WT and TRESK KO males behaviours at every temperature (**Table 7**, Mann-Whitney test p-values for 20 to 16 °C, 14 to 10 °C and 6 to 2 °C: > 0.999 for day 0 to 4; 0.556, > 0.999, 0.727, > 0.999 and > 0.999 for days 0 to 4, respectively, and 0.918, 0.665, 0.632, 0.546 and > 0.999 for days 0 to 4, respectively). We only obtained jumps data from 3 WT and 3 TRESK KO males treated with PBS, and the analysis is not shown here, as the resulting data is very preliminary.

With the cold ramp, we only obtained data on the temperature at which females started to stand on two paws. We found that Tacrolimus treatment did not vary the temperature at which WT neither TRESK KO females started to stand on two paws (**Figure 26**, **Table 8**). Unexpectedly, we found that threshold temperatures of the third day after saline solution injection were higher than the baseline values in WT females, which might be due to the low baseline value of those animals. TRESK KO animals injected with saline solution maintained their threshold temperature stable during experimental days (**Figure 26**, **Table 7**).

To sum up, we found no effects of Tacrolimus treatment on the cold sensitivity of females. In males, Tacrolimus seems to lightly increase the cold sensitivity of both WT and TRESK KO animals, although it is difficult to verify whether they are direct effects of the drug, as some TRESK KO males injected with PBS also showed increases in the sensitivity to the cold ramp. Considering those results and that TRESK depletion results in a decrease in the cold sensitivity of males, TRESK is not likely to mediate the effects of Tacrolimus on the cold sensitivity of mice.

			Cold plantar assay		Cold Ramp (from 30 to 2 ºC) "Standing" temp.		30 to 26 ºC		20 to 16 ºC		14 to 10 ºC		6 to 2 ºC	
			Latency (s)	*vs.* day 0 (p-value)	Threshold (ºC)	*vs.* day 0 (p-)	jumps (n)	*vs.* day 0 (p-)	jumps (n)	*vs.* day 0 (p-)	jumps (n)	*vs.* day 0 (p-)	jumps (n)	*vs.* day 0 (p-)
males	WT	baseline	5.31 ± 0.57		18.0 ± 2.6	–	0.0 ± 0.0	–	0.0 ± 0.0	–	1.3 ± 0.7	–	8.7 ± 4.6	–
		day 1	4.18 ± 0.33	Friedman	24.0 ± 2.1	*0.114*	0.0 ± 0.0	*> 0.999*	0.0 ± 0.0	*0.999*	0.0 ± 0.0	*0.684*	2.2 ± 1.3	*0.941*
		day 2	4.48 ± 0.48	ANOVA:	19.9 ± 2.9	*0.221*	0.0 ± 0.0	*> 0.999*	0.0 ± 0.0	*0.999*	0.8 ± 0.8	*> 0.999*	1.2 ± 0.8	*0.272*
		day 3	5.60 ± 1.08	*0.827*	21.5 ± 1.2	*0.941*	0.0 ± 0.0	*> 0.999*	0.0 ± 0.0	*0.999*	0.0 ± 0.0	*0.684*	1.3 ± 0.8	*0.684*
		day 4	4.68 ± 0.46		24.5 ± 1.4	*0.055*	0.0 ± 0.0	*> 0.999*	0.0 ± 0.0	*0.999*	0.0 ± 0.0	*0.684*	2.2 ± 2.0	*0.178*
	TRESK KO	baseline	6.63 ± 0.35	–	16.7 ± 1.6	–	0.0 ± 0.0	–	0.0 ± 0.0	–	5.5 ± 3.8	–	6.2 ± 2.9	–
		day 1	5.68 ± 0.97	*0.805*	19.9 ± 0.8	*0.401*	0.0 ± 0.0	***> 0.999***	0.0 ± 0.0	***> 0.999***	3.0 ± 3.0	***> 0.999***	6.2 ± 3.7	***> 0.999***
		day 2	4.62 ± 0.96	*0.143*	20.1 ± 0.9	*0.577*	0.0 ± 0.0	***> 0.999***	0.0 ± 0.0	***> 0.999***	1.8 ± 1.6	***> 0.999***	4.2 ± 2.5	***> 0.999***
		day 3	3.72 ± 0.31	***0.006***	20.9 ± 0.9	*0.071*	0.0 ± 0.0	***> 0.999***	3.0 ± 3.0	***> 0.999***	3.7 ± 3.7	***> 0.999***	1.3 ± 1.3	*0.577*
		day 4	4.78 ± 0.54	*0.401*	16.4 ± 1.6	*> 0.999*	0.0 ± 0.0	***> 0.999***	0.3 ± 0.3	***> 0.999***	2.3 ± 2.3	***> 0.999***	4.7 ± 4.7	*0.805*
females	WT	baseline	4.63 ± 0.32		19.2 ± 1.6	–	–	–	–	–	–	–	–	–
		day 1	4.52 ± 0.32	Friedman	17.7 ± 1.0	*0.577*	–	–	–	–	–	–	–	–
		day 2	3.86 ± 0.33	ANOVA:	19.0 ± 1.3	*> 0.999*	–	–	–	–	–	–	–	–
		day 3	4.55 ± 0.52	*0.339*	19.0 ± 0.8	*> 0.999*	–	–	–	–	–	–	–	–
		day 4	4.91 ± 0.25		20.5 ± 1.5	*> 0.999*	–	–	–	–	–	–	–	–
	TRESK KO	baseline	4.53 ± 0.31		20.9 ± 1.5	–	–	–	–	–	–	–	–	–
		day 1	5.12 ± 0.60	Friedman	20.0 ± 1.2	*> 0.999*	–	–	–	–	–	–	–	–
		day 2	4.43 ± 0.46	ANOVA:	21.7 ± 0.8	*> 0.999*	–	–	–	–	–	–	–	–
		day 3	4.52 ± 0.53	*0.804*	21.1 ± 0.6	*> 0.999*	–	–	–	–	–	–	–	–
		day 4	5.08 ± 0.91		21.7 ± 1.3	*> 0.999*	–	–	–	–	–	–	–	–

Statistics tests:

baseline *vs.* each day of Tacrolimus: Friedman multiple comparisons test (latency times, temperature to "stand up", number of jumps)

Table 7. Effects of Tacrolimus on the cold sensitivity of WT and TRESK KO mice. *Evaluation of the cold sensitivity of WT and TRESK KO males and females before and after Tacrolimus administration. 40 µg of Tacrolimus in 50 µL were administered IP after the sensitivity measurements on baseline, day 1 and day 2. Mean ± SEM of latency times to respond to the cold plantar assay, of temperature to stand on two paws on the cold ramp, and of the number of jumps at different ranges of warm (30 – 26 °C), innocuous cold (20 – 16 °C) and noxious cold (14 – 10 °C and 6 – 2 °C) temperatures. Statistical analysis significance of differences in the measurements before and different days after the treatment shown as p-values. N = 6 for WT males, TRESK KO males, WT females (except in the cold plantar assay, that n = 5), and TRESK KO females. Statistically significant values (threshold of significance of 5 %) highlighted using bold characters.*

			Cold plantar assay		Cold Ramp "Standing" temp.	
			Latency (s)	*vs.* day 0 (p-value)	Threshold (ºC)	*vs.* day 0 (p-value)
males	WT	baseline	4.65 ± 0.39		20.1 ± 1.4	–
		day 1	5.07 ± 0.41	Friedman	21.8 ± 1.4	*0.272*
		day 2	4.63 ± 0.47	ANOVA:	20.2 ± 1.8	*> 0.999*
		day 3	3.94 ± 0.19	*0.109*	19.9 ± 1.3	*> 0.999*
		day 4	3.75 ± 0.39		19.8 ± 1.7	*> 0.999*
	TRESK KO	baseline	6.78 ± 0.68	–	16.7 ± 1.4	–
		day 1	5.27 ± 0.79	*> 0.999*	19.2 ± 1.7	*> 0.999*
		day 2	4.63 ± 0.75	*0.941*	18.6 ± 1.8	*> 0.999*
		day 3	4.84 ± 0.51	*> 0.999*	19.5 ± 1.3	*0.483*
		day 4	3.40 ± 0.26	***0.005***	19.0 ± 0.9	*0.941*
females	WT	baseline	5.45 ± 0.55		15.7 ± 0.9	–
		day 1	5.13 ± 0.75	Friedman	18.8 ± 0.5	*0.468*
		day 2	4.92 ± 0.48	ANOVA:	21.6 ± 5.6	*0.344*
		day 3	5.43 ± 1.46	*0.933*	21.5 ± 0.8	***0.023***
		day 4	4.89 ± 0.60		20.8 ± 1.2	*0.081*
	TRESK KO	baseline	4.39 ± 0.21		18.3 ± 1.3	–
		day 1	4.78 ± 0.17	Friedman	19.8 ± 1.1	*> 0.999*
		day 2	3.95 ± 0.38	ANOVA:	20.3 ± 1.4	*0.483*
		day 3	4.49 ± 0.40	*0.672*	18.8 ± 1.2	*> 0.999*
		day 4	4.39 ± 0.44		19.3 ± 0.8	*> 0.999*

Statistics tests:
baseline *vs.* each day of PBS: Friedman multiple comparisons test (latency times, temperature to "stand up")

Table 8. Control measurements for the analysis of the cold sensitivity of WT and TRESK KO mice. *Evaluation of the cold sensitivity of WT and TRESK KO males and females before and after saline solution administration. 50 µL of PBS were administered IP after the sensitivity measurements on baseline, day 1 and day 2. Mean ± SEM of latency times in the cold plantar assay and of temperature to stand on two paws in the cold ramp. Statistical analysis significance of differences in the measurements before and different days after the treatment shown as p-values. N = 6 for WT and TRESK KO males, n = 4 for WT females, and n = 5 for cold plantar assay and n = 6 for cold ramp in TRESK KO females. Statistically significant values highlighted using bold characters.*

TRESK protects mice from heat hypersensitivity in physiological but not chronic pain conditions

TRPV1-expressing and TRPA1-expressing neurons are involved in noxious heat detection (Cavanaugh et al. 2009; Vandewauw et al. 2018), while different studies do not agree on whether MrgprD-expressing neurons have a role in heat sensing (Cavanaugh et al. 2009; Rau et al. 2009). Although most studies to date show that animals lacking TRESK have similar heat sensitivity in hind paws than WT animals, others showed that TRESK knock-out or knock-down animals present higher sensitivity to noxious heat than animals with the channel (see **Table 2**). As TRESK reduces the responsiveness of MrgprD-expressing, TRPA1-expressing and TRPV1-expressing neurons to some agonists (**Figure 19**), we wanted to validate whether its expression in animals is involved in their heat sensitivity in physiological conditions and in

pathological models by measuring the time it took for WT and TRESK KO males and females to respond to a heat beam (Hargreaves).

First, we found that TRESK KO males showed considerable lower latency times than WT males (8.2 ± 0.5 s for WT males and 5.8 ± 0.4 s for TRESK KO males; Mann-Whitney test p-value of 0.0004) and that TRESK KO females also tended to react first to the heat stimuli compared to WT females, although this comparison did not reach statistically significant levels (7.1 ± 0.4 s *vs.* 5.8 ± 0.4 s for WT and TRESK KO females, respectively; Mann-Whitney test p-value of 0.071). WT females also tended to show lower latency times than WT males, while TRESK KO males and females react to heat after similar times (Mann-Whitney test p-value of 0.076 for WT animals and unpaired T-test p-value of 0.956 for TRESK KO animals, **Figure 27**).

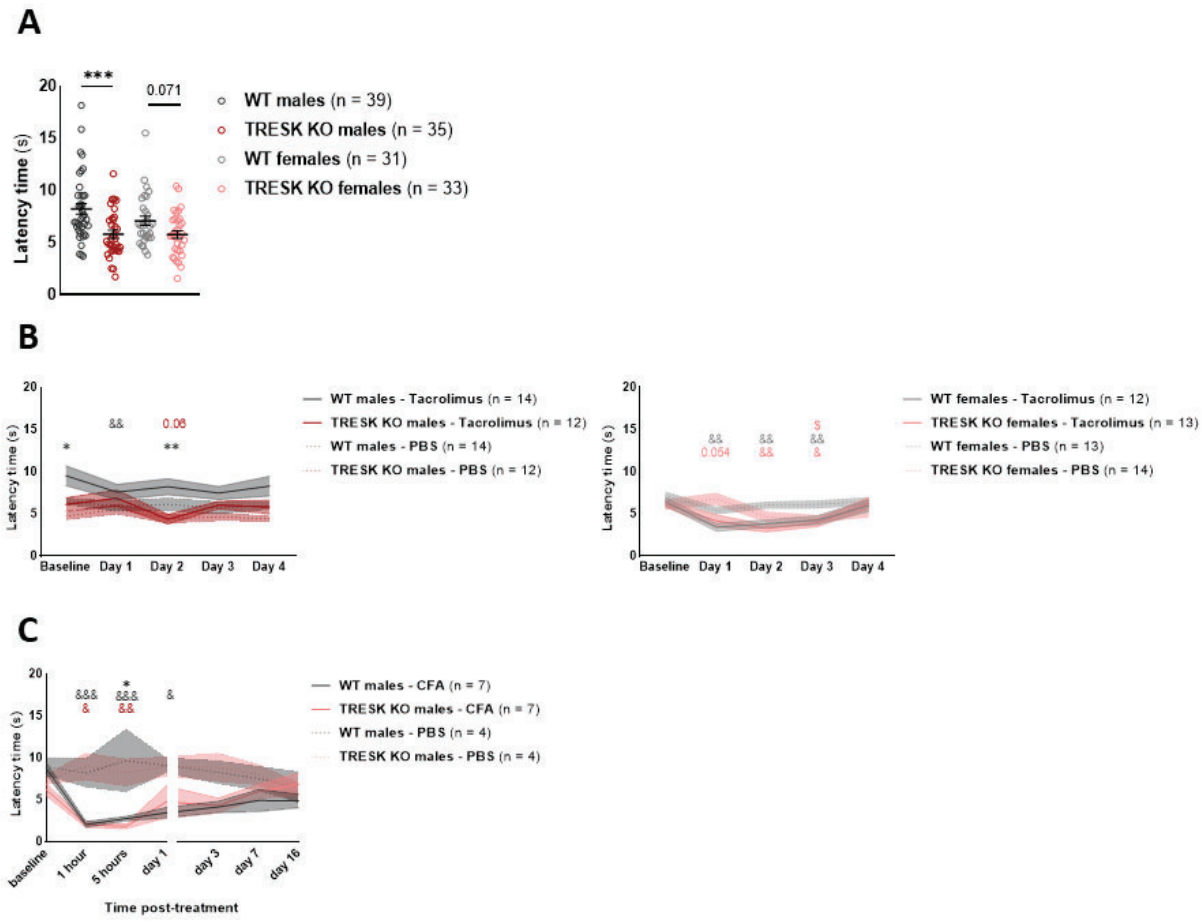

Figure 27. TRESK KO animals show increased heat sensitivity. *Evaluation of the heat sensitivity using the Hargreaves method.* ***(a)*** *Latency times to withdraw the hind paw from the infrared beam at 30% intensity in physiological conditions. Single dots indicate values from single animals, and lines indicate the mean and SEM for each group. Values of WT and TRESK KO animals are compared using the Mann-Whitney statistical test.* ***(b)*** *Latency times to withdraw the paw from the heat source before and after injection with 40 µg of Tacrolimus or saline solution (PBS) IP during 3 consecutive days (after baseline, day 1 and day 2 measurements). Statistical analysis detailed in* ***Table 9****.* ***(c)*** *Latency times to withdraw the paw from the heat source before and at different*

*time points after a unique intraplantar injection of 20 µL of CFA (1 mg / mL) or PBS in the hind paw (after the baseline measurement). Statistical analysis detailed in **Table 10**. For (b) and (c), lines and shaded areas indicate the mean and SEM for each group, respectively. The number of animals analysed is shown in parentheses in each figure. Statistical significant differences between WT and TRESK KO animals are shown using asterisks (* for p-value < 0.05, ** for p-value < 0.01, *** for p-value < 0.001 and numbers when p-values are close but do not reach the 5 % level of significance), between baseline values and each time point after CFA treatment values using ampersands (& for p-value < 0.05, && for p-value < 0.01, &&& for p-value < 0.001 and numbers when p-values are close but do not reach the 5 % level of significance) and between baseline values and each day after PBS treatment values using dollar/peso signs ($ for p-value < 0.05). The colours of the signs or numbers indicate which groups are compared.*

After validating that mice lacking TRESK tended to show increased heat sensitivity, we wondered whether calcineurin blocking using Tacrolimus might modify animals' heat sensitivity in a mechanism mediated by TRESK. To answer this question, we injected Tacrolimus and saline solution (negative control, PBS) in the intraperitoneal space of WT and TRESK KO males and females for three days and measured their latency times to respond to heat before the treatment and during the four following days. We observed that Tacrolimus injection resulted in an acute increase in the heat responsiveness of WT males, that showed similar latency times to those of TRESK KO males the first day after the treatment (**Figure 27**). However, even after the administration of Tacrolimus for two days more, WT males recovered their baseline heat sensitivity from the second to the fourth day after the first injection. Tacrolimus also seemed to increase TRESK KO males sensitivity the second day of the experiment, although statistical analysis did not show significant differences and TRESK KO males returned to baseline values the third and fourth days after the first injection (**Table 9**; Unpaired T-test comparing day 1 values of WT and TRESK KO males p-value of 0.595). The injection of saline solution had no effects on the sensitivity of WT and TRESK KO males (**Figure 27**, **Table 9**). Meanwhile, Tacrolimus treatment in females resulted in a clear decrease in latency times during the days post-injection with a fast recovery in both WT and TRESK KO animals on the fourth day of measurements, which is consistent with the reversible nature of Calcineurin-Inhibitor induced Pain Syndrome (CIPS; **Table 9**). Females injected with PBS did not show variations in their heat sensitivity, except for the reduction of the latency times of TRESK KO females the third day after the first injection (**Figure 27**, **Table 9**). The similar effects of Tacrolimus treatment in animals with and without the K_{2P} channel point to mechanisms besides TRESK being the main responsible for the increase in heat sensitivity in Tacrolimus-treated mice.

			Hargreaves				von Frey			
			Tacrolimus		PBS		Tacrolimus		PBS	
			Latency (s)	*vs.* day 0 (p-value)	Latency (s)	*vs.* day 0 (p-value)	50% threshold (g)	*vs.* day 0 (p-value)	50% threshold (g)	*vs.* day 0 (p-value)
males	WT	**baseline**	9.52 ± 1.19	–	6.49 ± 0.43	–	0.89 ± 0.14	–	1.04 ± 0.19	–
		day 1	7.59 ± 0.93	***0.005***	5.90 ± 0.65	*0.737*	0.97 ± 0.11	*0.958*	1.17 ± 0.12	*0.846*
		day 2	8.22 ± 0.95	*0.579*	6.12 ± 0.79	*0.971*	0.63 ± 0.12	*0.243*	0.93 ± 0.11	*0.896*
		day 3	7.48 ± 0.76	*0.275*	5.69 ± 0.77	*0.701*	0.64 ± 0.10	***0.038***	0.86 ± 0.12	*0.792*
		day 4	8.30 ± 1.18	*0.756*	5.99 ± 0.51	*0.726*	0.67 ± 0.12	*0.479*	0.86 ± 0.12	*0.702*
	TRESK KO	**baseline**	6.13 ± 0.80	–	4.72 ± 0.49	–	0.82 ± 0.12	–	0.97 ± 0.09	–
		day 1	6.86 ± 0.99	*0.789*	5.55 ± 0.64	*0.474*	0.68 ± 0.14	*0.822*	1.02 ± 0.12	*0.879*
		day 2	4.36 ± 0.58	*0.066*	4.43 ± 0.59	*0.989*	0.64 ± 0.13	*0.362*	0.99 ± 0.10	*0.9997*
		day 3	6.04 ± 0.47	*0.9999*	4.65 ± 0.52	*0.9999*	0.67 ± 0.13	*0.585*	1.02 ± 0.08	*0.969*
		day 4	5.80 ± 0.84	*0.991*	4.41 ± 0.34	*0.938*	0.37 ± 0.10	***0.028***	0.87 ± 0.15	*0.929*
females	WT	**baseline**	6.47 ± 0.52	–	7.16 ± 0.51	–	0.84 ± 0.14	–	0.77 ± 0.11	–
		day 1	3.40 ± 0.48	***0.002***	5.39 ± 0.48	*0.101*	0.47 ± 0.12	*0.095*	0.76 ± 0.12	*0.9999*
		day 2	3.84 ± 0.45	***0.006***	6.04 ± 0.43	*0.171*	0.24 ± 0.09	***0.005***	0.61 ± 0.12	*0.388*
		day 3	4.28 ± 0.53	***0.002***	6.12 ± 0.49	*0.142*	0.32 ± 0.11	***0.004***	0.49 ± 0.12	*0.068*
		day 4	5.97 ± 0.72	*0.919*	6.51 ± 0.47	*0.669*	0.32 ± 0.06	***0.003***	0.63 ± 0.14	*0.780*
	TRESK KO	**baseline**	6.19 ± 0.41	–	6.11 ± 0.63	–	0.74 ± 0.16	–	0.88 ± 0.12	–
		day 1	4.18 ± 0.72	*0.054*	6.79 ± 0.72	*0.654*	0.37 ± 0.12	***0.008***	0.89 ± 0.20	*> 0.999*
		day 2	3.27 ± 0.42	***0.002***	4.61 ± 0.67	*0.184*	0.41 ± 0.14	*0.051*	0.55 ± 0.11	*0.094*
		day 3	3.96 ± 0.46	***0.015***	4.45 ± 0.43	***0.046***	0.36 ± 0.11	*0.066*	0.68 ± 0.13	***0.029***
		day 4	6.28 ± 0.69	*0.9998*	5.52 ± 0.95	*0.953*	0.49 ± 0.11	*0.280*	0.70 ± 0.12	*0.402*

Statistics tests:

baseline *vs.* each day of treatment: row-matched one-way ANOVA multiple comparisons test (latency times, 50 % threshold force)

Table 9. Effects of Tacrolimus on the plantar heat and mechanical sensitivity of WT and TRESK KO mice. *Evaluation of the plantar heat and mechanical sensitivity of WT and TRESK KO males and females before and after Tacrolimus or saline solution (PBS) administration. 40 µg of Tacrolimus in 50 µL of PBS or 50 µL of PBS were administered IP after the sensitivity measurements of baseline, day 1 and day 2. Mean ± SEM of latency times for mice to respond to an infrared beam (Hargreaves) and threshold forces applied to the paw necessary to elicit nocifensive responses half of the application times (using the von Frey method). Statistical analysis significance of differences in the measurements before and different days after the treatment shown as p-values. Animals measured with Hargreaves: n = 12 WT males, TRESK KO males and WT females and n = 13 TRESK KO females (Tacrolimus-treated), and n = 14 WT males and TRESK KO females, n = 12 TRESK KO males and n= 13 WT females (saline controls). Animals measured with von Frey filaments: n = 12 for WT and TRESK KO males and n = 13 for WT and TRESK KO females (Tacrolimus), and n = 12 WT males, n = 10 TRESK KO males, n = 13 WT females and n = 14 TRESK KO females. Statistically significant values (threshold of significance of 5 %) highlighted using bold characters.*

		Hargreaves					Von Frey				
		CFA		PBS			CFA		PBS		
		Latency (s)	*vs.* day 0 (p-value)	Latency (s)	*vs.* day 0 (p-value)	CFA *vs.* PBS (p-value)	50 % threshold (g)	*vs.* day 0 (p-value)	50 % threshold (g)	*vs.* day 0 (p-value)	CFA *vs.* PBS (p-value)
males	WT										
	baseline	8.79 ± 0.70	–	8.98 ± 1.10	–	*0.053*	0.77 ± 0.13	–	0.97 ± 0.13	–	*0.338*
	1 hour	2.08 ± 0.35	***0.0003***	8.83 ± 1.75	*> 0.999*	*0.902*	0.37 ± 0.12	*0.220*	0.86 ± 0.28	*0.997*	*0.096*
	5 hours	2.76 ± 0.28	***0.0005***	9.68 ± 3.78	*> 0.999*	***0.020***	0.10 ± 0.03	***0.005***	0.82 ± 0.27	*0.992*	***0.006***
	day 1	3.46 ± 0.63	***0.027***	9.11 ± 0.93	*> 0.999*	*> 0.999*	0.20 ± 0.06	*0.050*	0.80 ± 0.15	*0.890*	***0.001***
	day 3	4.16 ± 0.69	*0.182*	8.30 ± 1.39	*> 0.999*	*0.971*	0.44 ± 0.18	*0.650*	1.02 ± 0.16	*0.999*	*0.061*
	day 7	4.93 ± 1.33	*0.156*	7.52 ± 1.48	*> 0.999*	*0.318*	0.48 ± 0.07	*0.352*	0.68 ± 0.30	*0.920*	*0.439*
	day 16	4.88 ± 0.82	*0.213*	6.50 ± 1.87	*> 0.999*	*0.383*	0.51 ± 0.13	*0.514*	0.77 ± 0.33	*0.990*	*0.395*
	TRESK KO										
	baseline	6.23 ± 0.76	–	7.39 ± 0.61	–	*0.114*	0.63 ± 0.16	–	0.71 ± 0.17	–	*0.770*
	1 hour	2.05 ± 0.37	***0.015***	8.96 ± 1.63	*> 0.999*	*0.686*	0.18 ± 0.06	*0.140*	0.88 ± 0.22	*0.961*	***0.004***
	5 hours	1.85 ± 0.28	***0.004***	8.24 ± 1.66	*> 0.999*	*0.886*	0.22 ± 0.05	*0.155*	1.02 ± 0.12	*0.712*	***< 0.0001***
	day 1	4.76 ± 1.92	*0.381*	8.97 ± 1.20	*> 0.999*	*> 0.999*	0.14 ± 0.05	*0.077*	1.03 ± 0.23	*0.717*	***0.001***
	day 3	4.34 ± 0.87	*> 0.999*	8.87 ± 1.72	*> 0.999*	*0.886*	0.33 ± 0.10	*0.489*	1.06 ± 0.20	*0.624*	***0.005***
	day 7	5.99 ± 0.85	*> 0.999*	7.99 ± 1.24	*> 0.999*	*0.829*	0.37 ± 0.09	*0.663*	0.66 ± 0.23	*0.999*	*0.194*
	day 16	6.87 ± 1.34	*> 0.999*	5.80 ± 1.25	*> 0.999*	*> 0.999*	0.39 ± 0.13	*0.666*	0.49 ± 0.15	*0.540*	*0.630*

Statistics tests:

baseline *vs.* each time point of treatment: Friedman multiple comparisons test (Hargreaves), row-matched one-way ANOVA multiple comparisons test (von Frey)

CFA *vs.* PBS: Mann-Whitney test (Hargreaves), unpaired T-test (von Frey)

Table 10. CFA effects on plantar heat and mechanical sensitivity. *Analysis of the plantar heat and mechanical sensitivity measured using the Hargreaves and von Frey "up and down" methods, respectively. Inducement of the CFA model of persistent pain by injecting 10 µL of CFA intraplantar to WT and TRESK KO animals. Control animals injected with 10 µL of PBS intraplantar. Latency times and threshold forces are indicated as mean ± SEM. P-values indicate the statistical significance of comparing the different time points after treatment with the baseline measurements (vs. day 0 columns) or of comparing the values of CFA and PBS-treated animals on the same time points (CFA vs. PBS column). N = 7 for CFA-treated and n = 4 for PBS-injected. Statistically significant p-values (threshold of significance of 5 %) are highlighted using bold characters.*

Apart from the reversible effects of calcineurin inhibition on pain conditions, we also wanted to study the possible role of TRESK in a model of persistent pain. Thus, we induced localized persistent inflammatory pain in WT and TRESK KO males by injecting Complete Freud's Adjuvant (CFA) subcutaneously in one of their hind paws. CFA injection resulted in a rapid increase of WT and TRESK KO males' heat sensitivity, that we found already one hour after the injection and that persisted until three days after the injection, although results only show statistically significant values for the first day after the injection in WT animals and for the first five hours after injection in TRESK KO animals (**Table 10**). Control animals injected with saline solution showed no variations in their sensitivity to heat during the 16 days of the experiment (**Figure 27**, **Table 10**).

TRESK has low contribution in plantar mechanical sensitivity in physiological and pain conditions

Callejo et al., 2013 showed that mechanical-like stimuli in the membrane of DRG neurons increased TRESK activity, and (Castellanos et al. 2020) that C-fibres lacking TRESK are activated when stimulated with lower forces than those that activate fibres with the channel. (Weir et al. 2019) found that TRESK reduces light touch and dynamic mechanical sensitivity, and (Guo et al. 2019) that it is involved in facial mechanical sensitivity. However, those same authors found that TRESK was not involved in the modulation of plantar mechanical sensitivity. Meanwhile, other studies knocking-down or knocking-out TRESK on rats and mice showed that the channel prevented animals' plantar mechanical hypersensitivity (Castellanos et al. 2020; Tulleuda et al. 2011; Yang et al. 2018). Here, we decided to use a battery of behavioural tests to evaluate the plantar punctate mechanical sensitivity of male and female mice of WT and TRESK KO strains.

We used different von Frey methods (see methods and (Deuis, Dvorakova, and Vetter 2017)) to determine the threshold forces applied to the plantar surface of the paw to provoke a response of WT and TRESK KO mice. All methods pointed to a low or inexistent role of TRESK in the modulation of plantar punctate mechanical sensitivity of males.

First, we used the plantar aesthesiometer in males, an automatic method to determine the threshold force at which animals withdraw the stimulated paw. Although graphs seem to point to a possible protective role of TRESK in the plantar mechanical sensitivity (**Figure 28**),

we found no statistically significant differences between the threshold forces measured with this method (threshold force of 4.86 ± 0.19 g and 5.32 ± 0.21 g for WT and TRESK KO males, respectively; unpaired T-test p-value of 0.110). Similarly, using the von Frey "up and down" method, a manual method that allows to find the threshold force at which animals' respond half of the times to the stimuli, we found no differences in the plantar mechanical sensitivities of WT and TRESK KO males and females (threshold force of 0.77 ± 0.05 g for WT males, 0.73 ± 0.06 g for TRESK KO males, 0.68 ± 0.05 g for WT females and 0.77 ± 0.06 for TRESK KO females; Mann-Whitney test p-values of 0.192 comparing WT males *vs.* females, 0.542 comparing TRESK KO males *vs.* females, 0.633 comparing WT *vs.* TRESK KO males and 0.252 comparing WT *vs.* TRESK KO females; **Figure 28**).

Using the Dynamic aesthesiometer and manual von Frey, we observed that animals can react to plantar mechanical stimuli with different responses (**Figure 28**). Ducourneau et al. 2014 described a new method using von Frey filaments to distinguish between detection ("touch" responses, scored "1") and nocifensive responses (withdrawal responses, scored from "2" to "4"), that we name here as von Frey "responses" method. Preliminary results in our laboratory showed differences between WT and TRESK KO males. Here, we compared the behaviours in response to different forces applied to WT and TRESK KO females' paws. We found that mechanical stimulation of the hind paw with increasing forces led to an increase in the touch and nocifensive responses. However, at forces higher than 0.16 g, the animals started responding less with "touch" responses in favour of nocifensive responses.

We found no differences in the area under the curve of the mean score and above the "noxious score" of "1.2" (see Methods and (Ducourneau et al. 2014); area under the curve and above "noxious score" of 4.2 ± 0.52 for WT and 4 ± 0.78 for TRESK KO females; unpaired T-test p-value of 0.831). When comparing the different reactions in response to different forces, we only find differences in the percentage of neurons responding to a stimulus of 0.6 g with nocifensive responses, although they do not reach statistically significant levels (percentages of noxious responses to a plantar stimulus of 0.6 g of 52.5 % and 74.3 % for WT and TRESK KO females, respectively; Fisher's exact test p-value of 0.060; **Figure 28**).

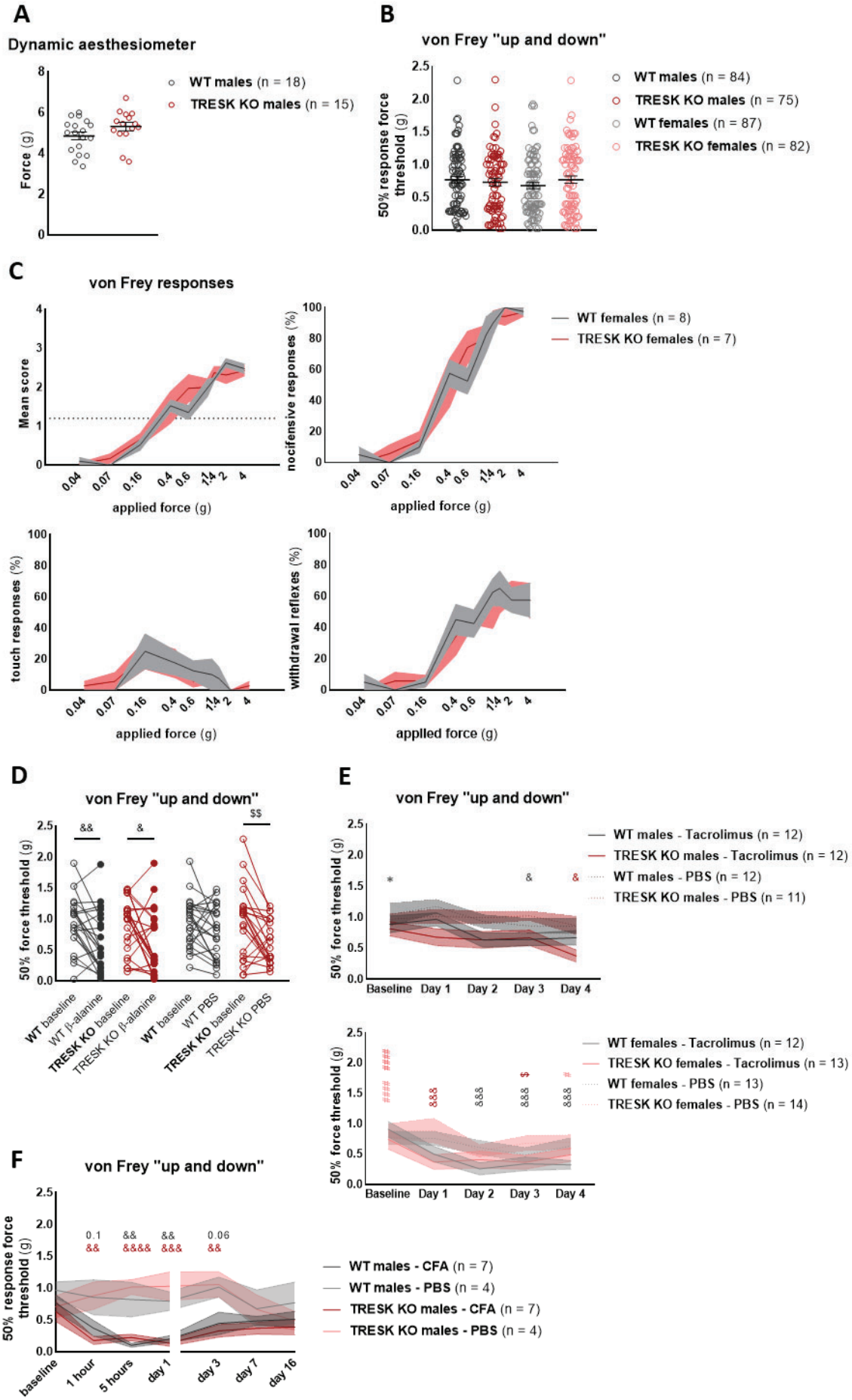
A
Dynamic aesthesiometer
Force (g)
WT males (n = 18)
TRESK KO males (n = 15)
B
von Frey "up and down"
50% response force threshold (g)
WT males (n = 84)
TRESK KO males (n = 75)
WT females (n = 87)
TRESK KO females (n = 82)
C
von Frey responses
Mean score
applied force (g)
nocifensive responses (%)
touch responses (%)
withdrawal reflexes (%)
WT females (n = 8)
TRESK KO females (n = 7)
D
von Frey "up and down"
50% force threshold (g)
WT baseline
WT β-alanine
TRESK KO baseline
TRESK KO β-alanine
WT baseline
WT PBS
TRESK KO baseline
TRESK KO PBS
E
von Frey "up and down"
50% force threshold (g)
Baseline
Day 1
Day 2
Day 3
Day 4
WT males - Tacrolimus (n = 12)
TRESK KO males - Tacrolimus (n = 12)
WT males - PBS (n = 12)
TRESK KO males - PBS (n = 11)
WT females - Tacrolimus (n = 12)
TRESK KO females - Tacrolimus (n = 13)
WT females - PBS (n = 13)
TRESK KO females - PBS (n = 14)
F
von Frey "up and down"
50% response force threshold (g)
baseline
1 hour
5 hours
day 1
day 3
day 7
day 16
WT males - CFA (n = 7)
WT males - PBS (n = 4)
TRESK KO males - CFA (n = 7)
TRESK KO males - PBS (n = 4)

Figure 28. WT and TRESK KO mice show similar plantar mechanical sensitivity. *Analysis of the plantar mechanical sensitivity of the hind paws using the automatic von Frey or dynamic aesthesiometer* ***(a)****, the von Frey "up and down" method* ***(b)*** *and the evaluation of the different types of responses to repeated application of von Frey filaments of different forces* ***(c)****. The different types of responses, shown in subsection c – right, are considered in the automatic von Frey and the manual von Frey, but the classification of the different types of responses is only considered in the method of repeated stimulation. (c) Top left: the mean score indicates the profile of responses, with lower scores being the more characteristic of non-nocifensive behaviours. Other plots indicate the percentage of different types of responses in repeated stimulation of the paw with the same force (see methods). From top to bottom and from left to right : touch responses (behaviours scored 1: detection responses not followed by leg or body movements), withdrawal reflexes (behaviours scored 2: withdrawal responses not followed by moving away from the stimuli or licking or biting the paw), and nocifensive responses (behaviours scored over 2: withdrawal reactions followed or not by other nocifensive behaviours). Baseline values of different groups were analysed using unpaired T-tests (for dynamic aesthesiometer data – a), Mann-Whitney test (for von Frey "up and down" data – b), and unpaired T-tests of the area under the curve (for von Frey responses data – c). When the percentage of nocifensive responses to a force of 0.6 g was analysed using the Fisher's exact test, the p-value was of 0.06 (subsection c – top right).* ***(d)*** *Effects of an intraplantar injection of 10 µL of β-alanine 50 mM or PBS on the mice's plantar mechanical sensitivity, evaluated using the von Frey "up and down" method before and 15 minutes after injections. Males and females are plotted together because there were no differences between their pre- and post-injection values. Statistical analysis of injection effects using the paired T-test for WT animals (12 males and 12 females per treatment) and the Wilcoxon test for TRESK KO animals (12 males and 12 females per treatment).* ***(e)*** *Threshold forces necessary to elicit a response half of the applications calculated using the von Frey "up and down" method before and after injection with 40 µg / 50 µL of Tacrolimus or 50 µL of PBS IP during 3 consecutive days (after baseline, day 1 and day 2 measurements). Statistical analysis detailed in* ***Table 9****. (f) Force threshold to withdraw the paw in 50 % of applications calculated using the von Frey "up and down" method before and at different time points after a unique intraplantar injection of 20 µg in 20 µL of CFA or 20 µL of PBS in the hind paw (after the baseline measurement). Statistical analysis detailed in* ***Table 10****. For (a) and (b), single dots show data from single animals and lines represent mean and SEM of each group; for (c), (e) and (f), lines and shadowed areas show means and SEM of each group, respectively, and, for (d), connected dots show data from single animals before and after β-alanine injection. The number of animals analysed in each group is shown between parentheses in each section. Statistical significant differences between WT and TRESK KO animals are shown using asterisks (* for p-value < 0.05), between males and females using pads (# for p-value < 0.05 and #### for p-value < 0.0001), between baseline values and each time point after β-alanine (d), Tacrolimus (e) or CFA (f) treatments values using ampersands (& for p-value < 0.05, && for p-value < 0.01, &&& for p-value < 0.001, &&&& for p-value < 0.0001 and numbers when p-values are close but do not reach the 5 % level of significance) and between baseline values and each day after PBS treatment values using dollar/peso signs ($ for p-value < 0.05 and $$ for p-value < 0.01). Colours of the signs or numbers indicate which groups are compared.*

Considering the results obtained with different techniques of manual and electronic von Frey, we could determine that animals lacking TRESK do not show changes in the plantar mechanical sensitivity compared to those with the channel. However, considering that TRESK protects MrgprD$^+$ neurons from hyperexcitability (**Figure 13**) and that that depletion of those neurons results in a decrease of noxious mechanical sensitivity and in limited development of mechanical hypersensitivity (Cavanaugh et al. 2009), we wanted to evaluate the role of TRESK in mice plantar mechanical sensitivity after potentiating the role of MrgprD$^+$ neurons. Thus, we injected β-alanine subcutaneously in the paw of WT and TRESK KO mice and evaluated their plantar mechanical sensitivity before and 15 minutes after the injection. We also injected saline solution (PBS) intraplantar in other animals to control for the mechanical effects of the injection and the possible effects of the diluent. We found that both WT and

TRESK KO animals showed decreased mechanical thresholds after β-alanine treatment (0.94 ± 0.09 g and 0.62 ± 0.10 g for WT animals before and after β-alanine treatment, respectively, and 0.92 ± 0.09 g and 0.61 ± 0.10 g for TRESK KO animals before and after β-alanine treatment, respectively; paired T-test p-value of 0.001 for WT animals and Wilcoxon test p-value of 0.0.17 for TRESK KO animals, respectively; **Figure 28**). TRESK KO animals injected with saline solution, however, also showed decreased mechanical threshold for response (0.95 ± 0.08 g and 0.80 ± 0.09 before and after PBS injection, respectively; Wilcoxon test p-value of 0.003), which does not allow the discard of the injection effects in the increase of the plantar mechanical sensitivity of TRESK KO animals injected with β-alanine. On the other side, we found no changes in the plantar mechanical sensitivity of WT animals before and after PBS injection (50% force thresholds of 0.96 ± 0.12 and 0.62 ± 0.07 before and after PBS injection, respectively; paired T-test p-value of 0.105; **Figure 28**). These results confirm the effects of β-alanine in the increase of the plantar mechanical sensitivity of WT animals, while point to a possible effect of acute mechanical disturbance by intraplantar injection in animals lacking TRESK (affected by both β-alanine and saline solution injections).

As explained in Chapter 4.5, treatment with calcineurin inhibitors such as Tacrolimus can produce Calcineurin-Inhibitor Pain Syndrome (CIPS) as side effects. However, the drug is also used to alleviate mechanical hypersensitivity in other cases (Yang et al. 2018). Although we found no differences in the baseline plantar mechanical sensitivities of WT and TRESK KO mice, considering that TRESK is regulated by calcineurin, we wondered whether the inactivation of the channel might modulate the mechanical sensitivity of animals treated with Tacrolimus. To answer this question, we treated WT and TRESK KO animals with Tacrolimus or saline solution (PBS, negative control) systemic and measured their plantar mechanical sensitivity before and during four days after the treatment.

WT and TRESK KO males treated with PBS did not show changes in their plantar mechanical sensitivity, while WT and TRESK KO females showed a decrease in the threshold force applied to the plantar surface to elicit responses on the day 3, and days 3 and 4 of the experiment, respectively. Those differences only reach statistically significant values on TRESK KO females the day 3 after treatment. Meanwhile, Tacrolimus treatment induced a decrease in the threshold forces necessary to elicit responses in all WT and TRESK KO males and females. The

effect of the treatment was more pronounced and sustained in females than in males (**Figure 28**, **Table 9**).

Tacrolimus produced similar effects in WT and TRESK KO males, that presented decreased mechanical threshold on day 3 and 4 after treatment, respectively. By their side, WT and TRESK KO females showed decreased threshold forces from the first day after the treatment and until the last and the third day of the treatment, respectively, although some of those decreases did not reach statistically significant levels (**Figure 28**, **Table 9**). Although, as explained, females treated with PBS also show increased plantar mechanical sensitivities and, thus, it is not possible to discard some habituation or recognition effects, the effects of Tacrolimus are more pronounced and sustained in time than the observed in PBS-treated females (**Figure 28**).

Summing these results up, we can say that calcineurin inhibition through Tacrolimus induces increases in the mechanical sensitivity in a TRESK-independent manner. However, as we still observed Tacrolimus effects 4 days after the treatment, it might be interesting to study the effects of TRESK for more time.

Although we found no effects of TRESK in the modulation of plantar mechanical sensitivity in physiological conditions (**Figure 28**), we wanted to study its possible contribution in chronic pain. Thus, we studied the plantar sensitivity of WT and TRESK KO males in the CFA model of persistent inflammatory pain. We found that both WT and TRESK KO males with intraplantar injected CFA showed remarkable increases in their plantar mechanical sensitivity from the very first moment after injection (1 hour post-injection), while we did not find any variation in the sensitivity of mice intraplantar injected with saline solution (PBS). We found that, in relation to baseline values, WT males showed a decreased 50% response force threshold calculated by the von Frey “up and down” method (see Methods) from 5 to 24 hours after CFA injection, although statistical analysis only show significant levels in the 5 hours after the injection time point. Those effects were only present 24 hours after CFA injection in TRESK KO males, although this difference did not reach statistically significant levels. When we compared the plantar sensitivity of animals treated with CFA and PBS to correct for the injection effects, and the experimental repetition and habituation processes, statistical tests indicate higher effects of the model of chronic pain from 1 hour to, at least, 3 days post-injection in both WT and TRESK KO animals (**Figure 28**, **Table 10**). Those effects did not reach

statistically significant levels in the measurements done 1 hour and 3 days after injection in WT males (**Table 10**). Summing this up, we did not observe any effect of TRESK in the development of the CFA persistent inflammatory pain model from 1 hour to, at least, 16 days after the beginning of the model.

Knocking out TRESK attenuates osteoarthritic mechanical joint pain

Although we found that TRESK impact in mice's plantar mechanical sensitivity was low (**Figure 28**), we wondered whether the channel modulated mechanical sensitivity in joints. To evaluate this, we took advantage of the knee-bending test (detailed in Methods) and found that TRESK KO males showed less aversive behaviours in response to knee flexion and extension than WT males (Knee bend score of 1.1 ± 0.2 in WT males and of 0.6 ± 0.1 in TRESK KO males; Welch's test p-value of 0.020; **Figure 29**). Thus, TRESK seemed to play a protective role in the joint mechanical sensitivity. However, as the knee-bending test is very invasive, it is difficult to ensure that the observed results are due to decreased sensitivity instead of to changes in animals' perception or anxiety, which might be mediated by CNS superior areas with TRESK expression. However, previous studies did not identify anxious phenotypes in mice lacking TRESK (Guo et al. 2019).

Osteoarthritis is a degenerative disease characterised by inflammation and the gradual deterioration of joint cartilage, resulting in chronic pain. As TRESK seemed to modulate the mechanical sensitivity of the knee joints, we wanted to assess its contribution to osteoarthritic pain. Thus, we studied the effects of knocking out the channel in monoarthritic mice induced by injecting 250 µg of monoiodoacetate (MIA) in one knee joint and compared the knee-bending scores and the plantar sensitivities of arthritic hind paws (ipsilateral) with healthy ones (contralateral) of the same animals from 1 to 28 days after the injection.

We found that both WT and TRESK KO males showed increased knee-bending scores in both treated and contralateral paws after MIA treatment, which indicates the development of the osteoarthritic model. Compared to baseline values, WT males presented increased knee-bending scores in the MIA-treated paw from 1 day to, at least, 28 days after the treatment. TRESK KO animals also presented increased knee-bending scores in the treated paw, which appeared clearly 2 days after the treatment and lasted until, at least, 28 days post-treatment, although differences were only statistically significant until the day 14 (**Figure 29**, **Table 11**).

Similarly to the observations on the baseline values, WT males tended to obtain higher knee-bending scores in the osteoarthritic paw than TRESK KO males (**Figure 29**, **Table 11**; unpaired T-test comparing WT and TRESK KO knee-bending scores p-values of 0.179, 0.002, 0.592, 0.087, 0.084, 0.056 and 0.029 for days 1, 2, 5, 7, 14, 21 and 28 after treatment, respectively).

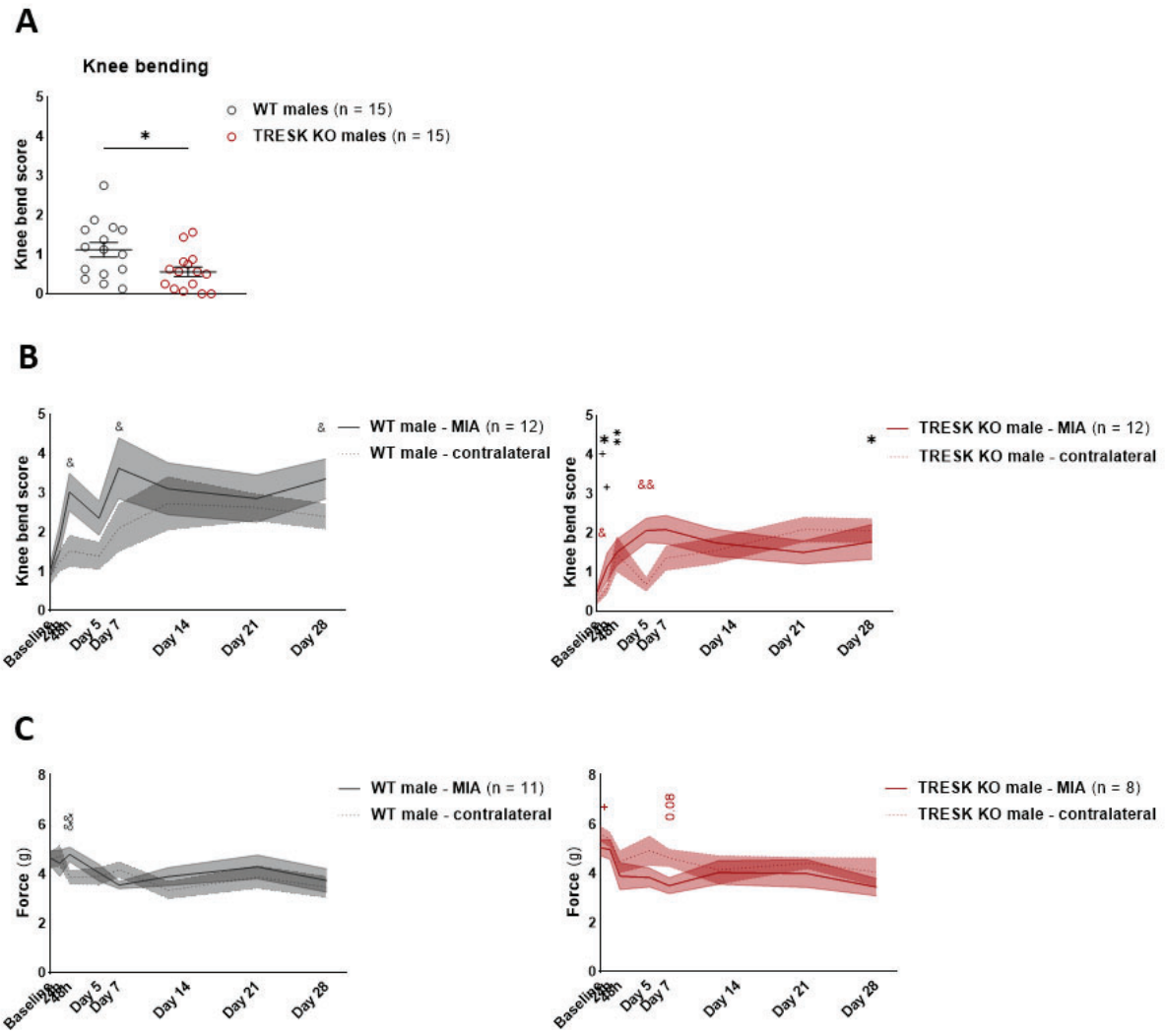

Figure 29. TRESK KO animals show decreased joint mechanical sensitivity. (a) *Knee joint mechanical sensitivity evaluated using the knee-bending score. Score resultant from adding punctuations from 5 flexion-extension cycles in the hind paw. Punctuations of [0] for no response, [0.5] for struggle at maximal flexion or extension, [1] for struggle to moderate flexion or extension or vocalization at maximal flexion or extension, and [2] for vocalization at moderate flexion or extension. The maximum score possible is 10. Left: Illustrative picture of the knee-bending technique. Right: Comparison of the knee-bend scores of WT and TRESK KO males in physiological states. Single dots indicate values from single animals, and lines the mean and SEM for each group. Statistical analysis using Welch's test.* ***(b)*** *Evaluation of the knee joint mechanical sensitivity of the two hind paws before and different time points after injecting one of the knee joint cavities with 250 µg of MIA to induce osteoarthritis in that paw.* ***(c)*** *Evaluation of the plantar mechanical sensitivity of the treated and the contralateral hind paws of the osteoarthritic mice analysed in section (b) using the Dynamic aesthesiometer. Lines and shadowed areas in sections (b) and (c) correspond to the mean and SEM of each group. Statistical analysis of the osteoarthritic model is detailed in* ***Table 11****. The number of animals analysed in each group is shown between parentheses on each figure. Statistical significant differences between WT and TRESK KO animals are shown using asterisks when*

they compare baselines (a) or MIA-treated paws (for p-value < 0.05, ** for p-value < 0.01) and using plus signs when they show differences in contralateral paws (+ for p-value < 0.05). Statistical significant differences between MIA-treated and contralateral paws are shown using ampersands (& for p-value < 0.05, && for p-value < 0.01, and numbers when p-values are close but do not reach the 5 % level of significance). Colours of the signs or numbers indicate which groups are compared.*

As said, when analysing the knee-bending scores of the contralateral paws, we also observed increases in the intensity and number of nocifensive responses during the development of the osteoarthritic model. Those increases appeared later than the effects on the osteoarthritic paw: on day 14 in WT males and on day 1 and 7 in TRESK KO males, and lasted until the day 28, at least (**Figure 29**, **Table 11**). Similar tendencies were observed in previous studies after the injection of high doses of MIA in the contralateral paw, although they were not that strong and were not clearly defined. Those effects are probably mediated by compensating mechanisms to avoid the pain resultant of supporting the body weight on the osteoarthritic paw. Still, when we compared the increases in the joint mechanical sensitivity of treated and contralateral paws, MIA-treated paw maintained higher knee-bending values than contralateral paws on days 2, 7 and 28 after treatment in WT males and on days 5 and 7 in TRESK KO males. From 5 to, at least, 28 days after the treatment, the knee-bending scores of contralateral paws of WT and TRESK KO males reached similar levels (**Table 11**).

MIA treatment affected the plantar mechanical sensitivity of WT and TRESK KO males to a lower extent. Both WT and TRESK KO males showed little increases in plantar sensitivity in the treated and contralateral paws. Increases in the plantar mechanical sensitivities of treated paws appeared only at day 7 after treatment in both WT and TRESK KO males, although differences only reach statistically significant levels in WT animals. Conversely, increases in the plantar mechanical sensitivities of untreated paws appeared later: only on day 14 in WT males and on days 21 and 28 on TRESK KO males (**Figure 29**, **Table 11**). These effects on the plantar mechanical sensitivity strengthen the thesis that the continued overload of the contralateral knee due to osteoarthritic pain in the treated paw results in allodynia in the untreated paw. TRESK depletion did not modify the effects of monoarthritis on the plantar mechanical sensitivity of the contralateral paw. When comparing the plantar mechanical sensitivity of ipsi and contralateral paws, we found that, 48 hours after treatment, WT males needed higher forces to respond with the treated paw compared to the contralateral. TRESK KO males required higher forces to respond with the contralateral than with the treated paw 7 days after treatment, although differences did not reach statistically significant values

(**Figure 29**, **Table 11**). TRESK expression did not modulate the effects of MIA on the ipsi and contralateral paws (**Table 11**; unpaired T-test comparing threshold forces of WT and TRESK KO p-values for days 1, 2, 5, 7, 14, 21 and 28 after treatment, respectively: 0.385, 0.457, 0.136, 0.695, 0.890, 0.807, 0.698 and 0.650 for the ipsilateral paw, and 0.033, 0.286, 0.235, 0.147, 0.360, 0.233, 0.363 and 0.417 for the contralateral paw).

In summary, although TRESK has low impact in the regulation of plantar mechanical sensitivity, its depletion has a protective role against joint mechanical hypersensitivity, in both physiological and osteoarthritic conditions. Moreover, we saw that the development of a model of monoarthritis in the knee results in an increase in joint and plantar allodynia in both the arthritic and the contralateral paws. Effects in the contralateral paw tend to appear later. TRESK expression increases the joint mechanical allodynia in the model of osteoarthritic pain. More than the half of people affected by osteoarthritis are women. Thus, it might be interesting to study the contribution of TRESK to the development of osteoarthritic pain also in female mice.

			Knee-bending score					Dynamic aesthesiometer – Force (g)				
			MIA-treated paw	MIA *vs.* day 0 (p-value)	Contralateral paw	control *vs.* day 0 (p-value)	MIA *vs.* contralateral (p-value)	MIA-treated paw	MIA *vs.* day 0 (p-value)	Contralateral paw	control *vs.* day 0 (p-value)	MIA *vs.* contralateral (p-value)
males	WT	**baseline**	0.98 ± 0.16	-	0.84 ± 0.21	-	*0.500*	4.67 ± 0.29	–	4.55 ± 0.32	–	*0.786*
		day 1	1.83 ± 0.36	***0.045***	1.25 ± 0.27	*0.449*	*0.137*	4.44 ± 0.53	*0.998*	4.75 ± 0.44	*0.995*	*0.585*
		day 2	3.02 ± 0.48	***0.004***	1.52 ± 0.41	*0.312*	***0.017***	4.80 ± 0.29	*0.988*	3.88 ± 0.27	*0.128*	***0.007***
		day 5	2.35 ± 0.43	***0.038***	1.40 ± 0.35	*0.122*	*0.120*	4.05 ± 0.34	*0.269*	3.91 ± 0.36	*0.768*	*0.910*
		day 7	3.63 ± 0.78	***0.019***	2.10 ± 0.61	*0.155*	***0.022***	3.56 ± 0.15	***0.014***	4.19 ± 0.32	*0.928*	*0.153*
		day 14	3.10 ± 0.66	***0.026***	2.73 ± 0.69	***0.037***	*0.575*	3.90 ± 0.36	*0.468*	3.35 ± 0.36	***0.047***	*0.348*
		day 21	2.85 ± 0.60	***0.029***	2.63 ± 0.35	***0.014***	*0.696*	4.29 ± 0.48	*0.982*	3.88 ± 0.47	*0.758*	*0.436*
		day 28	3.35 ± 0.51	***0.002***	2.40 ± 0.33	***0.002***	***0.040***	3.75 ± 0.48	*0.484*	3.47 ± 0.43	*0.398*	*0.689*
	TRESK KO	**baseline**	0.49 ± 0.12	-	0.26 ± 0.07	-	***0.046***	5.06 ± 0.32	–	5.64 ± 0.32	–	*0.160*
		day 1	1.13 ± 0.36	*0.252*	0.56 ± 0.13	***0.023***	*0.161*	4.99 ± 0.40	*0.9998*	5.39 ± 0.31	*0.994*	*0.418*
		day 2	1.50 ± 0.34	***0.032***	1.46 ± 0.46	*0.123*	*0.917*	3.90 ± 0.55	*0.109*	4.49 ± 0.45	*0.355*	*0.238*
		day 5	2.06 ± 0.32	***0.001***	0.69 ± 0.19	*0.192*	***0.006***	3.84 ± 0.39	*0.139*	4.94 ± 0.61	*0.745*	*0.203*
		day 7	2.08 ± 0.37	***0.004***	1.35 ± 0.32	***0.010***	*0.077*	3.51 ± 0.33	*0.082*	4.64 ± 0.36	*0.195*	*0.081*
		day 14	1.75 ± 0.35	***0.008***	1.54 ± 0.34	***0.007***	*0.678*	4.05 ± 0.48	*0.448*	4.16 ± 0.59	*0.321*	*0.811*
		day 21	1.50 ± 0.30	*0.065*	2.08 ± 0.32	***0.0004***	*0.177*	4.00 ± 0.57	*0.526*	4.43 ± 0.24	***0.012***	*0.429*
		day 28	1.77 ± 0.45	*0.089*	2.06 ± 0.30	***0.0004***	*0.589*	3.45 ± 0.35	*0.131*	4.07 ± 0.59	*0.087*	*0.203*

Statistics tests:

baseline *vs.* each time point of treatment: row-matched one-way ANOVA multiple comparisons test (knee-bending test, dynamic aesthesiometer)

MIA *vs.* contralateral paw: paired T-test (knee-bending test, dynamic aesthesiometer)

Table 11. Representative values and statistical analysis of the mechanical sensitivity indicators in a model of osteoarthritic mice. Knee joint and plantar mechanical sensitivity of MIA-treated and contralateral paws. Induction *of osteoarthritis in one hind paw of mice by injecting the knee with 250 µg of MIA. Mean ± SEM are the reference values for the knee bend score (joint sensitivity) and the threshold force (plantar sensitivity). "MIA vs. day 0" columns show the p-values resultant of comparing each time point values with the baseline values. "MIA vs. contralateral" columns show the p-values resultant of comparing treated and contralateral paw values of the same time points. N = 12 for the knee-bending, and n = 11 WT animals and n = 8 TRESK KO animals for dynamic aesthesiometer tests. Statistically significant p-values (threshold of significance of 5 %) are highlighted using bold characters.*

Discussion

TRESK in specific populations of primary sensory neurons

Perceiving the state of our environment and body is essential to survive. The system responsible for sensory perception is complex and tightly regulated to avoid decreased sensitivity or pain sensing without actual or potential harmful stimuli. Primary sensory neurons are the first connexion between body tissues and the CNS. TRESK is one of the main responsible of the modulation of primary sensory neurons' excitability. Thus, the study of the TRESK role in specific populations of sensory neurons and in sensory perception may allow to understand a mechanism involved in the endogenous regulation of sensory perception and to evaluate whether it may be a potential target to treat alterations in sensory perception.

Dobler et al., 2007 found *Kcnk18* transcripts in most of DRG neurons of all sizes, while Weir et al., 2019, in a more detailed study, identified the *Kcnk18* transcript in TG neurons of all sizes with markers corresponding to the neuronal populations of low-threshold mechanoreceptors NF1 and NF2, and the nociceptors populations NP2, PEP1 and PEP2. In DRGs, single-cell sequencing studies identified expression of the *Kcnk18* transcript in the same populations of low-threshold mechanoreceptors but in the NP1 instead of the PEP1 population of nociceptors (Jung et al. 2023; Usoskin et al. 2015). In a similar way, we found *Kcnk18* transcript expression in DRG and TG populations of all sizes and could validate its expression in the NP2 population of nociceptors, due to its coexpression with the *Mrgprd* and *Mrgpra3* transcripts, and in the NF1 and NF2 populations, due to the coexpression of the two transcripts in large-sized neurons.

TRESK in mechanical, heat and cold sensitivity

Different studies found that TRESK acts as a brake for neuronal excitability in different populations of primary sensory neurons and that, through this mechanism, its expression protects from hypersensitivity and allodynia. However, they show contradictory results regarding the different sensitivities modulated by the channel. Most of the studies agree in TRESK having a role in the protection from punctate mechanical and cold hypersensitivity in both male and female rodents, while its role in the modulation of heat sensitivity is more controversial (Castellanos et al., 2020; Guo et al., 2019; Tulleuda et al., 2011; Weir et al., 2019;

Yang et al., 2018) (**Table 2**). Surprisingly, we found that TRESK has almost no impact on the sensitivity of mice to cold temperatures and to punctate mechanical stimuli, while it prevents from heat hypersensitivity in a sex-independent manner.

We only found differences in the punctate mechanical sensitivity in the nocifensive but not touch behaviours of mice using specific techniques. Nevertheless, TRESK expression in Aδ-low threshold mechanoreceptors is involved in preventing mice responses to tactile stimuli (Usoskin et al. 2015; Weir et al. 2019), which might conditionate the observed effects of TRESK in the mechanical nociception studied in response to punctate stimuli. We also found that TRESK protects from the plantar mechanical hypersensitivity induced by low intensity disturbances (injecting saline solution subcutaneously), which points to a role of TRESK in the modulation of plantar mechanical sensitivity in a small range between noxious and innocuous stimuli.

Moreover, as mentioned in the introduction, differences in the results might be explained by the use of different animal models, by the different housing and experimental conditions, and by the variability between experimenters observed in the use of von Frey and Hargreaves techniques (Mogil 2017; Sadler, Mogil, and Stucky 2022). Here we propose that TRESK might modulate mechanical and thermal nociception at different degrees that are not always detectable depending on the experimental design.

Although Guo et al., 2019 found that TRESK prevents the TG-mediated heat sensitivity in female but not male animals, in this thesis and in previous studies in the laboratory (Castellanos et al. 2020), we found the role of TRESK in DRG-mediated mechanical and thermal sensitivity is similar in male and female mice.

In contrast with the lack of sex-mediated effects in the mechanical and thermal sensitivities of mice observed in other studies (Castellanos et al. 2020; Guo et al. 2019), we found that female mice tend to be more sensitive to heat than male mice. Although we found similar expression of the *Kcnk18* transcript in sensory ganglia from male and female mice, considering that TRESK modulates the heat sensitivity in mice, we hypothesise that TRESK activity might be mediating part of the differences in the heat sensitivity observed between male and female mice.

In this thesis and in the research previously published by Castellanos et al., 2020, it was found that TRESK expression reduced the number of DRG neurons responding to the TRPA1 agonist AITC, despite the unchanged expression of the TRPA1 in DRGs of TRESK KO mice. Moreover, in contrast to the effects expected, TRESK expression results in an increase in the nociceptive behaviours elicited by mice in response to AITC injected to the paw (Castellanos et al. 2020). As hypothesised in Castellanos et al., 2020, it is probable that other mechanisms are functionally compensating TRESK depletion in the DRG neurons of TRESK KO mice. These mechanisms are not including changes in the gene transcription of the other main K_{2P} channels in DRGs (Dobler et al. 2007; Kang and Kim 2006; Marsh et al. 2012), although changes in their protein expression or function can not be discarded. In a similar way, TRESK expression increases mice's sensitivity to mechanical joint movement evaluated using the knee-bending (see Methods).

TRESK expression also increases mice's sensitivity to mechanical joint movement in osteoarthritic conditions. Osteoarthritis development in one paw results in secondary effects appearing in the contralateral paw, probably due to weight redistribution or inflammation. TRESK is not involved in the modulation of these secondary effects. In a similar way, TRESK is not involved in the modulation of the secondary effects of joint deterioration and inflammation resulting in increased plantar mechanical sensitivity.

Among other populations, TRPA1 is expressed in the NP1 and NP2 populations of nociceptive neurons, which also express TRESK, and which might be involved in the modulation of the mechanical joint sensitivity in mice, thus explaining the unexpected results in the increased nociception in response to joint mobilisation. Single-cell sequencing and electrophysiology experiments in primary sensory neurons innervating the knee joint might help to unveil whether the observed behavioural effects are explained by compensating mechanisms activated by TRESK depletion in $TRPA1^{+}$ neurons.

Other explanation for this phenomenon is the expression of TRESK in inhibitory interneurons of the spinal cord, which might inactivate the propagation of the information of joint-innervating neurons to higher centres involved in sensory perception. As female mice show lower expression of the TRESK transcript in the spinal cord, it might be interesting to explore their responses to the mobilisation of the joint in the presence and the absence of the K_{2P} channel.

Finally, although animals were habituated to the manual retention, the knee-bending procedure is a very stressful procedure for them and, thus, it is possible that TRESK expression in different structures of the brain cortex might be mediating the animals' responses to the knee-bending test, although previous studies do not show TRESK effects in the results of tests evaluating mice anxiety (Guo et al. 2019).

Marsh et al., 2012 found that the inflammatory pain model induced by CFA injection presents decreases in TRESK, TASK 1, 2 and 3 and THIK2 levels in DRGs of rats, and that TRESK levels correlate with the spontaneous nocifensive behaviours elicited by the animals in this model. When evaluating the effects of mechanical and heat stimuli in mice nociception and although TRESK has been involved in the prevention of mechanical and heat hypersensitivity, we found that the channel can not protect from the pain hypersensitivity elicited in the model. The lack of TRESK effect might be due to the reduction of its expression in the model (Marsh et al. 2012) or due to the high effects of the inflammatory model apart from those involving TRESK. Nevertheless, it is possible that activating TRESK with agonists such as cloxyquin or nitroxoline, might compensate for its decreased expression and ameliorate the hypersensitivity effects mediated, in part, by the decrease of K_{2P} channels' currents.

Effects of TRESK modulation in nociception

Considering the role of TRESK in the modulation of the mechanical and thermal sensitivity and its activation through the phosphatase calcineurin (see Chapter 4.4), some authors hypothesised that the development the rare pain syndrome CIPS (Calcineurin-Inhibitor induced Pain Syndrome), which is characterised by severe and reversible pain in the lower limbs, might be mediated by the indirect inactivation of TRESK currents through calcineurin inhibition (Y. Huang et al. 2020; Prommer 2012; Smith 2009). Supporting this hypothesis, Yang et al., 2018 showed that mice treatment with the calcineurin inhibitor Tacrolimus increased TRESK phosphorylation and reduced the *Kcnk18* transcript expression.

Although different authors found that the treatment with Tacrolimus results in an amelioration of mechanical and thermal sensitivity in animals with neuropathic pain (Muthuraman and Sood 2014; Voda, Hama, and Sagen 2007), we found that intraperitoneal administration of the calcineurin inhibitor in male and female mice produced mechanical and

heat hyperalgesia, as it was previously reported by other authors (Y. Huang et al. 2020; Sato et al. 2007; Yang et al. 2018), and increased mice cold sensitivity at a lower extent.

Our results indicate that TRESK indirect inactivation by calcineurin inhibition mediates the heat hypersensitivity developed by male but not by female mice during the treatment with Tacrolimus. On the other side, we found that TRESK is not responsible for the mechanical and cold allodynia induced by Tacrolimus treatment in male and female mice. Although it should be considered that, in our experimental designs, we could not detect baseline differences between WT and TRESK KO mice sensitivities to mechanical and cold stimuli in most of the conditions, which might mask the detection of TRESK-mediated differences, it is also true that we observed similar Tacrolimus-induced changes in the mechanical and cold sensitivities of WT and TRESK KO animals.

These results suggests that other mechanisms apart from TRESK are the responsible for the alterations in mechanical and cold and in females' heat nociception in CIPS models of pain. Despite the effects of Tacrolimus in the development of CIPS are reversible, its effects on plantar cold and mechanical sensitivity of mice last for, at least, 2 days after the last Tacrolimus administration, depending on the sex of the animals. Thus, it can not be discarded whether TRESK (re)activation is involved in the recovery from Tacrolimus neuropathic effects.

$TRPA1^+$ and $MrgprD^+$ neurons are involved heat sensing and can be directly activated or sensitised by Tacrolimus (Arcas et al. 2019; Eriksson and Gasull Casanova 2019; Kita et al. 2019). The populations of non-peptidergic nociceptors NP1 and NP2 express both receptors and TRESK (Usoskin et al. 2015; Weir et al. 2019) and we found that TRESK prevents $MrgprD^+$ neurons from hyperexcitability while it has a dual effect in TRPA1-expressing neurons' responsiveness to chemical stimuli. Interestingly, TRESK prevents the activation of $TRPA1^+$ neurons from male mice while its expression promotes the activation of the same population of neurons from female mice. An increase in the responsiveness of the NP1 and NP2 populations of nociceptors due to TRESK inactivation might explain the selective role of the channel in the heat hypersensitivity developed by male mice in the CIPS pain model.

Conclusions

1. *Kcnk18* is highly expressed in DRG and TG sensory ganglia and, at lower levels, in the spinal cord, the brain cortex, the hippocampus and the cerebellum. *Kcnk18* expression is enriched in *Mrgprd*$^{+}$ and *Mrgpra3*$^{+}$ primary sensory neurons.

2. TRESK regulates MrgprD^{+} neurons excitability: its absence enhances neuronal firing and calcium responses to MrgprD activation. TRESK absence also increases the number of MrgprD^{+} neurons responding to cold stimuli in female mice.

3. Knocking out TRESK enhances the cold responsiveness in sensory neurons from females but not from males, with a main effect in high threshold cold-sensitive neurons. This difference does not affect the cold sensitivity of mice in physiological conditions.

4. TRESK channel prevents heat hypersensitivity in physiological conditions but not in persistent inflammatory pain conditions.

5. TRESK channel does not modulate plantar mechanical sensitivity in physiological and persistent pain conditions but increases joint mechanical sensitivity of mice in physiological and osteoarthritic conditions.

6. Inhibition of calcineurin by Tacrolimus enhances heat and mechanical sensitivity but does not modify cold sensitivity. Reversing TRESK activation through calcineurin inhibition with Tacrolimus does not modify heat, mechanical and cold sensitivity.

Bibliography

Abbafati, Cristiana et al. 2020. “Global Burden of 369 Diseases and Injuries in 204 Countries and Territories, 1990–2019: A Systematic Analysis for the Global Burden of Disease Study 2019.” *The Lancet* 396(10258): 1204–22.

Aida, Castellanos; “Role of the K2P Channel TRESK Nociceptive and Chronic Pain.”

Andres-Bilbe, Alba. 2020. “Mecanismes Neuronals de La Picor Aguda i Crònica En Neurones Sensorials: Implicació Del Canal TRESK.”

———. 2020. “The Background K+ Channel Tresk in Sensory Physiology and Pain.” *International Journal of Molecular Sciences* 21(15): 1–14.

Arcas, José Miguel et al. 2019. “The Immunosuppressant Macrolide Tacrolimus Activates Cold-Sensing TRPM8 Channels.” *Journal of Neuroscience* 39(6): 949–69.

Axelrod, Felicia B, and Max J Hilz. 2003. 23 Ch.B. Seminars in Neurology *The Autonomic Nervous System*.

Basbaum, Allan I., Diana M. Bautista, Grégory Scherrer, and David Julius. 2009. “Cellular and Molecular Mechanisms of Pain.” *Cell* 139(2): 267–84.

Bautista, Diana M. et al. 2008. “Pungent Agents from Szechuan Peppers Excite Sensory Neurons by Inhibiting Two-Pore Potassium Channels.” *Nature Neuroscience* 11(7): 772–79.

Beaulieu-Laroche, Lou et al. 2020. “TACAN Is an Ion Channel Involved in Sensing Mechanical Pain.” *Cell* 180(5): 956-967.e17. https://doi.org/10.1016/j.cell.2020.01.033.

Braun, Gabriella, Balázs Nemcsics, Péter Enyedi, and Gábor Czirják. 2011. “Tresk Background K+ Channel Is Inhibited by PAR-1/MARK Microtubule Affinity-Regulating Kinases in Xenopus Oocytes.” *PLoS ONE* 6(12).

Breivik, Harald et al. 2006. “Survey of Chronic Pain in Europe: Prevalence, Impact on Daily Life, and Treatment.” *European Journal of Pain* 10(4): 287–333.

Brohawn, Stephen G., Zhenwei Su, and Roderick MacKinnon. 2014. “Mechanosensitivity Is Mediated Directly by the Lipid Membrane in TRAAK and TREK1 K+ Channels.”

Proceedings of the National Academy of Sciences of the United States of America 111(9): 3614–19.

Busserolles, Jérôme, Xavier Gasull, and Jacques Noël. 2018. "Potassium Channels and Pain." In *The Oxford Handbook of the Neurobiology of Pain*, Oxford University Press, 263–312.

Cadaveira-Mosquera, Alba et al. 2012. "Expression of K2P Channels in Sensory and Motor Neurons of the Autonomic Nervous System." *Journal of Molecular Neuroscience* 48(1): 86–96.

Callejo, Gerard, Jonathan P. Giblin, and Xavier Gasull. 2013. "Modulation of TRESK Background K+ Channel by Membrane Stretch." *PLoS ONE* 8(5).

Castellanos, Aida et al. 2018. "Pyrethroids Inhibit K 2P Channels and Activate Sensory Neurons: Basis of Insecticide-Induced Paraesthesias." *Pain* 159(1): 92–105.

———. 2020. "TRESK Background K+ Channel Deletion Selectively Uncovers Enhanced Mechanical and Cold Sensitivity." *Journal of Physiology* 598(5): 1017–38.

Cavanaugh, Daniel J. et al. 2009. "Distinct Subsets of Unmyelinated Primary Sensory Fibers Mediate Behavioral Responses to Noxious Thermal and Mechanical Stimuli." *Proceedings of the National Academy of Sciences of the United States of America* 106(22): 9075–80.

Chae, Yun Jeong et al. 2010. 113 Anesthesiology *Discrete Change in Volatile Anesthetic Sensitivity in Mice with Inactivated Tandem Pore Potassium Ion Channel TRESK*. http://pubs.asahq.org/anesthesiology/article-pdf/113/6/1326/252499/0000542-201012000-00018.pdf.

Chen, Chao-Chen, Pierre Rainville, and M Catherine Bushnell. 1996. 68 Pain *Noxious and Innocuouscold Discriminationin Humans: Evidencefor Separateafferentchannels*.

Chiu, Isaac M. et al. 2014. "Transcriptional Profiling at Whole Population and Single Cell Levels Reveals Somatosensory Neuron Molecular Diversity." *eLife* 3: 1–32.

Crozier, R. A., S. K. Ajit, E. J. Kaftan, and M. H. Pausch. 2007. "MrgD Activation Inhibits KCNQ/M-Currents and Contributes to Enhanced Neuronal Excitability." *Journal of Neuroscience* 27(16): 4492–96.

Czirják, Gábor, and Péter Enyedi. 2006. “Zinc and Mercuric Ions Distinguish TRESK from the Other Two-Pore-Domain K+ Channels.” *Molecular Pharmacology* 69(3): 1024–32.

———. 2010. “TRESK Background K+ Channel Is Inhibited by Phosphorylation via Two Distinct Pathways.” *Journal of Biological Chemistry* 285(19): 14549–57.

———. 2014. “The LQLP Calcineurin Docking Site Is a Major Determinant of the Calcium-Dependent Activation of Human TRESK Background K+ Channel.” *Journal of Biological Chemistry* 289(43): 29506–18.

Czirják, Gábor, Zsuzsanna E. Tóth, and Péter Enyedi. 2004. “The Two-Pore Domain K+ Channel, TRESK, Is Activated by the Cytoplasmic Calcium Signal through Calcineurin.” *Journal of Biological Chemistry* 279(18): 18550–58.

Debreczeni, Dorina et al. 2023. “Critical Contribution of the Intracellular C-Terminal Region to TRESK Channel Activity Is Revealed by the Epithelial Na+ Current Ratio Method.” *Journal of Biological Chemistry* 299(6).

Dell, Ralph B., Steve Holleran, and Rajasekhar Ramakrishnan. 2002. “Sample Size Determination.” *ILAR Journal* 43(4): 207–12.

Deuis, Jennifer R., Lucie S. Dvorakova, and Irina Vetter. 2017. “Methods Used to Evaluate Pain Behaviors in Rodents.” *Frontiers in Molecular Neuroscience* 10: 1–17.

Dilek, Mustafa et al. 2021. “Activation of TRESK Background Potassium Channels by Cloxyquin Exerts Protective Effects against Excitotoxic-Induced Brain Injury and Neuroinammation in Neonatal Rats.” https://doi.org/10.21203/rs.3.rs-1188598/v1.

Dobler, Tina et al. 2007. “TRESK Two-Pore-Domain K+ Channels Constitute a Significant Component of Background Potassium Currents in Murine Dorsal Root Ganglion Neurones.” *Journal of Physiology* 585(3): 867–79.

Dong, Xinzhong et al. 2001. 106 Cell *A Diverse Family of GPCRs Expressed in Specific Subsets of Nociceptive Sensory Neurons Cord (Reviewed in Snider and McMahon, 1998). In Addi-Tion, C-Fibers Innervate a Variety of Peripheral Targets Including the Skin, Gut, Vasculature, and Muscle. Within*.

Ducourneau, Vincent R.R. et al. 2014. “Cancer Pain Is Not Necessarily Correlated with Spinal Overexpression of Reactive Glia Markers.” *Pain* 155(2): 275–91.

Egenberger, Brigitte, Georg Polleichtner, Erhard Wischmeyer, and Frank Döring. 2010. “N-Linked Glycosylation Determines Cell Surface Expression of Two-Pore-Domain K+ Channel TRESK.” *Biochemical and Biophysical Research Communications* 391(2): 1262–67.

Enyedi, Péter, Gabriella Braun, and Gábor Czirják. 2012. “TRESK: The Lone Ranger of Two-Pore Domain Potassium Channels.” *Molecular and Cellular Endocrinology* 353(1–2): 75–81.

Enyedi, Péter, and Gábor Czirják. 2010. “Molecular Background of Leak K+ Currents: Two-Pore Domain Potassium Channels.” *Physiological Reviews* 90(2): 559–605.

———. 2015. “Properties, Regulation, Pharmacology, and Functions of the K2P Channel, TRESK.” *European Journal of Physiology* 467(5): 945–58.

Eriksson, Emily, and Xavier Gasull Casanova. 2019. *Modulation of Pain Sensation by Calcineurin and TRESK Medical Science with a Major in Biomedicine*.

Fillingim, Roger B. et al. 2009. “Sex, Gender, and Pain: A Review of Recent Clinical and Experimental Findings.” *Journal of Pain* 10(5): 447–85.

Finno, Carrie J. et al. 2022. “Cisplatin Neurotoxicity Targets Specific Subpopulations and K+ Channels in Tyrosine-Hydroxylase Positive Dorsal Root Ganglia Neurons.” *Frontiers in Cellular Neuroscience* 16.

Grotz, W. H. et al. 2001. “Calcineurin-Inhibitor Induced Pain Syndrome (CIPS): A Severe Disabling Complication after Organ Transplantation.” *Transplant International* 14(1): 16–23.

Guo, Zhaohua et al. 2019. “TRESK K+ Channel Activity Regulates Trigeminal Nociception and Headache.” *eNeuro* 6(4).

Guo, Zhaohua, and Yu Qing Cao. 2014. “Over-Expression of TRESK K+ Channels Reduces the Excitability of Trigeminal Ganglion Nociceptors.” *PLoS ONE* 9(1).

Han, Ji Yoon, Ja Hyun Jang, Joonhong Park, and In Goo Lee. 2018. “Targeted Next-Generation Sequencing of Korean Patients with Developmental Delay and/or Intellectual Disability.” *Frontiers in Pediatrics* 6.

Häring, Martin et al. 2018. “Neuronal Atlas of the Dorsal Horn Defines Its Architecture and Links Sensory Input to Transcriptional Cell Types.” *Nature Neuroscience* 21(6): 869–80.

Herweijer, Geraldine et al. 2014. “Characterisation of Primary Afferent Spinal Innervation of Mouse Uterus.” *Frontiers in Neuroscience* (8 JUN).

Hong, Gyu Sang et al. 2016. “Tentonin 3/TMEM150c Confers Distinct Mechanosensitive Currents in Dorsal-Root Ganglion Neurons with Proprioceptive Function.” *Neuron* 91(1): 107–18.

Huang, Weiyuan et al. 2021. “TRESK Channel Contributes to Depolarization-Induced Shunting Inhibition and Modulates Epileptic Seizures.” *Cell Reports* 36(3): 109404. https://doi.org/10.1016/j.celrep.2021.109404.

Huang, Yuying et al. 2020. “Calcineurin Inhibition Causes A2D-1–Mediated Tonic Activation of Synaptic NMDA Receptors and Pain Hypersensitivity.” *Journal of Neuroscience* 40(19): 3707–19.

Hwang, Hee Youn et al. 2015. “TWIK-Related Spinal Cord K+ Channel Expression Is Increased in the Spinal Dorsal Horn after Spinal Nerve Ligation.” *Yonsei Medical Journal* 56(5): 1307–15.

Imbrici, Paola et al. 2020. “Altered Functional Properties of a Missense Variant in the TRESK K+ Channel (KCNK18) Associated with Migraine and Intellectual Disability.” *Pflügers Archiv - European Journal of Physiology* 472(7): 923–30. https://link.springer.com/10.1007/s00424-020-02382-5.

International Association for the Study of Pain Terminology Working Group. 2020. “IASP Revises Its Definition for the First Time Since 1979.” *International Association for the Study of Pain*: 4. http://186.42.188.158:8090/guias/TRATAMIENTO DEL DOLOR ONCOLOGICO EN ADULTOS.pdf.

Jiménez-Trujillo, Isabel et al. 2019. “Gender Differences in the Prevalence and Characteristics of Pain in Spain: Report from a Population-Based Study.” *Pain Medicine (United States)* 20(12): 2349–59.

Jo, Sally et al. 2019. “Comparing Electrical Stimulation and Tacrolimus (FK506) to Enhance Treating Nerve Injuries.” *Muscle and Nerve* 60(5): 629–36.

Jung, Min et al. 2023. “Cross-Species Transcriptomic Atlas of Dorsal Root Ganglia Reveals Species-Specific Programs for Sensory Function.” *Nature Communications* 14(1).

Kamuene, Jordie M., Yu Xu, and Leigh D. Plant. 2021. “The Pharmacology of Two-Pore Domain Potassium Channels.” In *Handbook of Experimental Pharmacology*, Springer Science and Business Media Deutschland GmbH, 417–43.

Kandel, E R, J D Koester, S H Mack, and S A Siegelbaum. 2021. *Principles of Neural Science, 6e.* 6th ed. eds. Michael Weitz and Kim J. Davis. United States of America: McGraw Hill. https://accessbiomedicalscience-mhmedical-com.sire.ub.edu/book.aspx?bookid=3024 (February 3, 2024).

Kang, Dawon, Changyong Choe, and Donghee Kim. 2005. “Thermosensitivity of the Two-Pore Domain K+ Channels TREK-2 and TRAAK.” *Journal of Physiology* 564(1): 103–16.

Kang, Dawon, and Donghee Kim. 2006. “TREK-2 (K2P10.1) and TRESK (K2P18.1) Are Major Background K+ Channels in Dorsal Root Ganglion Neurons.” *American journal of Physiology. Cell Physiology* 291(1): 138–46.

Kang, Dawon, Evan Mariash, and Donghee Kim. 2004. “Functional Expression of TRESK-2, a New Member of the Tandem-Pore K + Channel Family.” *Journal of Biological Chemistry* 279(27): 28063–70.

Karashima, Yuji et al. 2007. “Bimodal Action of Menthol on the Transient Receptor Potential Channel TRPA1.” *Journal of Neuroscience* 27(37): 9874–84.

Keshavaprasad, Bharat et al. 2005. “Species-Specific Differences in Response to Anesthetics and Other Modulators by the K2P Channel TRESK.” *Anesthesia & Analgesia* 101(4): 1042–49. http://journals.lww.com/00000539-200510000-00021.

Kim, Gyu Tae et al. 2020. “Upregulation of Tresk Channels Contributes to Motor and Sensory Recovery after Spinal Cord Injury.” *International Journal of Molecular Sciences* 21(23): 1–15.

Kita, Tomo et al. 2019. “FK506 (Tacrolimus) Causes Pain Sensation through the Activation of Transient Receptor Potential Ankyrin 1 (TRPA1) Channels.” *The Journal of Physiological Sciences* 69(2): 305–16. https://doi.org/10.1007/s12576-018-0647-z.

Klein, Amanda et al. 2021. “Pruriception and Neuronal Coding in Nociceptor Subtypes in Human and Nonhuman Primates.” *eLife* 10.

Lafrenière, Ronald G. et al. 2010. “A Dominant-Negative Mutation in the TRESK Potassium Channel Is Linked to Familial Migraine with Aura.” *Nature Medicine* 16(10): 1157–60.

Lengyel, Miklós et al. 2019. “Chemically Modified Derivatives of the Activator Compound Cloxyquin Exert Inhibitory Effect on TRESK (K2P18.1) Background Potassium Channel.” *Molecular Pharmacology* 95(6): 652–60.

Lengyel, Miklós, Gábor Czirják, David A. Jacobson, and Péter Enyedi. 2020. “TRESK and TREK-2 Two-Pore-Domain Potassium Channel Subunits Form Functional Heterodimers in Primary Somatosensory Neurons.” *Journal of Biological Chemistry* 295(35): 12408–25.

Lengyel, Miklós, Alice Dobolyi, Gábor Czirják, and Péter Enyedi. 2017. “Selective and State-Dependent Activation of TRESK (K2P18.1) Background Potassium Channel by Cloxyquin.” *British Journal of Pharmacology* 174(13): 2102–13.

Levine, David N. 2007. “Sherrington’s ‘The Integrative Action of the Nervous System’: A Centennial Appraisal.” *Journal of the Neurological Sciences* 253(1–2): 1–6.

Lindsay, Nicole Mercer et al. 2021. 13 Sci. Transl. Med *Brain Circuits for Pain and Its Treatment*. https://www.science.org.

Litwic, Anna, Mark H. Edwards, Elaine M. Dennison, and Cyrus Cooper. 2013. “Epidemiology and Burden of Osteoarthritis.” *British Medical Bulletin* 105(1): 185–99.

Liu, Canhui et al. 2004. “Potent Activation of the Human Tandem Pore Domain K Channel TRESK with Clinical Concentrations of Volatile Anesthetics.” *Anesthesia & Analgesia*: 1715–22. http://journals.lww.com/00000539-200412000-00026.

Llimós-Aubach, Júlia et al. “TRESK Background Potassium Channel in MrgprA3 + Pruriceptors Regulates Acute and Chronic Itch.” https://doi.org/10.1101/2024.01.25.577205.

Ma, Qiufu. 2010. “Labeled Lines Meet and Talk: Population Coding of Somatic Sensations.” *Journal of Clinical Investigation* 120(11): 3773–78.

Madisen, Linda et al. 2010. “A Robust and High-Throughput Cre Reporting and Characterization System for the Whole Mouse Brain.” *Nature Neuroscience* 13(1): 133–40.

Madrid, Rodolfo et al. 2009. “Variable Threshold of Trigeminal Cold-Thermosensitive Neurons Is Determined by a Balance between TRPM8 and Kv1 Potassium Channels.” *Journal of Neuroscience* 29(10): 3120–31.

Marsh, Barnaby, Cristian Acosta, Laiche Djouhri, and Sally N. Lawson. 2012. “Leak K + Channel MRNAs in Dorsal Root Ganglia: Relation to Inflammation and Spontaneous Pain Behaviour.” *Molecular and Cellular Neuroscience* 49(3): 375–86.

Mickle, Aaron D., Andrew J. Shepherd, and Durga P. Mohapatra. 2016. “Nociceptive TRP Channels: Sensory Detectors and Transducers in Multiple Pain Pathologies.” *Pharmaceuticals* 9(4).

Mills, Sarah E.E., Karen P. Nicolson, and Blair H. Smith. 2019. “Chronic Pain: A Review of Its Epidemiology and Associated Factors in Population-Based Studies.” *British Journal of Anaesthesia* 123(2): e273–83.

Mogil, Jeffrey S. 2017. “Laboratory Environmental Factors and Pain Behavior: The Relevance of Unknown Unknowns to Reproducibility and Translation.” *Lab Animal* 46(4): 136–41.

———. 2020. “Qualitative Sex Differences in Pain Processing: Emerging Evidence of a Biased Literature.” *Nature Reviews Neuroscience* 21(7): 353–65. http://dx.doi.org/10.1038/s41583-020-0310-6.

Muthuraman, Arunachalam, and Shailja Sood. 2014. “Pharmacological Evaluation of Tacrolimus (FK-506) on Ischemia Reperfusion Induced Vasculatic Neuropathic Pain in Rats.” *Journal of Brachial Plexus and Peripheral Nerve Injury* 05(01): e64–74. http://www.thieme-connect.de/DOI/DOI?10.1186/1749-7221-5-13.

Nguyen, Minh Q., Claire E. Le Pichon, and Nicholas Ryba. 2019. “Stereotyped Transcriptomic Transformation of Somatosensory Neurons in Response to Injury.” *eLife* 8: 1–22.

Pavinato, Lisa et al. 2021. “Kcnk18 Biallelic Variants Associated with Intellectual Disability and Neurodevelopmental Disorders Alter Tresk Channel Activity.” *International Journal of Molecular Sciences* 22(11).

Pergel, Enikő, Miklós Lengyel, Péter Enyedi, and Gábor Czirják. 2019. “TRESK (K2P18.1) Background Potassium Channel Is Activated by Novel-Type Protein Kinase C via Dephosphorylation.” *Molecular Pharmacology* 95(6): 661–72.

Pettingill, Philippa et al. 2019. “A Causal Role for TRESK Loss of Function in Migraine Mechanisms.” *Brain* 142(12): 3852–67.

Pitcher, Thomas, João Sousa-Valente, and Marzia Malcangio. 2016. “The Monoiodoacetate Model of Osteoarthritis Pain in the Mouse.” *Journal of Visualized Experiments* 2016(111).

Plotnikoff, Ronald et al. 2015. “Osteoarthritis Prevalence and Modifiable Factors: A Population Study Chronic Disease Epidemiology.” *BMC Public Health* 15(1).

Pogorzala, Leah A., Santosh K. Mishra, and Mark A. Hoon. 2013. “The Cellular Code for Mammalian Thermosensation.” *Journal of Neuroscience* 33(13): 5533–41.

Prommer, Eric. 2012. *Calcineurin-Inhibitor Pain Syndrome*. http://journals.lww.com/clinicalpain.

Racine, Mélanie et al. 2012. “A Systematic Literature Review of 10 Years of Research on Sex/Gender and Pain Perception - Part 2: Do Biopsychosocial Factors Alter Pain Sensitivity Differently in Women and Men?” *Pain* 153(3): 619–35.

Rainville, Pierre, Chao-Chen Chen, and M. Catherine Bushnell. 1999. “Psychophysical Study of Noxious and Innocuous Cold Discrimination in Monkey.” *Experimental Brain Research* 125(1): 28–34. http://link.springer.com/10.1007/s002210050654.

Raja, Srinivasa N. et al. 2020. “The Revised International Association for the Study of Pain Definition of Pain: Concepts, Challenges, and Compromises.” *Pain* 161(9): 1976–82.

Ran, Chen, and Xiaoke Chen. 2019. “Probing the Coding Logic of Thermosensation Using Spinal Cord Calcium Imaging.” *Experimental Neurology* 318: 42–49.

Ran, Chen, Mark A. Hoon, and Xiaoke Chen. 2016. “The Coding of Cutaneous Temperature in the Spinal Cord.” *Nature Neuroscience* 19(9): 1201–9.

Ranade, Sanjeev S. et al. 2014. “Piezo2 Is the Major Transducer of Mechanical Forces for Touch Sensation in Mice.” *Nature* 516(729): 121–25.

Rau, Kristofer K. et al. 2009. “Mrgprd Enhances Excitability in Specific Populations of Cutaneous Murine Polymodal Nociceptors.” *Journal of Neuroscience* 29(26): 8612–19.

Royal, Perrine et al. 2019. “Migraine-Associated TRESK Mutations Increase Neuronal Excitability through Alternative Translation Initiation and Inhibition of TREK.” *Neuron* 101(2): 232-245.e6.

Ruck, Tobias et al. 2022. “K2P18.1 Translates T Cell Receptor Signals into Thymic Regulatory T Cell Development.” *Cell Research* 32(1): 72–88.

Sadler, Katelyn E., Jeffrey S. Mogil, and Cheryl L. Stucky. 2022. “Innovations and Advances in Modelling and Measuring Pain in Animals.” *Nature Reviews Neuroscience* 23(2): 70–85.

Sánchez-Miguel, Dénison Selene et al. 2013. “TRESK Potassium Channel in Human T Lymphoblasts.” *Biochemical and Biophysical Research Communications* 434(2): 273–79.

Sano, Yorikata et al. 2003. “A Novel Two-Pore Domain K+ Channel, TRESK, Is Localized in the Spinal Cord.” *Journal of Biological Chemistry* 278(30): 27406–12.

Sato, Yuki, Tatsushi Onaka, Eiji Kobayashi, and Norimasa Seo. 2007. “The Differential Effect of Cyclosporine on Hypnotic Response and Pain Reaction in Mice.” *Anesthesia and Analgesia* 105(5): 1489–93.

Schewe, Marcus et al. 2016. “A Non-Canonical Voltage-Sensing Mechanism Controls Gating in K2P K+ Channels.” *Cell* 164(5): 937–49.

Schreiber, Julian Alexander et al. 2023. “Cloxyquin Activates HTRESK by Allosteric Modulation of the Selectivity Filter.” *Communications Biology* 6(1).

Shinohara, Tokuyuki et al. 2004. “Identification of a G Protein-Coupled Receptor Specifically Responsive to β-Alanine.” *Journal of Biological Chemistry* 279(22): 23559–64. http://dx.doi.org/10.1074/jbc.M314240200.

Smith, Howard S. 2009. “Calcineurin as a Nociceptor Modulator.” *Pain physician* 12(4): E309-18. http://www.ncbi.nlm.nih.gov/pubmed/19668290.

Tattersall, Glenn J. et al. 2012. “Coping with Thermal Challenges: Physiological Adaptations to Environmental Temperatures.” In *Comprehensive Physiology*, Wiley, 2151–2202.

Tavares-Ferreira, Diana, Pradipta R. Ray, et al. 2022. “Sex Differences in Nociceptor Translatomes Contribute to Divergent Prostaglandin Signaling in Male and Female Mice.” *Biological Psychiatry* 91(1): 129–40. https://doi.org/10.1016/j.biopsych.2020.09.022.

Tavares-Ferreira, Diana, Stephanie Shiers, et al. 2022. 14 Sci. Transl. Med *Spatial Transcriptomics of Dorsal Root Ganglia Identifies Molecular Signatures of Human Nociceptors*. https://www.science.org.

Tsagareli, Merab G., and Ivliane Nozadze. 2020. “An Overview on Transient Receptor Potential Channels Superfamily.” *Behavioural Pharmacology* 31(5): 413–34.

Tulleuda, Astrid et al. 2011. “TRESK Channel Contribution to Nociceptive Sensory Neurons Excitability: Modulation by Nerve Injury.” *Molecular Pain* 7(1): 30. http://www.molecularpain.com/content/7/1/30.

Usoskin, Dmitry et al. 2015. “Unbiased Classification of Sensory Neuron Types by Large-Scale Single-Cell RNA Sequencing.” *Nature Neuroscience* 18(1): 145–53. http://dx.doi.org/10.1038/nn.3881.

Vandewauw, Ine et al. 2018. “A TRP Channel Trio Mediates Acute Noxious Heat Sensing.” *Nature* 555(7698): 662–66.

Voda, Jan, Aldric Hama, and Jacqueline Sagen. 2007. “FK506 Reduces the Severity of Cutaneous Hypersensitivity in Rats with a Spinal Cord Contusion.” *Neuroscience Research* 58(1): 95–99.

Wang, Changming et al. 2019. “Facilitation of MrgprD by TRP-A1 Promotes Neuropathic Pain.” *FASEB Journal* 33(1): 1360–73.

Wang, Feng et al. 2018. “Sensory Afferents Use Different Coding Strategies for Heat and Cold.” *Cell Reports* 23(7): 2001–13.

Wei, X. et al. 2018. “Tacrolimus-Induced Pain Syndrome After Bone Marrow Transplantation: A Case Report and Literature Review.” *Transplantation Proceedings* 50(10): 4090–95.

Weir, Greg A. et al. 2019. “The Role of TRESK in Discrete Sensory Neuron Populations and Somatosensory Processing.” *Frontiers in Molecular Neuroscience* 12: 1–11.

Woo, Seung Hyun et al. 2015. “Piezo2 Is the Principal Mechanotransduction Channel for Proprioception.” *Nature Neuroscience* 18(12): 1756–62.

Woolf, Clifford J. 2010. “What Is This Thing Called Pain?” *Journal of Clinical Investigation* 120(11): 3742–44.

Wooten, Matthew et al. 2014. “Three Functionally Distinct Classes of C-Fibre Nociceptors in Primates.” *Nature Communications* 5.

Wright, Paul D. et al. 2013. “Cloxyquin (5-Chloroquinolin-8-Ol) Is an Activator of the Two-Pore Domain Potassium Channel TRESK.” *Biochemical and Biophysical Research Communications* 441(2): 463–68.

Xiao, Rui, and Shawn Xu. 2020. “Annual Review of Physiology Temperature Sensation: From Molecular Thermosensors to Neural Circuits and Coding Principles.” *The Annual Review of Physiology is online at* 83: 205–35. https://doi.org/10.1146/annurev-physiol-031220-
.

Xie, Keyu, Xu Cheng, Tao Zhu, and Donghang Zhang. 2023. “Single-Cell Transcriptomic Profiling of Dorsal Root Ganglion: An Overview.” *Frontiers in Neuroanatomy* 17.

Yalcin, Ipek et al. 2009. “Differentiating Thermal Allodynia and Hyperalgesia Using Dynamic Hot and Cold Plate in Rodents.” *Journal of Pain* 10(7): 767–73. http://dx.doi.org/10.1016/j.jpain.2009.01.325.

Yang, Yue et al. 2018. “Decreased Abundance of TRESK Two-Pore Domain Potassium Channels in Sensory Neurons Underlies the Pain Associated with Bone Metastasis.” *Science Signaling* 11(552).

Yarmolinsky, David A. et al. 2016. “Coding and Plasticity in the Mammalian Thermosensory System.” *Neuron* 92(5): 1079–92.

Yoo, SieHyeon et al. 2010. “Regional Expression of the Anesthetic-Activated Potassium Channel TRESK in the Rat Nervous System.” 465(1): 79–84.

Zeisel, Amit et al. 2018. “Molecular Architecture of the Mouse Nervous System.” *Cell* 174(4): 999-1014.e22.

Zheng, Yang et al. 2019. “Deep Sequencing of Somatosensory Neurons Reveals Molecular Determinants of Intrinsic Physiological Properties.” *Neuron* 103(4): 598-616.e7. https://doi.org/10.1016/j.neuron.2019.05.039.

Zhou, Jun et al. 2017. “Reversal of TRESK Downregulation Alleviates Neuropathic Pain by Inhibiting Activation of Gliocytes in the Spinal Cord.” *Neurochemical Research* 42(5): 1288–98.

Zhou, Jun, Cheng-Xiang Yang, Ji-Ying Zhong, and Han-Bing Wang. 2013. “Intrathecal TRESK Gene Recombinant Adenovirus Attenuates Spared Nerve Injury-Induced Neuropathic Pain in Rats.” *NeuroReport* 24(3): 131–36. https://journals.lww.com/00001756-201302130-00006 (January 27, 2024).

Zylka, Mark J., Frank L. Rice, and David J. Anderson. 2005. “Topographically Distinct Epidermal Nociceptive Circuits Revealed by Axonal Tracers Targeted to Mrgprd.” *Neuron* 45(1): 17–25. https://linkinghub.elsevier.com/retrieve/pii/S0896627304008037.